Improved Estimations of Energy Consumption for Dredging Activities Based on Actual Data

S. A. Lamers
TU Delft

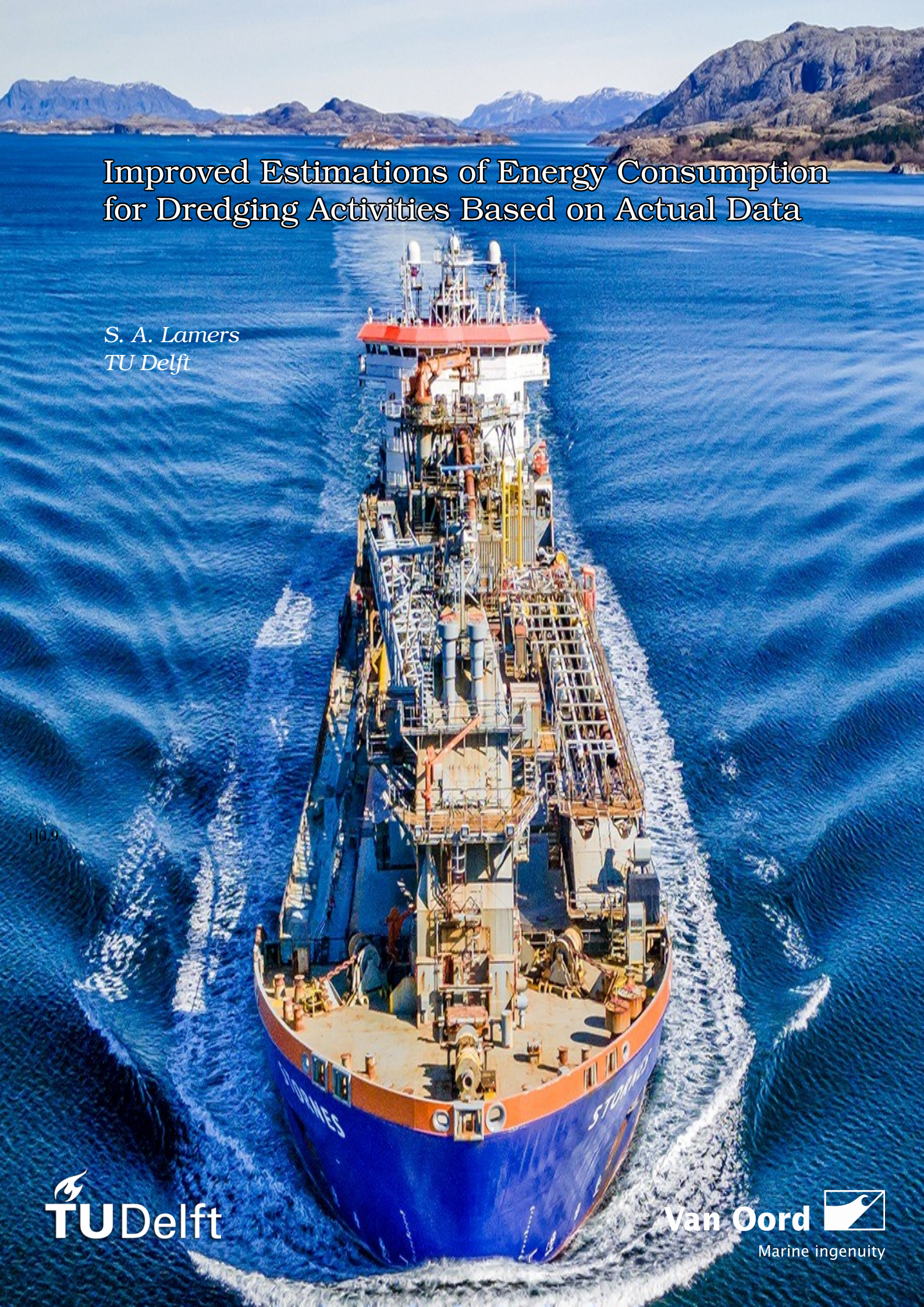

TU Delft

Van Oord
Marine ingenuity

Improved Estimation of Energy Consumption for Dredging Activities Based on Actual Data

by

S.A. Lamers

A thesis presented for the degree of
Master of Science at the Delft University of Technology
To be defended publicly on Wednesday September 14, 2022.

Studentnumber: 4478754
Committee: Prof. dr. ir. M. Van Koingsveld, TU Delft (chair)
M. De Geus, Van Oord
M. Jiang, TU Delft
C. Van Rhee, TU Delft
J. Antolinez, TU Delft
Hydraulic Engineering
Delft University of Technology
The Netherlands
June 2022

Preface

This research is carried out in order to complete the Hydraulic Engineering program at the faculty of Civil Engineering and Geosciences of the Delft University of Technology, in order to obtain a master's degree.

During this eleven month period, this research has been conducted with guidance of Van Oord, a marine contractor. The motivation of this research concerns the upcoming consequences of climate change in the dredging sector, whereas improvement of estimating energy consumption is becoming more important. During my research, Van Oord always provided me with kindness and support. They made me feel like Van Oord was my home and always stood out for me. I want to thank the company for providing me the opportunity to develop myself inside the boundaries of their company. In addition, I would like to thank everyone else who has supported me during the process.

To begin with, I would like to thank Martin de Geus, my daily supervisor at Van Oord. Thanks to your enthusiasm and support, I showed real process on personal and practical level, which lead me to where we are right now. Thanks to your ability to no only demonstrate knowledge but also to convey it to me really supported me in becoming the engineer that I am right now. Furthermore I would like to thank my chair of my committee Mark van Koningsveld for his constant enthusiasm when I was presenting my research. Your way of discussing with someone, instead of against them, has taught me a new skill which I am hoping to develop more in the future. Next, I would like to thanks Man Jiang, member of my committee, for always being there for me when I needed some other perspective in doing the research. Our discussions were not only very thoughtful, I also enjoyed them by heart. Many thanks for supporting me in rough times. I would like to thank my other committee members, Cees van Rhee and José Antolínez for supporting me through the process and providing feedback. At last many thanks to all my friends and family, especially Koosje who did a great job in handling me while I was managing this roller coaster, must have been tough. Other thanks to my friends from the Maison, Joost, Willem, Joppe and Pepijn, could not have performed this without the discussions we had or the support you provided me. It was a long run in which I did not expect the process to be so learnful.

Stijn Lamers
Amsterdam, June 2022

Abstract

The consequences of climate change are happening now, and will increase in the years to come. Understanding the energy consumption of dredging operations is becoming increasingly important for dredging contractors such as Van Oord. With the emergence of more complex dredging situations, including dredging at limited depths and short sailing distances, it has become more difficult to provide an accurate estimate. This research was conducted to evaluate Van Oord's current estimation method, called VOHOP, and to provide an improved estimate of the energy consumption for dredging activities based on historical data. Therefore, the main objective of the study is as follows:

"To improve the estimation of energy consumption for dredging activities based on actual data."

To achieve this goal, the method that is selected for creating improvement is comparing estimation methods with actual data where the difference gives insight in how to improve the estimation method, explained more briefly: EST vs ACT = DIFF. A literature review is first conducted to indicate what a dredging cycle looks like. After analyzing the different phases, consisting of sailing empty, loading, sailing full and disposing, the parameters that play a role in the consumption of energy during the dredging process are stated. For example for the sailing stages parameters that play a role are: sailing distance and sailing speed. Due to the relatively less elaborate calculation of energy consumption for the sailing stages, an improvement of estimation accuracy for these phases is considered to be valuable. Next, existing alternative methods for estimating energy consumption for the sailing phases are explored and the method proposed by Holtrop & Mennen (HM), including modifications created for limited depth estimations, is selected as the most appropriate because it takes into account a larger number of parameters (such as depth, draught and distance), which is expected to increase the accuracy. After comparing the current estimation method VOHOP, with the method proposed by HM including modifications, one of the main findings is that the modified HM approach has a lower outcome of energy consumption compared to VOHOP especially for larger depths. After comparing, the starting point of the selected estimation method (EST) is created. The comparison of the modified HM method and VOHOP is done by means of the simulation software OpenCLSim in Python.

To validate the accuracy of either VOHOP or modified HM, comparative material consisting of actual data provided by Van Oord is used. Multiple projects (20+) that have been performed by a trailing suction hopper dredger (TSHD) of Van Oord are analyzed after which three are selected. The selection is based on the amount of data available for a project and the difference in depth and distance, to use data that is suitable for comparison. After filtering out non-representative data (missing data points or too large time steps), the actual data is analyzed where a distinction is made between acceleration, free sailing and deceleration. Using the suitable data for comparison contributes to the actual data (ACT) part of this research.

The selected actual data is compared with the modified HM approach for estimating energy consumption, which contributes to the DIFF part. For the free sailing part, a main finding when comparing the modified HM with the actual data is the deviation (lower estimation compared to actual data) for increasing depth estimations (analyzed for depths up to 60 m). A possible reason for this is due to the applied modifications for the modified HM approach that are observed to have less impact on the estimation for increasing depths with respect to the draught. However, estimates for limited depth also show a deviation as the results are more sensitive and show an asymptotic behaviour for which a correction is recommended. It is therefore concluded that the modified HM approach needs corrections for both estimating deeper situations as for situations with more limited depths. After analysing the resistance components of the modified HM approach in different situations, consisting of different ratios of depth and draught, the reason for the large deviation in the modified HM method for deeper situations and the greater sensitivity for more limited depths is found in the contribution of the wave resistance term R_w. This is found out after comparing and determining the contribution of all resistance terms for multiple situations gathered from real time projects of actual data containing increasing depths and draughts. A correction to the wave resistance calculation is made using actual data, finding a fitting between increasing wave resistance for increasing vessel draught with respect to water depth. The result is a proposed HM method containing a less sensitive estimation method that takes into account the draught of the vessel related to the water depth for both deeper situations and shallower situations.

The acceleration and deceleration phases of the actual data are considered inappropriate for comparison with the modified HM approach, since the used power in the actual data contains the effect of slip, causing the vessel to use more power for reaching a certain velocity than actually required according to modified HM. Therefore, to improve the estimation of the acceleration and deceleration, a generalised fit is found in the actual data

for the power in relation to time. This fit is generated for different ranges of depth and is coupled with the sailed distance to quantify whether the distance has any effect on the results. It is found that at a short sailing distance a significantly lower velocity is achieved, which in turn affects the power used. By taking into account depth and distance, an estimation fit results that takes into account a larger number of parameters (velocity, distance, depth and draught) than the VOHOP method, and is therefore expected to produce more accurate results. With the estimation fits created for acceleration and deceleration and the corrected estimation method, HM proposed, for free sailing, the outcome is a newly created estimation tool that is based on historical data.

The improvement of the newly developed estimation method is validated by comparing VOHOP and the new estimation tool with eight cases from historical data. The cases are selected at different depths and different distances and are found in the selected projects for this research. The results show an increase in accuracy for the acceleration phase, while the other two phases, free sailing and deceleration, show fluctuating results. The reason for the fluctuation in the free sailing phase is the difference in duration of the phase caused by the definition of acceleration and free sailing, where the new estimation tool considers part of the free sailing as acceleration. The results indicate that the power usage is more accurately estimated by the new estimation tool, which indicates that the fluctuations of energy estimates are caused by a miss-estimation of duration instead of power usage. For deceleration, the fluctuating results can be attributed to the fluctuating pattern of deceleration, which may be caused by external factors such as traffic or currents, making it difficult to predict the energy consumption for this part of the sailing phase. All in all, the new estimation tool exhibits greater accuracy for the overall energy consumption estimation compared to the current estimation method VOHOP. In addition, the estimation of power consumption during free sailing shows improvement, indicating that incorrect estimates of energy during free sailing are more likely to be caused by inaccurate estimations of the duration instead of inaccurate estimations of power.

In conclusion, the results show that when considering depth, distance and draught as input parameters and applying a data based correction, the accuracy of the estimation method increases. Where the results do show an improvement, it is recommended that further research be conducted on the estimation of energy consumption and sailing duration for acceleration and deceleration. Several assumptions were made in this study to simplify the analysis such as constant wave climate, where a follow-up study could verify these assumptions or even improve the results of the study by implementing additional consequences for these assumptions. Moreover, this study took into account a certain number of parameters and observed only one vessel type, where adding more parameters or considering more vessel types would give a clear picture of the reliability of the estimation method and energy consumption. A further study is needed to perform the same procedure of improving the estimation also for the other phases of a dredging cycle, since these phases do contribute to a large extent of the total energy consumption of a dredging cycle. Finally, using a larger amount of data for this study could reduce the uncertainty of the results and increase the reliability. In addition, an increase in the quality of the data further increases the reliability of the results.

Contents

Acronyms

AE Auxiliary Engine
AIS Automatic Identification System

CO_2 Carbon Dioxide
CSD Cutter Suction Dredger

EEDI Energy Efficiency Design Index
ETS European Trading System

GHG Green House Gas
GPS Global Positioning System

HM Holtrop & Mennen

IMO International Maritime Organization
ITTC International Towing Tank Conference

LR Loading Rate

ME Main Engine

OpenCLSim Open Complex Logistics Simulation

RTK Real Time Kinetics

SE Sailing Empty
SF Sailing Full
SFC Specific Fuel Consumption
STEAM Ship Traffic Emission Assessment Model

TSHD Trailing Suction Hopper Dredger

VOHOP Van Oord Hopper Estimation Tool

1 Introduction

1.1 Background Description

The effects of human-caused global warming are happening now, are irreversible on the timescale of people alive today, and will worsen in the decades to come (Jackson, 2017). Since the maritime sector is a major contributor to CO_2 emissions with a yearly emission of 1 billion metric tonne of CO_2, a reduction in environmental pollution is necessary (Van der Bilt, 2019; Statista, 2021). Dredging activities are related to a high fuel combustion, and thus a high emission of greenhouse gas (GHG) is associated with performing these activities (Murphy, 2012). In order to reduce environmental pollution, it is important to gain a better understanding of the amount of GHG released during certain dredging activities. Before creating a better view on the amount of fuel consumed, first the amount of energy consumed is determined. With upcoming penalties for excessive pollution, dredging companies need more insight into their prior estimates of energy consumption to adjust their tender planning. This thesis presents an improved method for estimating the amount of energy consumption that occurs in certain dredging operations. The result is an estimation method that is able to accurately predict the amount of energy consumption, giving dredgers a better view of their GHG emissions.

Before providing more information on the impact of environmental awareness in the dredging industry, a brief overview of the dredging industry itself is given. A problem analysis is then given, followed by the scope and research objective of this thesis. Next, the research approach and the thesis outline are described to provide an overview of the steps taken to arrive at certain results.

1.1.1 Dredging Activities

Dredging is the process of carrying out an excavation operation underwater, in shallow or deep seas, with the purpose to collect bottom sediments and dispose at a different location (Haldar, 2013). Dredging activities, carried out by specialized dredge vessels, can have a wide variety of reasons including navigational purposes, environmental remediation, flood control, and the placement of engineering structures. Dredging is also carried out to extract material for land reclamation and sand nourishment (Vivian, 2009). Dredging projects can be divided into two types: capital dredging and maintenance dredging. Capital dredging is defined as the initial dredging activity, i.e., the creation of navigation channels for example. Maintenance dredging is carried out to maintain the situation created by dredging, i.e. maintaining the required depth of a navigation channel. Since nature will attempt to return the situation to an equilibrium that fits with local hydrodynamic conditions, maintenance dredging is of great importance as the dredging activity is deviating from the equilibrium situation. Dredging projects are offered at the market in the form of a tender. A contractor can bid on the tender and win the project depending on the dredging strategy it proposes.

Due to climate change, sea levels are rising, which has many consequences. One measure to protect us from rising sea water is to maintain nourishments on the coasts by carrying out dredging operations. Moreover, additional dredging could be considered to be carried out to achieve a higher level of protection to protect the coasts for the future environmental problems. Despite dredging being considered highly efficient and regarding the large variety in functions (EuDA, 2022), dredging does require a large amount of energy. With rising sea levels, dredging is inevitable due to its simplicity and wide portfolio (EuDA, 2022). Therefore, it is important to better estimate the environmental impacts of dredging. Improving energy estimates could potentially lead to more environmentally friendly project strategies that result in lower environmental impact and give a better view on the total impact with an eye on energy consumption and the amount to mitigate.

1.1.2 Environmental Status

Because the impact of countries on the environment has never been more important than it is today, some countries have set climate goals for the coming years to reduce the impact of climate change. In 2015, a group

of 196 parties made a set of rules and plans to address the problem of climate change, this is called the Paris Agreement (UNCC, 2021). One of the main goals is to limit global temperature rise by reducing greenhouse gas emissions and achieve a climate-neutral world by the middle of the century. To meet the requirements of the Paris Agreement, Rijkswaterstaat has set a goal of being energy neutral by 2030 (Rijkswaterstaat, 2021). This means that Rijkswaterstaat wants to generate as much energy as it consumes. For 2030, the European Union has set itself the target of reducing greenhouse gas emissions by 40% relative to 1990 (ECN & Planbureau voor de Leefomgeving, 2014). In addition, the European Commission has set out a target, the Green Deal, to reduce the emission of GHG with 55% in 2030 compared to 1990, and measures are undertaken by the so called Fit for 55% package (Kort, 2021), (EUC, 2020). This package consists of more than ten legislative proposals which are supposed to realize this reduction in GHG emission. The ultimate goal: Europe to be climate neutral by 2050 (Kort, 2021). In addition, Europe should no longer contribute to global warming (Jiang et al., 2022).

Despite the need to reduce the GHG emissions, it is financially not the most convenient way for a contractor to operate as bio- or e-fuels are more costly. However, policies are made for contractors to make it more desirable to make a more environmental friendly project strategy. For example, Rijkswaterstaat has introduced the CO_2 ladder. This concept holds that contractors that apply for a tender, and are able to show that measures are taken to reduce their environmental impact for the project, get a favourable position for the tender (Rijkswaterstaat, 2021). Contractors with considerable environmental measures end up at a higher position on the CO_2 ladder where a higher position leads to a lower registration fee for the tender and could lead to discounts on their eventual tender price. An important aspect of the CO_2 ladder is that the contractor has to actually realize their promises otherwise a sanction of 1.5 times the given discount is applied (Rijkswaterstaat, 2021).

Another method that is used to reduce the carbon emission of companies is the European Trading System (ETS) which started in 2005. This system works with a "cap and trade" principle. A cap is set on the total amount of certain GHG that may be emitted by the installations or companies covered by the system. Over time, this cap will be reduced so that the total emissions will also be reduced (European Commission, 2022). Inside the cap, companies can trade their emissions allowances. Buying allowances from others will give you the right to emit more GHG while the party that sold their allowance will have to reduce their emissions. The amount of GHG that are produced are monitored, exceeding your allowance limit leads to heavy fines (European Commission, 2022). The ETS concept has a large influence on the dredging industry as energy consumption estimations are inaccurate at the moment. This could lead to exceeding of their emission allowances resulting in sanctions.

Due to the strict measures that are taken to reduce GHG emissions, the importance of an accurate CO_2 emission estimation has become significant. The contractor is able to have a better view on whether the actual energy consumption (and thus GHG emissions) is exceeding their planned value. With better estimations, the mistakes made in planned emissions will be reduced. Contractors will be able to adapt their strategy so that the allowed amount of GHG is emitted. In addition, an accurate estimation also improves their position on the tender market as more insights will give the opportunity to suppose an either favourable but most of all feasible dredging strategy (with no miss-estimates afterwards).

1.2 Problem Analysis

With the increasing attention to environmental pollution regarding the upcoming taxes and sanctions for GHG emissions, it is important for dredging contractors to gain a better insight in energy estimates. The significance of total duration of a dredging project is decreasing while the importance of environmental awareness is rising. Contractors must give priority to sharpening their estimation tools on energy consumption so that strategies with a low environmental impact can be conducted while still remaining competitive on the tender market.

Dredging contractor Van Oord does have an estimation tool for predicting the power production and energy consumption (and thus CO_2 production). However, due to new data collections, the estimating tool is potentially outdated with a less accurate estimation as result. The current tool does not comply to the complex projects that appear in real world nowadays and only gives an estimation for more standard situations (10 nautical miles sailing distance and 300 μ grain size). Therefore Van Oord cannot adapt their strategy based on a certain tender in order to conduct it in the most optimal way. At the moment, the estimation tool of Van Oord is based on basic parameters that do not take variations in dredging projects with it and therefore does not give a realistic result for more complex tenders that arise nowadays. It is necessary to implement certain parameters that do have an influence and take them into account when making an estimation.

Problem Statement

To formulate the main problem: The current estimation tools are considered not up to date for the future situation with respect to the environmental problems and more complex dredging situations ahead (shallow depth, short distances and certain constraints). Because of upcoming fines for excessive emission patterns, it is important for Van Oord and other contractors to have a better understanding of the amount of CO_2 that will be produced before a dredging project is undertaken. It is unknown to contractors which alternative will produce the best result, both in terms of CO_2 emissions and costs, knowing that in the future certain penalties will be imposed for excessive CO_2 production patterns. Gaining more insight in the energy consumption for dredging activities gives in its way a better view on emission patterns and costs as the energy consumption is linked to these factors. An improved model for estimating energy consumption should be developed to better understand CO_2 production for different types of dredging projects. The model allows the contractor to see in advance which dredging strategy is more optimal and how it differs from other alternatives in terms of environmental pollution. In addition, it should also allow the contractor to either choose a more environmentally friendly strategy and still maintain a competitive position in the market.

1.3 Research Scope

The research on the estimation of energy consumption is based on a trailing suction hopper dredger (TSHD) owned by Van Oord of which the identity remains confidential. The reason to use the TSHD as a proof of concept is because this vessel is considered to be representative for dredging projects that concern this thesis. Besides, there is a large amount of actual data available for this vessel compared to others. In this way, the results of the evaluation and the improvement of the estimation can be compared to historical data of the TSHD. It is important to keep in mind that the results of the thesis are all based on only a TSHD and no other type of vessel is considered (such as a cutter suction dredger).

1.4 Research Goal

The overall aim of the research is: To improve the estimation of energy consumption for dredging activities, in order to enable the comparison of different dredging strategies with a view on energy consumption. This is achieved by analyzing historical data provided by Van Oord in combination with the software tool OpenCLSim. Different historical projects carried out by the TSHD are compared to each other in terms of estimations and actual data. Based on this, an improved estimation method is created. The output of the research contains the creation of an improved estimation tool which is not only suitable for the standard dredging projects, but also shows improved estimations for more complex dredging projects (for example short sailing distance or shallow depth dredging).

To elaborate more on the research objective, some more specifications within the project aim are given. The objective is achieved by evaluating the different factors that influence the estimation in the current situation and subsequently developing a more accurate estimation model which produces the estimated amount of energy consumption as outcome, specified for a specific dredging project. This research is carried out as a follow-up on the energy consumption analysis of Van der Bilt (2019) and the research on estimation of energy consumption for IWT carried out by Segers (2020). The model is supposed to give a better estimation on the energy consumption than the current estimation model used by Van Oord called VOHOP. In addition, the model enables users to implement different strategies for the same dredging project in order to get a view on what alternative has the optimal environmental outcome while remaining competitive on the tender market. With the rising sanctions on CO_2 production, this model can eventually become leading for both environmental considerations as cost considerations. It is the main goal for the model to be able to have different input while still an accurate estimate is the outcome. To summarize, the research objective is:

To improve the estimation of energy consumption for dredging activities based on actual data.

To achieve the research objective, the following research questions are stated:

(i.) What does a dredging process look like and what variables play a role?

(ii.) What is the current estimation method for quantifying energy consumption based on?

(iii.) What other estimation models exist to quantify energy consumption?

(iv.) How to develop and validate a model to evaluate and improve the estimation of energy consumption?

1.5 Research Approach

In this section an indication is given on how the problem is treated and how the research objective and questions are handled. The methodology of performing the research is shown. The research approach consists of the following parts:

- Introduction
- Literature Study
- Materials and methods
- Results
- Discussion
- Conclusion

The research approach selected for this research is shown.

First of all, the relevance and importance of the research is stated. Due to the upcoming consequences of climate change, dredging contractors, such as Van Oord, have to gain insight in energy consumption, so that alternative strategies can be selected to reduce emissions. Certain penalties in excessive energy use increase the desire for a sustainable way of carrying out dredging activities. However, the current energy estimation methods are considered outdated as new complex dredging situations arise such as short sailing distances. This defines the problem that appears nowadays, with subsequently the research objective: to create an improved estimation method for estimating energy consumption for dredging activities based on actual data. In this research the data that is used to create an improved estimation method is provided by Van Oord. The scope of the research is limited to a TSHD owned by Van Oord. This part of the research approach is treated in Chapter 1 and is considered as the introduction.

In the literature study, written in Chapter 2, it is stated why estimating the energy consumption in dredging projects is important and why improvement is required. The basics of a dredging cycle are shown to give a clear vision of what a dredging process looks like. After this, the various factors that play a role in the current estimation method, called VOHOP, of energy consumption are indicated. Subsequently, some existing estimation models are treated in order to compare them to VOHOP. The method proposed by Holtrop & Mennen is selected combined with certain modifications that already exist for this estimation method.

The next step of the research approach is the materials and methods. This is first treated in Chapter 3, Estimation Analysis (EST), where an elaborate explanation is given of the Holtrop & Mennen method that is used for comparison. The different components of this estimation method are indicated consisting of different type of resistance terms and certain modifications that are applied according to literature. After clearly indicating the calculation method and the modifications that are applied, the modified Holtrop & Mennen approach is compared to the current estimation method (VOHOP). This step is done in order to show whether there are differences in the results between these two methods.

Moreover, the materials and methods part consists of examining the historical data (ACT) provided by Van Oord. This step is carried out in order to compare the historical data with the modified Holtrop & Mennen method and the VOHOP method to show how accurate these estimations are. However, first the data is filtered to ensure the workability of the data. Part of the filtering process is removing zero-valued sensordata and removing outliers to ensure the data to be suitable for comparison. Now that the data is considered to be suitable, certain projects carried out by the TSHD are selected to be researched. This selection is done based on the amount of data available for the projects and the reliability of the data. Three projects are selected of which the actual data is compared to the VOHOP estimations and the modified Holtrop & Mennen estimations. The selection and analysis of the actual data is part of the materials and methods of this research and is treated in Chapter 4, Historical Data Analysis.

To finalize the materials and methods part, the actual data, selected in Chapter 4, is compared to the selected estimation method from Chapter 3. For this comparison there are two scenarios that are likely to occur. Scenario 1 exists of EST $\approx$ ACT. In this case, the estimation method shows similar results as the actual data. The definition of this scenario is set on a maximum deviation of 20%. For this scenario, a correction factor is created in order to improve the accuracy of the estimation. However if the second scenario, EST $\neq$ ACT (so a difference of more than 20%) appears, the method of improvement has to be examined. The reason behind

miss-estimation is identified and it is determined whether applying a correction factor suffices. If applying a correction factor is considered unsuitable, another method is applied. This alternative method consists of analyzing power fits of the actual data and creating a estimation that is based on this fit for different type of situations such as varying distances or varying depths. After analyzing the comparison and creating either a correction factor or a estimation fit, the material and methods part is completed with as an end results an estimation method that is based on the actual data. This last part of comparing and creating the improvement is carried out in the first part of Chapter 5, Application & Results.

The second part of Chapter 5, Application & Results, consists of a case study for different type of situations to verify whether the improved estimation method has an actual improvement. In this case study both VOHOP and the newly created estimation method are compared to cases of actual data and the energy consumption is calculated. After comparison the resulting improvement is shown in order to draw conclusions. This is part of the results of the research approach.

Chapter 6 contains the discussion and the conclusion. First the research discussion is treated in which an overall summary of the research is given, followed by the interpretations and implications of the research. After this the observed limitations and recommendations are mentioned. After given a detailed overview of what the exact recommendations are, the conclusion of the research is stated. The conclusion consists of summarizing the research objective of the research and showing step by step what methods are used in order to find the results of the research. The findings of each chapter are concisely described and finalized by the drawn conclusions. This chapter is ended by showing an indication of the results and stating the recommendations of the research.

2 | Literature Study

In this chapter a literature study is done to answer the first three sub-questions:

(i.) *What does a dredging process look like and what variables play a role?*

(ii.) *What is the current estimation method for quantifying energy consumption?*

(iii.) *What other methods exist for quantifying energy consumption?*

Literature provides answers on what the energy consumption and its estimation is based on during a dredging project. In Section 2.1 the basics of a dredging cycle are shown to give a better understanding of what a dredging cycle looks like. Section 2.2 zooms into the dredging phases and mentions what factors play a role. It is important to mention which of the factors can be influenced by the contractor side and which of the factors are set by other external parties. Next, Section 2.3 gives an overview of other existing estimation methods and emphasizes important differences. An important part of the first three sections is to express where the gap of knowledge is on estimating the energy consumption for dredging cycles. At last, the answer to the first three sub-questions is given in Section 2.4.

2.1 System Analysis

This section details the dredging cycle performed by the TSHD. The different phases of the cycle are mentioned. A broader analysis of certain equipment used during the dredging process is also given, and it is highlighted which equipment is used at which stage of the dredging cycle.

2.1.1 Basics of the Dredging Cycle

Within the cycle of a dredging project, a distinction is made between different dredging phases. When calculating the energy required for a particular dredging project, the phases within the project are split up as discrete events and calculated separately. The four phases that represent a dredging cycle are: sailing empty, dredging, sailing full and disposal. Each completed cycle is called a trip and a dredging project is completed after a number of trip sequences until all material has been excavated or placed in the proper location. Thus, the total time required for a dredging project can be described as the following equation, where n is the number of trips required to complete the project:

$$t_{project} = \sum_{i=0}^{n} (t_{sailing,empty} + t_{dredging} + t_{sailing,full} + t_{disposing}) \tag{2.1}$$

With the four stages in mind, a schematization of a whole cycle is shown in Figure 2.1.

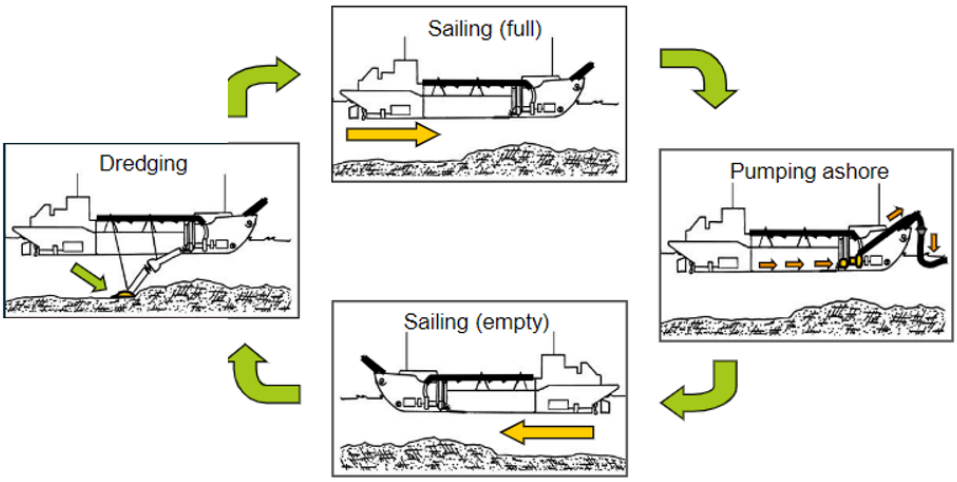

Figure 2.1: Stages of a dredging cycle

To give a better understanding of how long the process takes and what the volumes of dredged material are for a hopper, Figure 2.2 gives a picture of the dredging process during one trip (Van der Bilt, 2019). Different colors represent different stages of the dredging cycle. As shown in the figure, for the sailing phases, there is no change in weight during a cycle. However, for the dredging and disposal phases, there is a slight change of direction in the line. The phases are, also in the legend of the figure, divided into two parts. For the dredging phase, this distinction is due to overflow. First, the mixture of sand and water is loaded into the hopper until the overflow point is reached. After the overflow has occurred, the dredging process continues. However, when the overflow begins, low-density material will cause a loss in efficiency because it is the first material to be lost as the process continues. Therefore the deflection occurs in the figure. The deflection of the curve is considered greater if more fine material is dredged instead of coarse material (Van der Bilt, 2019). A small deflection can also be observed for the disposal phase. This occurs only for disposal through pipelines and not for dumping through bottom doors. The first part of the disposing stage (unloading stage 1 in the figure) is also called the bulk stage, where the second part (unloading stage 2 in the figure) is also referred to as clean-up stage. The reason for the deflection of the curve is that further on in the disposal process there is less sandy material in the hopper, so the hopper loses efficiency (Van der Bilt, 2019).

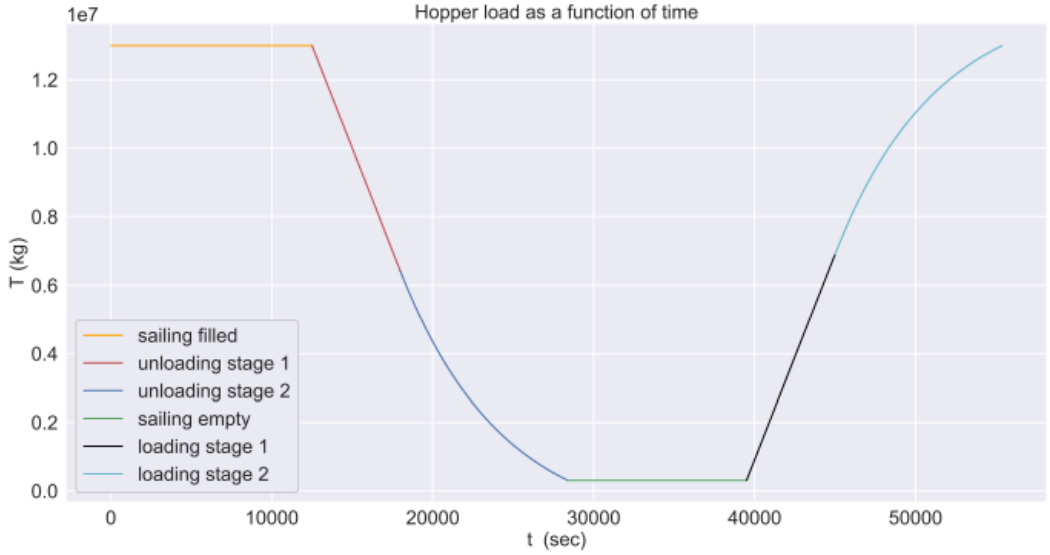

Figure 2.2: Hopper load as function of time (Van der Bilt, 2019)

Now that the process of a dredging cycle is explained, it is important to know what type of equipment is used per phase. Before determining which equipment is used per phase, the type of equipment itself is described.

Equipment

On board of the vessel different types of equipment are located that are used for different purposes. The equipment has a characteristic energy consumption and power production for a certain phase. Van der Bilt (2019) described each type of equipment in a clear way, which is represented in the following list.

- **Propulsion system**
  The propulsion system is used to accelerate and decelerate the vessel. It is also used to keep the vessel moving during free sailing. The characterized power percentages differ for speeding up, free sailing and slowing down. The propeller system is used during all phases. When (un)loading, the propulsion system is used to set the trailing speed.

- **Jet Pumps**
  Jet pumps are used to pump water under high pressure into the soil by means of a nozzle (Vosta, 2019). This loosens the soil which makes it able to import it onto the vessel. The jet pumps are used during loading and unloading. In the unloading stage, the material is used to liquidize the sand inside the vessel (Van der Bilt, 2019)

- **Thruster system**
  The thruster system is used to improve the manoeuvrability of the vessel by using a jet stream on each side of the vessel. This enables the vessel to not only move forwards or backwards but also to left and right. Thrusters are not used during sailing but only during dredging and dumping, where the main focus is on dumping as it uses the thrusters more than during the dredging process (Van Rhee, 2020).

- **Dredge pumps**
  The dredge pumps are used to transport the mixture of soil and water. The dredge pumps are only used during loading and unloading (Van Rhee, 2020). There are two types of dredging pumps: in-board dredging pumps and underwater dredge pumps (Van der Bilt, 2019). The inboard dredge pumps are used to transport the mixture inside the vessel, where underwater dredge pumps are used during dredging at large depths to deal with the underwater pressure.

- **Board net**
  The board net is the system that is in control of all other elements that require electricity on board. This contains small machines, lights, power outlet and other on board small equipment. It is operating during all stages of the dredging cycle.

To summarize, Table 2.1 provides an overview on which type of equipment is used per phase.

	Dredging	**Sailing full**	**Disposing**	**Sailing empty**
Propeller system	x	x	x	x
Jet Pumps	x		x	
Thruster system	x		x	
Dredge pumps	x		x	
Board net	x	x	x	x

Table 2.1: Equipment per phase

2.2 Variable Analysis

This section gives a vision on which factors play a role in estimating the energy consumption during a dredging project. First, a more clear vision is given on what a tender is based on. Certain factors that influence the energy consumption in each phase are mentioned and it is analyzed on what their part is when estimating the energy consumption in that phase. The relation between executing a phase and the CO2 production is emphasized.

A dredging contractor, like Van Oord, is able to create its own dredging strategy to execute a certain tender. However, there are limitations as the tender itself contains boundaries. These boundaries are set at the start of a tender and the contractor is not able to adapt them. Therefore these so-called *project aspects* are less important when determining which strategy is optimal (Van Rhee, 2020). However, it still has high priority to accurately estimate the factors that influence the energy consumption inside these *project aspects*. After determining the boundaries of the tender, the solution space for the contractor is defined. Inside this solution space, the contractor is able to optimally adapt its strategy. Factors that play a role in this are called *operational aspects*.

After performing a literature study, the *project aspects* and the *operational aspects* inside a tender are determined. A brief analysis on the contribution to the energy consumption of each factor within these aspects is given underneath. After the analysis, the current estimation method used by Van Oord is elaborated. Each phase is treated separately and important elements that are used during the estimation calculations are mentioned. The description of the aspects is described by Van der Bilt (2019).

Project Aspects

- **Sailing Distance**
  The sailing distance is considered as a pre-determined factor within a tender as it is prescribed where the material needs to be extracted and where to deposit it. The sailing route is then usually set on the shortest reachable distance between the two points if no restrictions are set. Keep in mind that this route does vary for different type of vessels as some particular vessels might not be able to sail the same route as others due to variations in depth. The length of the sailing distance influences the amount of energy that is consumed during the dredging project. A larger sailing distance requires a larger energy consumption. The existing variations for this factor are short, moderate or long distances. The specifications for these distinctions are elaborated in a further paragraph.

- **Excavation depth**
  Both the initial depth of the dredged material as the required depth is defined beforehand. For this factor it is important to notice that for different depths it might require different vessels to execute the dredging activity. This could result in a different energy consumption pattern. The larger the depth the more power is required to dredge the material inside the vessel, and thus the more energy is consumed.

- **Dredged material**
  The type of material has a large influence on the amount of power that is required to cut the soil. A distinction is made between coarse, moderate or fine sediments. The order of magnitude of power needed to dredge clay or sand is kPa, where cutting rock is considered to be in the order of MPa (Miedema, 2015). Also the transportation of the material is considered to require more energy for coarse material compared to relatively fine material (Van der Schrieck, 2015). The type of material is determined on beforehand and is therefore a *project aspect*. However, as it does contribute to the amount of energy that is required for the project, it is required to make an accurate estimation of the amount of energy needed. Another aspect is the overflow difference per material. The considered loss of fines during overflowing is expected higher than for coarse grains as the settling process of fines is much slower than for coarse grains. Therefore fine materials are lost faster when overflowing occurs (Miedema & Vlasblom, 1996).

Operational aspects

- **Sailing speed**
  As the use of a dredging vessel is combined with additional costs it is desired to sail at full speed to reduce the duration of a project. However, sailing at a lower speed is paired with lower energy consumption due to less drag force. Nowadays, estimation methods consider the vessels to always sail at full speed (if there are no speed restrictions). Despite, the sailing stage is not always on full speed as time is required for the vessel to speed up and slow down when departing and arriving. The duration and power required for speeding up and slowing down, even as sailing free, is related to the dimensions of the ship and its corresponding resistance (Segers, 2020).

- **Trail speed**
  The trail speed is defined as the speed at which the draghead moves when dredging the soil. In general the trail speed is set to the speed at which the production is the highest. Subsequently, the duration of filling the dredging vessel is minimized which causes reduction of costs. However, a higher trail speed also requires more energy. This is because a higher suction power is required for the material to be loaded onto the vessel due to a higher pipe resistance.

- **Unloading method**
  The three unloading methods that are mainly used are: Dumping, rainbowing and pipeline transport (Laboyrie et al, 2018). Dumping is done by opening the bottom doors of a dredging vessel and considered to be most efficient and most environmental friendly. However not all dredging vessels are able to perform dumping through bottom doors. Moreover dumping is not always possible as it cannot be done at very shallow depths. For pipeline transport the amount of energy required depends on the resistance of the pipeline which the pump has to handle. In addition, unloading can also be done using a combination of the unloading methods depending on what options are feasible considering parameters such as depth or distance.

- **Unloading production**
  In general the unloading production is set on the maximum production possible. For dumping through bottom doors it is not possible to change the unloading rate. For rainbowing and pipeline transport it possible to make adaptions in the unloading strategy. As already mentioned, unloading at the maximum velocity does demand the highest amount of power, and thus energy, due to the effect of resistance. Therefore this is not the optimal strategy (Van der Schrieck, 2015).

- **Loading rate**
  When determining the loading rate it is important to take the effect of overflowing into account. The loading process consists of three parts: Loading without overflow, loading with build up of water above overflow level and continuation of loading while overflowing occurs (Van Rhee, 2020). It is key to stop the dredging process on the right moment so that the amount of dredged incoming material is not lower than lost dredged material due to overflowing. The optimal moment is chosen with help of loading curves. However there are consequences on filling the vessel to its maximum capacity. First, the draught of the vessel is increasing with increasing load inside the hopper. This makes it more difficult to reach certain locations. Moreover, The vessel requires more power to reach the same speed when fully loaded, which results in a higher energy consumption.

- **Type of vessel**
  According to Van Rhee (2020) there are four type of TSHD's considering their size: small, medium, large and jumbo. The selection of the vessel size is important as small vessels require less energy but have to perform more dredging cycles to dredge the same amount of material where a larger vessel could execute the same process in less cycles. However, smaller vessels are able to reach shallower deposition locations where larger vessel might have to deposit their material by means of pipeline transport. It depends on the type of project which size suffices the best with an eye on energy consumption.

2.3 Estimation Methods for Energy Consumption

In this section, the importance of improvement of the current estimation methods is emphasized. Subsequently the current method is elaborated and the factors that play a role in estimating are highlighted. At last a literature study is done on which other possible estimation methods could be implemented that already exist. A comparison is made on the level of accuracy which gives insight on the form in which the eventual model is set.

2.3.1 VOHOP Estimation Method

The current estimation method for estimating energy consumption for a TSHD is an estimation tool developed by Van Oord that converts input characteristics into output values such as power production, energy consumption and fuel consumption. The name of the current method is VOHOP. The program uses the value of the Specific Fuel Consumption (SFC) for a certain type of fuel which has a characteristic value. VOHOP calculates the amount of fuel that is consumed by the following formula's where the minimum value is used:

$$F_{cycle} = P_{\%} * P_{max} * t_{cycle} * SFC \tag{2.2}$$

$$F_{max} = \alpha * P_{inst} * SFC \tag{2.3}$$

Where:

F_{cycle} = fuel consumption per cycle [l]

P% = power distribution percentage [-]

$P_{max,cycle}$ = maximum installed power [kW]

t_{cycle} = duration of a cycle [h]

SFC = fuel use in [l/kWh]

F_{max} = fuel consumption when all installed power is in use [l/h]

P_{inst} = total installed power [kW]

This results in the following formula:

$$F = min(F_{max}, (\frac{F_{cycle}}{t_{cycle}})) \tag{2.4}$$

Where F is the fuel consumption in [l/h]. Subsequently, the energy consumption is determined by dividing the fuel consumption by the SFC (which is the power) and multiplying with the required time, also formulated as:

$$E = P * t = P_{\%} * Pmax * t \tag{2.5}$$

After defining the energy consumption, it is important to determine in what way this energy estimation is done. Equation 2.2 and 2.3 show that the estimation (for fuel consumption) is based on the required power production and a certain percentage, a distribution factor, is added to the power consumption. A similar case is shown in Figure 2.3 (Van der Bilt, 2019). The percentage is added because the maximal pump power is not used in reality as efficiency losses cause a lower pump production to be executed. This percentage that is assigned to each power consumption is based on historical data per vessel and is a reference to a standardized dredging project. However in reality, dredging projects vary a lot from the standard situation. Therefore these estimations are inaccurate when variations occur. It is key to improve the estimation on the required power of a dredging cycle so that the energy consumption can be estimated without diverting from the actual power usage.

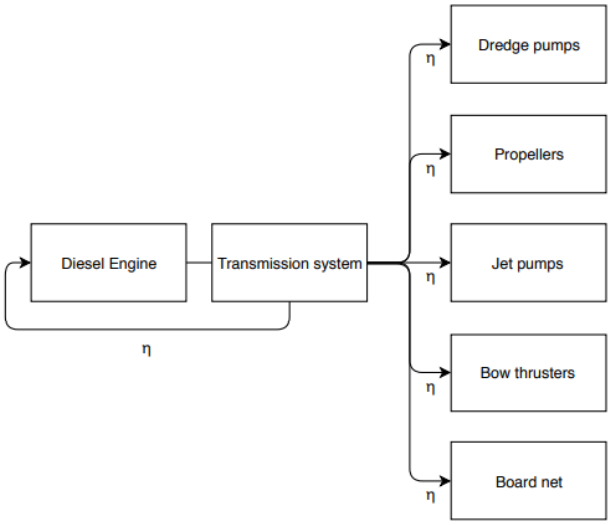

Figure 2.3: Efficiency of equipment (Van der Bilt, 2019)

As mentioned, VOHOP uses Equation 2.5 to estimate the energy consumption of a dredging cycle. The values of P_{max} and $P\%$ are set values as they are set per vessel in the estimation model of Van Oord. This causes deviations from actual results when making estimations, as the estimation is now only based on time, t. However, this research provides a methodology to achieve a more accurate estimation. This is done by analyzing which parameters play a role in determining time, t, and applying certain correction factors to the estimations. The analysis starts with defining the important parameters that play a role when calculating the time needed for a dredging cycle.

Inside the estimation tool for TSHD's, the parameters that define the time needed for a dredging cycle can be found. By tracing down the formulas that are used, multiple parameters are defined for each phase of the dredging cycle. In Table 2.2 each phase is shown and the parameters that play a role.

Parameter/Phase	Dredging	Sailing Full	Disposing	Sailing Empty
Dredging Depth	x		x	
Hopper Density	x		x	
Dmf	x		x	
Unloading Method	x		x	
Excavation Method	x		x	
Suction Velocity	x		x	
Loading Rate	x		x	
Trail Speed	x		x	
Sail Distance Full		x		
Sail Distance Empty				x
Sail Speed Full		x		
Sail Speed Empty				x
Available Pump Power			x	
Discharge Distance			x	

Table 2.2: Parameters per phase

2.3.2 Dredging Phase

In this paragraph the estimation of the dredging phase is elaborated for the current method Van Oord uses. As mentioned in Table 2.1, during the dredging phase all energy systems are in use. The total required energy during the dredging phase is then:

$$E_{dredge} = \sum_{i=0}^{n} t_{dredge} * (P_{propeller} + P_{jet} + P_{thruster} + P_{pump} + P_{board}) \tag{2.6}$$

At the moment, the estimation model is based on the power percentage shown in Equation 2.2. This percentage is based on historical data provided by Van Oord. However, as already mentioned, during the dredging phase the amount of power required depends on various parameters that vary for projects deviating from the standard dredging projects, shown in Table 2.2. The power usage that results from the distribution factors are shown underneath:

$$P_{prop} = P\% * P_{inst} \text{ kW} \tag{2.7}$$

$$P_{thrust} = P\% * P_{inst} \text{ kW} \tag{2.8}$$

$$P_{board} = P\% * P_{inst} \text{ kW} \tag{2.9}$$

$$P_{pump} = P\% * (P_{pump1} + P_{pump2} + ...) \text{ kW} \tag{2.10}$$

$$P_{jet} = P\% * P_{inst} \text{ kW} \tag{2.11}$$

With a set value for P % and P_{inst}, the total energy is retrieved by calculating the total time that is required for dredging. In order to calculate the energy for the dredging phase, the production rate executed by the dredging pumps must be found as the dredging time, t_{dredge}, depends on it. The dredging time is calculated as follows:

$$t_{dredge} = t_{suction} + t_{agitation} + t_{after,overflow} \tag{2.12}$$

The exact determination of the suction time ($t_{suction}$) and time after overflow ($t_{after,overflow}$) is left out as it is considered to be out of the scope of this research or the used equations are made confidential by Van Oord. However, a part of the determination is shown in the following paragraph by showing the suction formula, which is used to determine the suction time.

There are two factors where the maximum production in the dredging phase is limited by, either the available vacuum or the available jet production where the lowest value is the limiting factor. It is important to mention that a higher velocity does not always cause a higher production as resistance plays a role (Van der Schrieck, 2015). Figure 2.4 shows that for different situations, the maximum production is not found at the highest velocity, but at a point that is to be determined in the middle.

For a situation where the jet production is the limiting factor, one can reduce the vacuum as this will not change the limiting factor until it reaches the same level as the jet production. This causes the required head for the needed production to reduce (Van der Bilt, 2019). Following the highest point in the curve for different values of available vacuum results in the following graph (in this case for three different values)(Van der Bilt, 2019):

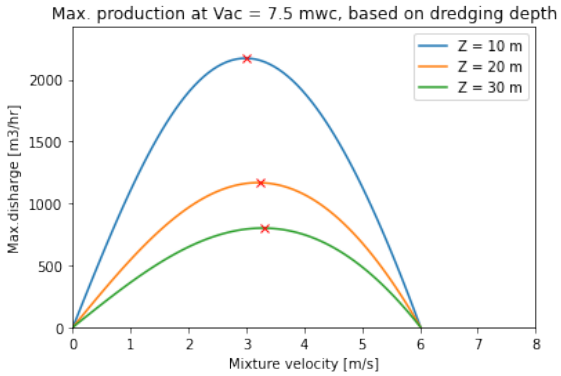

Figure 2.4: Production for varying velocities (Janssen, 2022)

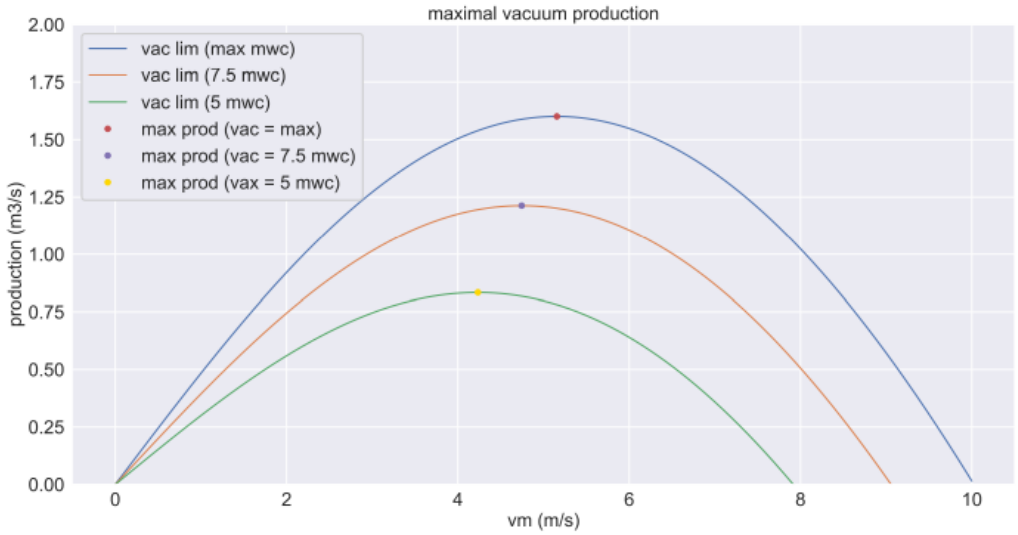

Figure 2.5: Maximal production (Van der Bilt, 2019)

If the same procedure of plotting the maximum production for every possible available vacuum is done, an optimal workline can be found for which the production is maximal. At this line the energy losses are minimal (Van der Bilt, 2019). The result is shown in Figure 2.6 at the yellow dot.

By combining the vacuum production equation with the jet production equation, one can find the work point of that specific vacuum. Eventually, the optimal production can be determined by calculating the maximum mixture density for which the given vacuum is able to deliver. This can be calculated by means of the 'suction formula' or 'vacuum formula' (Van der Schrieck, 2015):

$$Vac = (1 + \alpha + \xi_s + \lambda * \frac{L_s}{D_s}) * \frac{v_s^2}{2g} * \frac{\rho_m}{\rho_w} - (Z - A) * \frac{\rho_m}{\rho_w} - Z \tag{2.13}$$

Where:

Vac = available vacuum [mwc]

α = inlet loss factor [-]

ξ_s = resistance factor for non-straight parts [-]

λ = resistance factor straight parts [-]

L_s = length of suction pipe [m]

D_s = diameter of suction pipe [m]

v_s = suction velocity [m/s]

ρ_m = mixture density $[kg/m^3]$

Z = extraction depth [m]

A = depth of the submerged pump relative to the waterline [m]

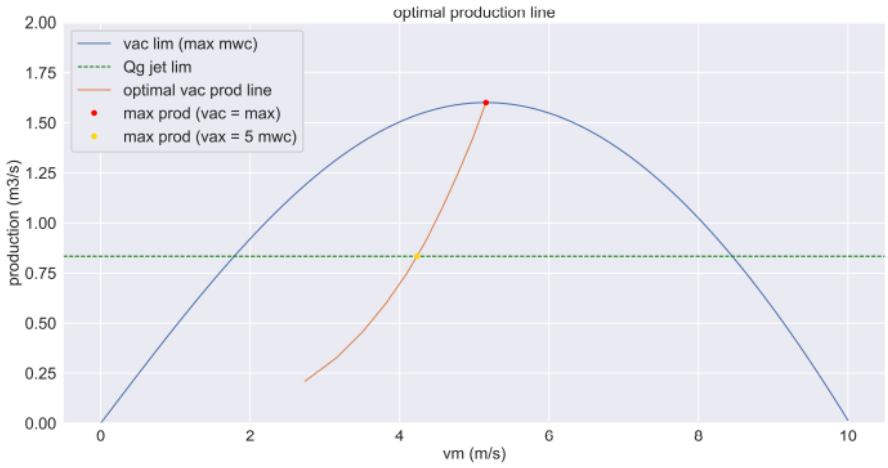

Figure 2.6: Production workline (Van der Bilt, 2019)

2.3.3 Disposing Phase

There are multiple ways of disposing the dredged material: dumping, pipeline transport and rainbowing. In this section the disposing method for dumping is first shortly described. Subsequently the disposing through pipeline transport and rainbowing is discussed.

Dumping

During the dumping stage the same equipment is used as during the dredging stage. The energy that is required can be expressed as follows:

$$E = \sum_{i=0}^{n} t_{dump} * (P_{prop} + P_{thrust} + P_{board} + P_{jet} + P_{ibp}) \tag{2.14}$$

Where the required power per equipment is set per vessel and the time is given in minutes. VOHOP uses a set percentage of the max installed power for that certain type of equipment. Each equipment type has its own percentage that is based on empirical data. However, if the situation changes (for example shorter distance) the percentage stays the same. This lead to the following equations:

$$P_{prop} = P\% * P_{inst} \text{ kW} \tag{2.15}$$

$$P_{thrust} = P\% * P_{inst} \text{ kW} \tag{2.16}$$

$$P_{board} = P\% * P_{inst} \text{ kW} \tag{2.17}$$

$$P_{ibp} = P\% * (P_{pump1} + P_{pump2}) \text{ kW} \tag{2.18}$$

$$P_{jet} = P\% * P_{inst} \text{ kW} \tag{2.19}$$

The time needed for dumping is considered to be t_{dump} = 900s or 15 min, with small fluctuations per project. This is significantly a shorter time than the time needed for other disposal methods. However, dumping is not always possible due to restrictions or inability to reach the disposal area.

Pipeline Transport and Rainbowing

The equation for energy consumption for disposing through pipeline transport is almost similar to the equation for dumping. However, the time required is dependent on other parameters and the percentages that were added to the required power differ from the situation where dumping occurs. For pipeline transport and rainbowing the formula to calculate the energy consumption is:

$$E = \sum_{i=0}^{n} t_{pipe} * (P_{prop} + P_{thrust} + P_{board} + P_{jet} + P_{pump}) \tag{2.20}$$

$$P_{prop} = P\% * P_{inst} \text{ kW} \tag{2.21}$$

$$P_{thrust} = P\% * P_{inst} \text{ kW} \tag{2.22}$$

$$P_{board} = P\% * P_{inst} \text{ kW} \tag{2.23}$$

$$P_{jet} = P\% * P_{inst} \text{ kW} \tag{2.24}$$

$$P_{pump} = P\% * (P_{dpump1} + P_{dpump2}) \tag{2.25}$$

The time required for pipeline transport depends on multiple parameters and can be divided into three parts:

$$t_{pipe} = t_{p,clean} + t_{p,bulk} + t_{clean} \tag{2.26}$$

Where:

$t_{p,clean}$ = pumping time cleaning quantity [min]

$t_{p,bulk}$ = pumping time bulk quantity [min]

t_{clean} = cleaning time pipeline [min]

Where pumping time cleaning quantity, $t_{p,clean}$, is the time needed for the pump to pump the total cleaning volume through the pipeline with a certain cleaning production. This is expressed as:

$$t_{p,clean} = \frac{V_{clean}}{P_{hop,c}} \tag{2.27}$$

Where cleaning volume depends on the total load (L_{tot}) inside the hopper and the bulk volume (V_{bulk}). The cleaning production rate of the hopper depends on the available pump power (P_{avail}) and the loading rate (LR). In equation form expressed as:

$$V_{clean} = L_{tot} - 250 - V_{bulk} \tag{2.28}$$

$$P_{hop,c} = MIN(\alpha * Pmax, P_{p,bulk}) = MIN(\alpha * Pmax, P_{available} * \sqrt{LR}) \tag{2.29}$$

for this equation a large number of parameters needs to be determined, which is beyond the scope of this research.

The pumping time bulk quantity is the time required to pump the bulk volume through the pipeline. This is calculated with a similar equation:

$$t_{p,bulk} = \frac{V_{bulk}}{P_{h,bulk}} = \frac{V_{bulk}}{P_{apump} * \sqrt{LR}} \tag{2.30}$$

At last, the cleaning time pipeline, depends on the discharge distance only:

$$t_{clean} = \frac{d_{disch} * \alpha}{300} \tag{2.31}$$

Which is 0 for rainbowing.

2.3.4 Sailing Phases

The estimation for energy consumption for the sailing stages are calculated with the same equations for sailing full as for sailing empty, with varying values for parameters. In the following equations the terms SU and SD express a parameter during Speed Up and Slow Down respectively.

$$E = P_{prop,SU} * t_{SU} + P_{prop,SD} * t_{SD} + P_{board} * t_{tot} + P_{prop,free} * (t_{tot} - t_{SD} - t_{SU}) \tag{2.32}$$

Speed up (SU)

$$E_{SU} = P\%_{SU} * P_{inst,prop} * t_{SU} = \frac{100 - P\%_{SD}}{2} + P\%_{SD} * P_{inst,prop} * t_{SU} \tag{2.33}$$

Where the values for the P% and $P_{inst,prop}$ are constant values for a vessel.

$$t_{SU} = \frac{Correction}{v} \tag{2.34}$$

Where the correction is applied for short distances. The correction is based on the speed of the vessel (v), the sailing distance, certain restrictions if present and the trail speed. The exact formula is:

$$Correction = MIN(GrossSpeed, \sqrt{(Speed * 60 * Distance)} + \frac{1}{2} * v\_trail) \tag{2.35}$$

Where the speed is set for a vessel. The distance and the trail speed is a varying parameter which changes per project and has an influence on the total time t. The gross speed is calculated by means of the following equation, in which the max speed is set for a vessel and in this research it is assumed that there are no restrictions:

$$Grossspeed = \frac{Distance}{Sailtimefullspeed + sailtimereducedspeed} * 60 = \frac{Distance}{\frac{Distance-(restrictions)}{MaxSpeed} * 60 + restrictions} * 60 \tag{2.36}$$

Slow Down (SD)

$$E_{SD} = P\%_{SD} * P_{inst,prop} * t_{SD} \tag{2.37}$$

Where the values for the P% and $P_{inst,prop}$ are constant for a vessel.

$$t_{SD} = \frac{Correction - v_{trail}}{v} \tag{2.38}$$

Free Sailing

For free sailing under speed restrictions:

$$P_{free} = ((0.1 * P_{inst,prop} * P\%_{free}) + \alpha * P_{inst,prop} * P\%_{free} * (\frac{GrossSpeed}{v_{max}})^3) \tag{2.39}$$

For free sailing under squat restriction:

$$P_{free} = (((0.1 * P_{inst,prop} * P\%_{free}) + \alpha * P_{inst,prop} * P\%_{free} * (\frac{GrossSpeed}{v_{max}})^3)) * \frac{P_{inst,prop} * P\%_{free}}{\sqrt{P_{inst,prop} * P\%_{free}}} \tag{2.40}$$

For no restrictions:

$$P_{inst,prop} * P\%_{free} \text{ kW} \tag{2.41}$$

The equations that express the value for the gross speed are mentioned in Equation (2.36). The values for the installed power and the power percentages are set values for a vessel.

$$t_{tot} = \frac{d_{tot} - d_{SU} - d_{SD}}{Correction} * 60 + t_{SU} + t_{SD} \tag{2.42}$$

Where the distance, d, differs for sailing empty and sailing full depending on whether a certain sailing route is possible to sail with a loaded hopper.

$$d_{SD} = \frac{Correction + v_{trail}}{2} * t_{SD}/60 \tag{2.43}$$

$$d_{SU} = \frac{Correction}{2} * t_{SU}/60 \tag{2.44}$$

Board Net

$$E_{board} = P\% * P_{inst,board} * t_{tot} \tag{2.45}$$

2.3.5 VOHOP Estimation Assessment

The current method that is used by Van Oord is analysed per phase in the previous paragraphs. The method uses a distribution factor (P%) that is based on empirical data as a correction factor on the installed power. However, with the complex dredging situations that arise, a method that estimates energy based on physical relations instead of empirical relations might result in more accurate results. To explain some more, a method where required power is a function of depth and distance might give a more representative result in combination with the empirical factors that are already used.

It is important to notice that there is a large difference in amount of parameters taken into account per phase. For the dredging and disposing phase a relatively large amount of parameters is taken into account. Therefore this estimation is considered to be more elaborate. The sailing phases are based on a relatively small a amount of parameters. It is key to find out whether the estimation method is inaccurate because of these less elaborate estimations for the sailing phases. However, the estimation does take a difference in acceleration, free sailing and slowing down into account.

2.4 Alternative Estimation Methods

There are several estimation methods for estimating the amount of energy during a dredging cycle. This section describes certain methods and gives an overview of what parameters are taken into account for the different methods. Subsequently some advantages and disadvantages are given for each method.

International Maritime Organization

Due to the challenging targets that are set by the European Union on the emission of GHG, the International Maritime Organization (IMO) is forced to introduce measures to reduce the emission patterns. Therefore a CO_2 index is developed to indicate, and thus estimate, the amount of GHG emission a certain vessel has. The index is named Energy Efficiency Design Index (EEDI) (Van de Ketterij & Stapersma, 2009). The EEDI is set to determine whether certain vessels are allowed to operate at certain locations. The index is formulated in the following way with main engine (ME) and auxiliary engine (AE)(Van de Ketterij & Stapersma, 2009):

$$EEDI = \frac{(\sum C_{FME} * SFC_{ME} * P_{ME}) + P_{AE} * C_{AE} * SFC_{AE}}{Deadweight * V_{ref}} \tag{2.46}$$

Where:

C_F = conversion factor between fuel consumption and CO2 emission [-]

SFC = specific fuel consumption [g/kWh]

P = average power consumption [kW]

V_{ref} = vessel speed [m/s]

$EEDI$ = Energy Effeciency Design Index [g CO_2/ tonne m]

The EEDI is developed to give an estimation on the amount of GHG emission a vessel has. However, the method has some drawbacks. For example, the formula expresses the benefit of a certain (dredging) activity in terms of deadweight and speed. As some dredging vessels only perform the dredging activity such as a Cutter Suction Dredger (CSD), this formula is inapplicable because the CSD leaves the transportation of the material to other vessels (Van de Ketterij & Stapersma, 2009). Another disadvantage is that the method focuses only on the free sailing part of the energy consumption, while other phases can also have a large share in the energy consumption. An energy index based only on the free sailing part cannot make a distinction between ships that carry out other dredging phases in an energy efficient way and ships that do so less efficiently (Van de Ketterij & Stapersma, 2009). Van de Ketterij & Stapersma (2009) offer a number of recommendations to ensure that the EEDI index gives a better reflection on reality. For a TSHD, this means that all phases of a dredging process should be included in the calculation and considered separately. In addition, a standard situation should be created from which the index can be derived.

Top-down and Bottom-up approach

The main methodologies for estimating ship emissions are top-down and bottom-up approach (Miola, 2011). The top-down approach calculates the energy consumption without considering the vessels' characteristics (Miola, 2011). The bottom-up approach is based on data collected from the Automatic Identification System (AIS). Therefore estimations conducted based on this approach have a higher space-time resolution because the estimate is based on ship static and dynamic information such as fuel type, ship speed, ship dimensions and location. To elaborate a bit more on AIS data: AIS data contains static and dynamic information. Static information contains the vessel type and length. Dynamic information includes the vessel its position, speed and duration. Due to the short transmission time for an AIS system, the emission pattern of a vessel can be estimated quite accurately. By applying extrapolation and interpolation methods, gaps in the AIS data can be filled in (Weng, 2020). Previous studies have shown that the bottom-up approach, which uses the AIS data, have proven the reliability of the emission estimates (Weng, 2020). As the top-down approach is considered less accurate than the bottom-up approach, only the bottom-up approach will be elaborated further. Although the estimation of energy consumption with the bottom-up approach is considered to be more accurate than others, there are disadvantages to this method: There are certain areas where an AIS system does not work completely and it is not always suitable to use AIS to estimate CO_2 emissions in ports. Finally, AIS data may not be detected if the vessel has to travel long distances. While this is not often the case for dredging vessels, it is important to take into account (Miola, 2011).

STEAM method

The Ship Traffic Emission Assessment Model (STEAM) is a hybrid of the top-down method and the bottom-up method (Goldsworthy & Goldsworthy, 2013). It displays high spatial and temporal resolution and can calculate emissions based on AIS data, ship information and power-based emission information (Weng, 2020). The equation that is applied in the STEAM method according to Weng (2020) is:

$$E_{i,j,k,l} = \sum P_j * LF_{j,l} * T_{j,k,l} * EF_{i,j,k}/10^6 \tag{2.47}$$

Where:

E = ship pollutant emissions [tonne]

i = emission substance

j = engine type ME, AE and boiler

k = fuel type

l = navigational status of the vessel

P = installer power [kW]

LF = load factor

T = operating time [hr]

EF = emission factor of pollutants [g/kWh]

The STEAM model is considered as a realistic estimate because it also reflects the relationship between delivered power and instantaneous speed. The model takes into account an additional calculation of the load factor, LF, through direct observation by AIS data (Moreno, 2015). The estimation method is comparable to the current estimation method. Nevertheless, the STEAM model only shows the emission value during free sailing, while acceleration and deceleration also plays a role and other phases during the dredging process have to be taken into account.

Bolt Method

The method proposed by Bolt (2003), is an estimation method for Inland Waterway Transport (IWT). The total power that is used by the vessel is based on the resistance that is acting on the vessel. The resistance terms are divided into three parts: frictional resistance, wave resistance and residual resistance. The estimation is based on the velocity of the vessel and the resistance it has to overcome. An advantage of this method, opposed to other methods that take resistance into account, is the enhancement of resistance for limited water depths. This enhancement is caused by an increase of current for a shallower situation:

$$u = \frac{A_m/A_c}{(1 - A_m)/(A_c - F_{nh}^2)} * V \tag{2.48}$$

With:

u = return current velocity [m/s]

A_m = area of immersed midship Section [m^2]

A_c = cross-section of the waterway [m^2]

V = velocity of the vessel [m/s]

F_{nh} = Froude number based on depth [-]

h = water depth [m]

With this advantage of taking into account currents, the method also has some disadvantages. Some of the disadvantages, as proposed by Bolt have to do with the difference between IWT vessels and seagoing vessels. This is of great importance for this research, as the dredging vessels are seagoing vessels. Some disadvantages (Bolt, 2003), are:

- This method is strictly applicable for IWT, as seagoing vessels sail with a larger velocity, that increases the significance of the wave resistance.

- The shape of an IWT vessel is more prismatic than for a seagoing vessel
- Seagoing vessels normally sail through deep and wide waters, where IWT transport concerns more shallow and small waterways.
- Seagoing vessels experience more resistance due to the appearance of waves at deep waters, higher wind velocities and a larger wind scope.

Holtrop & Mennen Method

The method proposed by Holtrop & Mennen (1982) can give an insight on how estimations for dredging vessels should be done. This method calculates the energy consumption of a vessel based on the speed, its dimensions and the fairway characteristics. By calculating the encountered resistance acting on the vessel for a certain speed, the consumed power and energy is determined. To start with, the standard values that can be measured for a certain vessel are required such as: length (Ls), beam (B), draught (T), speed (Vs) and the characteristic values of the waterway: water depth (h0) and ambient current (Uc). With these values the underwater resistance can be calculated and with this the necessary power a vessel has to deliver can be determined. From the required power the fuel consumption can be calculated. Finally, the fuel consumption can then be translated into emissions (Van Koningsveld, 2021; Segers, 2020). Figure 2.7 gives an overview of the steps taken in this method.

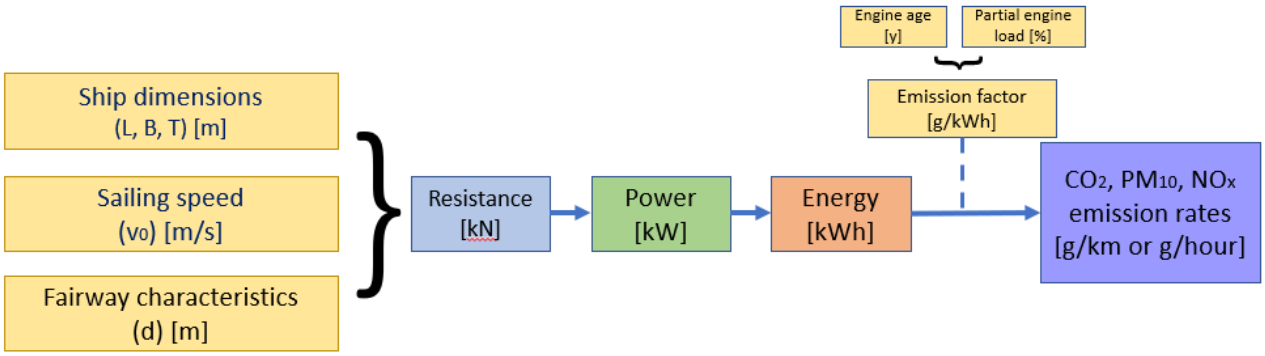

Figure 2.7: Holtrop and Mennen methodology on estimating emissions (Segers, 2020)

The resistance was determined using the method described by Holtrop & Mennen (1982). This method takes into account a number of parameters such as speed, surface area, Reynolds number, flow and vessel dimensions. In addition, empirical data is used, which gives the method a realistic picture (Van Koningsveld, 2021; Segers, 2020). However, this method is very detailed and will be discussed in more detail in a later section. Once the resistance is determined the steps to the required power and the final emission are relatively simple. The power is calculated by multiplying the total resistance by the vessel speed. The energy consumption is then calculated by multiplying the total power by the total time. Despite the advantage that many parameters are taken into account for this approach, the estimation can only be applied for the transportation of the vessel and does not include the loading and unloading phase. Nonetheless it does give an indication on the energy consumption of IWT vessels when stationary (Van Koningsveld, 2021). This gives some insight on the energy consumption of a dredging vessel, although a dredging vessel requires a much higher amount of energy due to the activity it is performing when stationary and due to the shorter duration of loading/unloading for IWT, where dredging vessels have a longer loading duration.

Modifications

The method proposed by Holtrop & Mennen is already modified in different forms of which two of them are shortly described to give an idea of what corrections exist, and why they are proposed.

- **Zeng (2018)**
  The modification proposed by Zeng is applied to the frictional resistance calculation. The correction implies an enhancing effect on resistance for limited water depths. The correction is applied on designated regions that are based on the waterline length of the vessel in relation with the difference between the water depth and the draught of the vessel:

$$(h - T)/L_{wl} \tag{2.49}$$

The method proposed Zeng introduces a correction that is applied on the friction coefficient, C_f (Zeng, 2018). The exact correction is explained further in this research.

- **Karpov (Rotteveel, 2013)**
  The modification proposed by Karpov is applied on the wave resistance terms and the residual resistance terms of the Holtrop & Mennen (1982) calculation. It takes into account a different velocity value to calculate with for different values of the Froude number based on depth and the relation between depth and the draught of the vessel. A limited depth will enhance the resistance terms, resulting in a higher overall velocity.

In the mentioned corrections, the main focus is on limited depth profiles. The result of the applied correction will be shown further in this research.

2.5 Conclusion

The literature study conducted in this chapter has shown the factors involved in determining an estimate to the amount of energy consumption. The factors could be divided into project aspects and operational aspects where the former includes standard boundaries and the latter includes the solution space for the contractor. In addition, the literature study gives a view on what a dredging cycle looks like and what phases of a dredging cycle exist. By describing which type of equipment is used per phase, a clear overview is given on the whole dredging process. The first sub-question is answered by giving a clear overview on what a dredging cycle is based on and mentioning which factors play a role during a dredging process. It also gives insight in which parameters might be important in forming an estimation model such as water depth, sailing distance, hopper density and suction velocity (as mentioned in Table 2.2).

After analyzing these factors, the estimation for each phase inside the dredging cycle was investigated for the current estimation method. It is shown that the estimation for the dredging phase and the disposing phase are more elaborated than the sailing phases, where only a sailing distance and sailing speed play a role. This highlights the existing gap in the current estimation method for the sailing stages. By explaining the estimation pattern for each phase for the current estimation method, the second sub-question is also answered. Following this, a number of existing estimation methods were named and elaborated. Mainly the STEAM model, the approach mentioned by Bolt (2003) and Holtrop & Mennen (1982) are considered as useful methods for giving insight on developing an estimation model as these methods include either more parameters (like resistance which is in its place based on velocity, depth and vessel characteristics) or make use of static and dynamic data. The main conclusion regarding the literature study on existing methods is that there is currently no general estimation model for dredging phases other than the sailing phases. Moreover, the estimation methods do not take acceleration and deceleration into account. By naming the current method and describing the existing methods briefly, the third sub-question is also answered.

The literature study and the analysis on the current estimation method, paired with the alternative estimation methods, highlights the gap in literature on the estimation models.The current method is detailed for determining the energy consumption during the dredging stage and the disposing stage with many different parameters taken into account. However, the estimation for the sailing stages only takes a low amount of parameters into account as shown in Table 2.2. Where the current method only mentions speed and distance, other alternative methods take more parameters into account with as significant parameter the factor of resistance. However, on the other side, these alternative methods are mainly based on only the sailing stages and do not take into account that a sailing stage does exist out of three stages, speeding up, free sailing and slowing down. Where the current method misses extra information for the sailing stages but does take acceleration en deceleration into account, for the alternative methods it is the other way around. The method proposed by Holtrop & Mennen (1982) is considered to be a method with potential to be more accurate. The reason for leaving out the STEAM method and the method proposed by Bolt (2003), is because for the estimation method that is chosen it is important to take into account the resistance terms as this factor is increasingly important for seagoing vessels, especially the wave resistance (Bolt, 2003). The reason that the Holtrop & Mennen approach is selected prior to the method proposed by Bolt, is because Bolt mentions that for estimating the energy consumption for one particular vessel is not applicable for that estimation method. Besides, the approach is not applicable for more detailed calculations of energy consumption (Bolt, 2003). Therefore, in the next chapter a more elaborate analysis is done on the VOHOP estimation and on the Holtrop & Mennen method. The focus is on analysing both methods zoomed in on the sailing stages only, as these represent a large gap for VOHOP and Holtrop & Mennen. It is key to determine which method is more accurate based on historical data so that subsequently an improvement of the estimation method can be done in order to increase accuracy.

3 | Estimation Analysis

In this chapter, the VOHOP estimation method for the sailing phases is evaluated and compared with the method proposed by Holtrop & Mennen. Important parameters are highlighted and taken into account within the comparison. The estimation models are used as input for a simulation through OpenCLSim and a simulation is given. By doing this, the input for the to-be-created simulation model is formed, which contributes to the first part of the fourth sub-question:

(iv.) How to **develop** and validate a model to evaluate and improve the estimation of energy consumption?

3.1 Holtrop & Mennen

In this section the estimation method used by Holtrop & Mennen (1982) for energy consumption is described in more detail. Keep in mind that only the energy consumption for sailing stages is taken into account. The calculation method for determining power usage that is proposed by Holtrop & Mennen (also mentioned as HM in this research) is shown. Subsequently some modifications are mentioned that are applied to the method to make it more accurate for certain situations. With Equation (2.5) already mentioned, the total power that is used during sailing is divided into two parts (Segers, 2020):

$$P_{tot} = P_{board} + P_{propulsion} \tag{3.1}$$

Where the P_{board} can be defined as:

$$P_{board} = 0.05 * P_{inst} \tag{3.2}$$

After defining the required power for the board net, only the required power for propulsion is needed. The power needed for a ship to reach a certain velocity depends on the resistance that acts on the vessel (Segers, 2020). The propulsion power must overcome the resistance of the vessel to induce movement. However, the calculation for the total resistance is divided into multiple parts. This section will treat each part separately. In essence, the formula for the effective power, the power needed to travel with a certain speed overcoming resistance, is given underneath:

$$P_e = V_0 * R_{tot} \tag{3.3}$$

Where:

P_e = effective power [kW]

V_0 = vessel speed [m/s]

R_{tot} = total resistance [kN]

The factor of resistance is a complex factor and there are multiple methods to calculate this value because it depends on a high number of parameters. For this research, estimating the resistance is done by means of the method developed by Holtrop and Mennen (1982):

$$R_{tot} = R_F(1 + k_1) + R_{APP} + R_W + R_B + R_{TR} + R_A \tag{3.4}$$

Where:

R_F = frictional resistance according to the ITTC-1957 friction formula [kN]

$1 + k_1$ = form factor describing the viscous resistance of the hull form in relation to R_F [-]

R_{APP} = resistance of appendages [kN]

R_W = wave-making and wave-breaking resistance [kN]

R_B = additional pressure resistance of bulbous bow near the water surface [kN]

R_{TR} = additional pressure resistance of immersed transom stern [kN]

R_A = model-ship correlation resistance [kN]

The resistance parameters can be divided into four parts: friction, waves, pressure and residual. The total resistance is calculated by adding these values together. In the following sections each individual resistance component will be discussed.

3.1.1 Resistance due to friction

In this section the factors that play a role in the resistance due to friction are explained and calculated. Besides the skin friction that acts on the vessel, the viscosity and any appendages also have an influence. The resistance due to friction is therefore expressed as:

$$R_{friction} = R_F(1 + k_1) + R_{APP} \tag{3.5}$$

Frictional resistance R_F

A prediction of the frictional resistance can be done by using a function of the Reynolds number (Roh, 2017). The frictional resistance is assumed to act the same as resistance of an equivalent flat plate of the same area and length as shown in Figure 3.1.

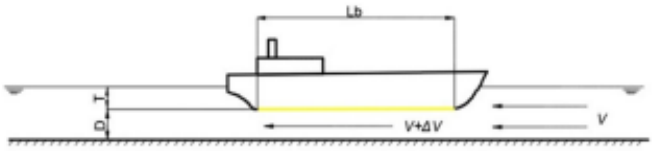

Figure 3.1: Schematisation of flat area (Segers, 2020)

This leads to the following equation.

$$R_F = \frac{1}{2}\rho C_F S_T V^2 \tag{3.6}$$

Where:

ρ = density of sea water $[kg/m^3]$

C_F = frictional resistance coefficient [-]

S_T = wetted surface area of the vessel $[m^2]$

V = vessel speed [m/s]

First the frictional resistance coefficient, C_F, is treated. According to the International Towing Tank Conference (ITTC), the value of the frictional resistance coefficient can be calculated by (ITTC, 2002):

$$C_F = \frac{0.075}{(\log R_e - 2)^2} = \frac{0.075}{(\log \frac{V * L_a}{\nu} - 2)^2} \tag{3.7}$$

Where:

R_e = Reynolds number [-]

V = vessel speed [m/s]

L_a = length of vessel at waterline [m]

ν = kinematic viscosity $[m^2/s]$ ($\approx 1 * 10^{-6}$)

However, according to Zeng (2018), the value for C_f also depends on the depth and the dimensions of the vessel. Therefore a correction is used for calculating C_f, which uses three different type of values for C_f according to the situation and its depth consisting of: C_{deep}, C_{F0} and $C_{shallow}$. Where C_{F0} is the method as Equation (3.7) proposes. However a correction is used, for a situation where (d-T)/L_{wl} > 1::

$$C_f = C_{F0} + (C_{deep} - C_{katsui}) * \frac{S_B}{S_T} \tag{3.8}$$

and for situations where (d-T)/$L_{wl} \leq 1$:

$$C_f = C_{F0} + (C_{shallow} - C_{katsui}) * \frac{S_B}{S_T} * (\frac{V_B}{V})^2 \tag{3.9}$$

Where:

S_B = area of flat bottom [m^2]

C_{katsui} = Katsui friction coefficient [-]

$C_{shallow}$ = shallow friction coefficient [-]

C_{deep} = deep friction coefficient [-]

V_B = velocity under vessel taking shallow water effects into account [m/s]

The Katsui coefficient is determined by the following equation (Zeng,2018):

$$C_{katsui} = \frac{0.0066577}{(log(R_e) - 4.3762)^a} \tag{3.10}$$

Where the coefficient 'a', is calculated as (Zeng, 2018):

$$a = 0.042612 * log(R_e) + 0.56725 \tag{3.11}$$

Next, the deep and shallow frictional coefficient C_{deep} and $C_{shallow}$ are calculated as (Zeng, 2018):

$$C_{deep} = \frac{0.08169}{(log(R_e) - 1.717)^2} \tag{3.12}$$

$$C_{shallow} = \frac{0.08169}{(log(R_e) - 1.717)^2} * (1 + (\frac{0.003998}{(log(R_e) - 4.393) * ((d-T)/L_{wl})^{-1.083}} \tag{3.13}$$

At last, the velocity under the vessel with shallow water effects taken into account, V_B, is for d/T $\leq$ 4 (Zeng, 2018):

$$V_B = 0.4277 * V * e^{(d/T)^{-0.07625}} \tag{3.14}$$

Otherwise, V_B = V. With the vessel speed and depth as variable and the length of the vessel as set for the TSHD, the frictional resistance coefficient can be determined. However, when investigating the influence of different depths for the energy consumption of a vessel, the modification proposed by Zeng (2018) is not of much influence regarding the TSHD. As the Zeng (2018) equation is based on the relation (d-T)/$L_{wl} < 1.0$, the scope of this research will always fulfill this requirement as depths with a maximum value of -60 meters are observed and the length of the vessel is above 100 m (which causes the equation to always end up lower than 1.0).

The wetted surface area of the vessel, S, can be calculated by the following equation according to Holtrop & Mennen (1982):

$$S = L_a(2T + B)\sqrt{C_M}(0.453 + 0.4425C_B - (0.2862C_M) - (0.003467\frac{B}{T}) + 0.3696C_{WP}) + 2.38\frac{A_{BT}}{C_B} \tag{3.15}$$

Where:

L_a = length of the vessel at waterline [m]

T = draught of the vessel [m]

B = width of the vessel [m]

C_M = midship section coefficient [-]

C_B = block coefficient [-]

C_{WP} = water plane area coefficient [-]

A_{BT} = wet transverse sectional area of the bulb [m^2]

Where the block coefficient is 0.85 according to Vlasblom (2007) for dredge vessels. The block coefficient of a vessel is the ratio of underwater volume of the vessel to the volume of a rectangular block having the same overall lengths. To visualize this, Figure 3.2a gives an illustration of the ratio (Jassal, 2022).

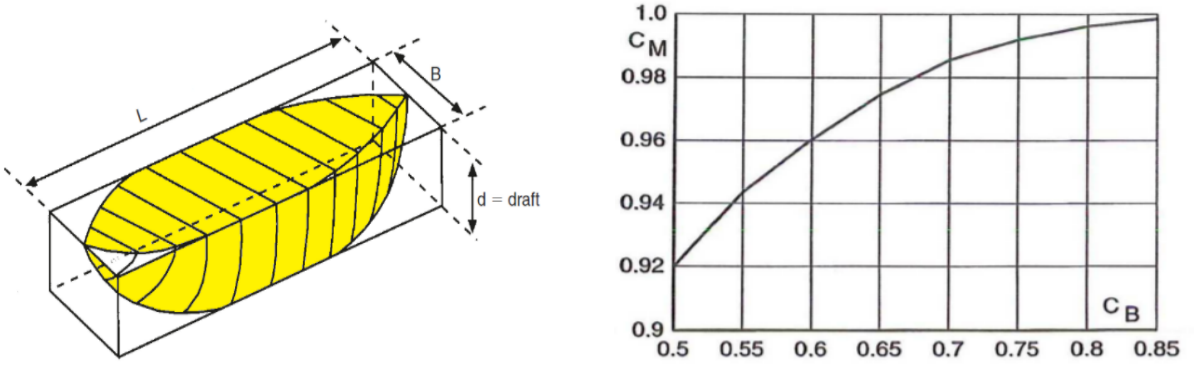

(a) Visualization of block coefficient (Segers, 2020) (b) Midship coefficient (Bertram & Schneekluth, 1998)

Figure 3.2: Resistance coefficients

The midship section coefficient, C_M is the ratio between the area of a midship section that is actually under the water surface and that of a rectangle with the same depth and width (Wartsilia, 2022). According to Betram & Schneekluth (1998), the midship section coefficient is dependant on the value of the block coefficient as shown in Figure 3.2b. Therefore with a value of 0.85 for C_B, the value for C_M is ≈ 1.

The water plane area coefficient, C_{WP}, can be calculated with the known value for the block coefficient (Bertram & Schneekluth, 1998). The coefficient is defined as the ratio between the waterplane area and that of a rectangle with the same length and width. A calculation method that is used to calculate the value of the water plane coefficient is (Bertram & Schneekluth, 1998):

$$C_{WP} = \frac{(1 + 2C_B)}{3} \tag{3.16}$$

At last, the wet transverse sectional area of the bulb, A_{BT}, is defined. The bulbous bow is a round protrusion at the stern of the vessel, see Figure **??**. It helps to reduce the drag by inducing the flow around the hull. This reduces the resistance acting on the ship (Chakraborty, 2021). According to Ventura (2022), the formula for A_{BT} is:

$$A_{BT} = C_{BB} * B * T * C_M \tag{3.17}$$

Where a typical value for C_{BB} is ≈ 0.2. With the previous equations, the value of R_F can now be determined.

Viscous resistance, $(1 + k_1)$

The form factor, $(1+k_1)$, describes the viscous resistance of the hull in relation to the frictional resistance. The value of the form factor can be expressed as (Roh, 2017):

$$1 + k_1 = 0.93 + 0.487118 * C_{14}(\frac{B}{L_a})^{1.06806} * (\frac{T}{L_a})^{0.46106} * (\frac{L_a}{L_R})^{0.121563}(\frac{L_a^3}{\nabla})^{0.36486} * (1 - C_P)^{-0.60247} \tag{3.18}$$

Where:

C_P = prismatic coefficient [-]

L_R = length of run [m]

∇ = displacement of water [m^3]

C_{14} = coefficient based on C_{stern} of TSHD [-] (≈ 1)

The value for ∇, the volume of displaced water, can be calculated by:

$$\nabla = C_b * B * T * L_a \tag{3.19}$$

The prismatic coefficient, C_P can be expressed as the ratio of the volume of displacement to the volume of a prism having a length equal to the length between perpendiculars and a cross-sectional area equal to the midship sectional area (Rawson, 2001). According to Holtrop & Mennen (1982), it can be described as:

$$C_P = \frac{C_B}{C_M} \tag{3.20}$$

With the value for C_P known, the length of the run, L_R, can be defined. This is done by the following equation (Roh, 2017):

$$\frac{L_R}{L_a} = 1 - C_P + \frac{0.06 C_P * l_{cb}}{4C_P - 1} \tag{3.21}$$

In this equation, the value for l_{cp} also referred to as the longitudinal position of the center of buoyancy (either forward (+) or afterward (-)), can be described by the following equation (Segers, 2020):

$$l_{cb} = -13.5 + 19.4 C_P \tag{3.22}$$

The value of the viscous resistance can now be determined by using the above equations.

Resistance of appendages, R_{APP}

The appendage resistance is a frictional resistance factor, that usually is considered small (in the order of 10 times smaller than the frictional resistance)(Rawson, 2001). The formula that expresses the appendage resistance is (Roh, 2017):

$$R_{APP} = \frac{1}{2} \rho C_F S_{APP} V^2 (1 + k_2) \tag{3.23}$$

Where k_2 depends on the combination of appendages that differs per ship. The different combinations that exist are given in Appendix A. However for simplicity the value for k_2 is determined as 2.5 (Segers, 2020). The value for S_{APP} is estimated to be approximately 10% of the total wetted area S (Rawson, 2001).

3.1.2 Wave resistance, R_W

The wave resistance, R_W, is dependant on the size and shape of the hull. During the sailing stages, the vessel creates waves that act as resistance on the vessel. Higher waves, generated by a higher velocity, result in higher resistance (Segers, 2020). As the Froude number, F_n, is dependant on the velocity of the ship, this equation has changing variables related to the velocity. Before determining the changing variables, the Froude number is determined (Navalapp, 2022):

$$F_n = \frac{V}{\sqrt{g L_w}} \tag{3.24}$$

The wave resistance is then determined from:

$$R_W = c_1 c_2 c_5 \nabla \rho g * exp(m_1 F_n^{-0.9} + m_2 * cos(\lambda F_n^{-2})) \tag{3.25}$$

With:

$$c_1 = 2223105 * (c_7 * *3.78613) * ((T/B) * *1.07961) * (90 - i_E) * *(-1.37165) \tag{3.26}$$

For $B/L_{wl} < 0.11$:

$$c_7 = 0.229577 * (B/L_w l) * *0.33333 \tag{3.27}$$

For $B/L_{wl} > 0.25$:

$$c_7 = 0.5 - 0.0625 * (L_w l/B) \tag{3.28}$$

And for $0.11 < B/L_{wl} < 0.25$:

$$c_7 = B/L_w l \tag{3.29}$$

Further, where:

$$c_2 = exp(-1.89 * \sqrt{c_3}) \tag{3.30}$$

$$c_5 = 1 - (0.8 * A_T)/(B * T * C_M) \tag{3.31}$$

In these expressions c_2 is a parameter which accounts for the reduction of the wave resistance due to the action of the bulbous bow. Similarly, c_5 expresses the influence of a transom stern on the wave resistance. In the

expression A_T represents the immersed part of the transverse area of the transom at zero speed (Holtrop & Mennen, 1982). The other parameters can be determined from the following equations. For L/B $<$ 12:

$$\lambda = 1.446C_P - 0.03L/B \tag{3.32}$$

For L/B $>$ 12:

$$\lambda = 1.446C_P - 0.36 \tag{3.33}$$

Further, where:

$$m_1 = 00140407L/T - 1.75254\nabla^{1/3}/L + -4.79323B/L - c_{16} \tag{3.34}$$

With, for $C_P < 0.8$:

$$c_{16} = 8.07981C)P - 13.8673C_P^2 + 6.984388C_P^3 \tag{3.35}$$

For $C_P > 0.8$:

$$c_{16} = 1.73014 - 0.7067C_P \tag{3.36}$$

Further, where:

$$m_2 = c_{15}C_P^2 * exp(-0.1F_n^{-2}) \tag{3.37}$$

In these equations, the coefficient c_{15} is equal to -1.69385 for $L^3/\nabla < 512$, whereas $c_{15} = 0.0$ for $L^3/\nabla > 1727$. For values of $512 < L^3/\nabla < 1727$, c_{15} is determined from:

$$c_{15} = -1.69385 + (L/\nabla^{1/3} - 8)/2.36 \tag{3.38}$$

The half angle of entrance, i_E, is the angle of the waterline at the bow in degrees with reference to the centre plane but neglecting the local shape at the stem (Holtrop & Mennen, 1982). If i_E is unknown, use can be made of the following formula:

$$i_E = 1+89*exp(-((L_{wl}/B)^{0.80856})*((1-C_{wp})^{0.30484})*((1-C_p-0.0225*lcb)^{0.6367})*((L_R/B)^{0.34574})*((100*\nabla/(L_{wl}^3))^{0.16302})) \tag{3.39}$$

This formula, obtained by regression analysis of over 200 hull shapes, yields i_E values for exceptional combinations of hull-form parameters (Holtrop & Mennen, 1982). The coefficient that determines the influence of the bulbous bow on the wave resistance is defined as:

$$c_3 = (0.56 * A_{BT}^{1.5})/(B * T * (0.31 * \sqrt{A_B T} + T_F - h_B)) \tag{3.40}$$

Where h_B is the position of the centre of the transverse area A_{BT} above the keel line and T_F is the forward draught of the ship (Holtrop & Mennen, 1982). In this way, the wave resistance can be determined.

3.1.3 Pressure resistance

The total resistance that is formed due to pressure consists of two factors: resistance due to the bulbous bow and resistance due to the immersed transom stern. This leads to the following expression:

$$R_{pressure} = R_B + R_{TR} \tag{3.41}$$

Resistance due to bulbous bow, R_B

A bulbous bow creates resistance by the pressures that acts on the water surface. The amount of resistance of dependant on the shape of the bulbous bow. The resistance can be expressed as (Roh, 2017):

$$R_B = \frac{0.11exp(-3P_B^{-2}) * F_{ni}^3 A_{BT}^{1.5} \rho g}{1 + F_{ni}^2} \tag{3.42}$$

Where:

P_B = coefficient for the emergence of bulbous bow [-]

F_{ni} = Froude number based on immerion of bulbous bow [-]

The values for P_B and F_{ni} can be calculated with the following equations respectively:

$$P_B = \frac{0.56\sqrt{A_{BT}}}{T_F - 1.5h_B} \tag{3.43}$$

$$F_{ni} = \frac{V}{\sqrt{g(T_F - h_B - 0.25\sqrt{A_{BT}}) + 0.15V^2}} \tag{3.44}$$

Where:

T_F = forward draft of the ship [m]

h_B = position of the centre of the transverse area [m]

Resistance due to immersed transom, R_{TR}

The resistance that is built up due to the immersed transom is created the same way as the bulbous bow, because of its shape (Roh, 2017). The expression to calculate the resistance is:

$$R_{TR} = \frac{1}{2}\rho C_6 A_T V^2 \tag{3.45}$$

Where:

A_T = immersed area of transom $[m^2]$

C_6 = coefficient determined by Froude number [-]

the immersed area of the transom, A_T, is calculated by (Segers, 2020):

$$A_T = 0.2 * B * T \tag{3.46}$$

Subsequently, the value for C_6 is determined by the Froude number, F_{nT}, that is based on the immersion of the transom. The Froude number is expressed as:

$$F_{nT} = \frac{V}{\sqrt{2gA_T/(B + B * C_{WP})}} \tag{3.47}$$

If the Froude has a value ($F_{nT} \geq 5$), C_6 will be 0, otherwise:

$$C_6 = 0.2(1 - 0.2F_{nT}) \tag{3.48}$$

3.1.4 Residual resistance, R_A

The model-ship correlation resistance, R_A, is part of the residual resistance. This factor describes the difference between the calculated resistance and the resistance that is present in reality. It is used to function as a fine-tuning factor for the estimated resistance (Roh, 2017). It is mainly based on the effects on the hull roughness and the still-air resistance and can be expressed as:

$$R_A = \frac{1}{2}\rho C_A S V^2 \tag{3.49}$$

Where C_A is a coefficient calculated as:

$$C_A = 0.006(L_a + 100)^{-0.16} - 0.00205 + 0.003\sqrt{L_a/7.5}C_B^4 C_2(0.04 - C_4) \tag{3.50}$$

Inside the equation the value of C_4 is T_F/L_a, with a maximum of 0.04.

3.1.5 Karpov

After analyzing all resistance parts of the HM equation, some extra information on modifications of the estimation method is given. One of the modifications proposed by Karpov (Rotteveel, 2013) (as mentioned in Chapter 2), is to apply an enhancing modification on the vessel speed that is used in the calculations for decreasing depth. This modification is then only applied for the wave resistance part and the residual resistance part. The first part of the modification is based on the Froude number where the velocity is related to the depth:

$$F_{nh} = V_0/\sqrt{gh} \tag{3.51}$$

Subsequently different values for the relation between the water depth, h, and the draught of the vessel, T, give a determination of the correction factor α_{xx}. The exact determination of α_{xx} is shown in Appendix A.1. At last, the modified velocity that is used for the calculation of wave resistance terms and residual resistance terms is then:

$$V_2 = V_0/\alpha_{xx} \tag{3.52}$$

Where V_2 is the modified velocity. The effect of the modification is to increase the resistance for decreasing water depth (Rotteveel, 2013). In this research the modified version of HM (modified by Karpov) is used. The reason to use the modification instead of the original approach is because the correction shows a higher resulting power profile compared to the original HM approach. The difference is shown in Table 3.1. The table shows that the modified approach, so including the correction of Karpov, shows a higher required power for limited depths, where the same power is required for deeper situations. Figure 3.3 and 3.4 show the difference in share of the total resistance of the resistance terms for original HM and for modified HM including Karpov modification. It can be observed that for deeper depths the distribution is similar, however for limited depths the distribution is changing for the modified HM method. Subsequently, Section 3.2 shows the need for a higher estimation of HM compared to VOHOP, where the need for a higher estimation is more schematised in Chapter 5. Therefore the estimation method that is used is the HM approach including the Karpov correction, also referred to as modified HM approach.

	Original HM [kW] Power [kW]	HM incl Karpov Power [kW]	Diff Hm,karpov/HM [HM,karpov/HM]
d = 12 m	9761	15342	1.57
d = 14 m	9732	11314	1.16
d = 20 m	9696	9749	1.01
d = 40 m	9673	9673	1.00

Table 3.1: Holtrop & Mennen vs Holtrop & Mennen inlc Karpov (v = 14 knots, T = 6 m)

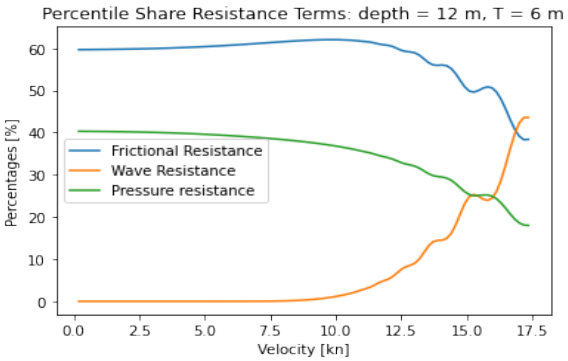

(a) Shallow depth HM excluding Karpov correction

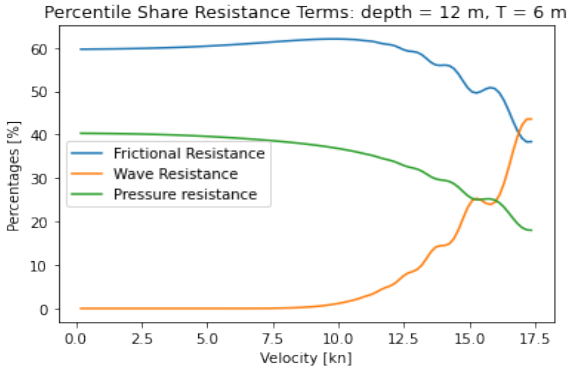

(b) Deep depth HM excluding Karpov correction

Figure 3.3: Distribution of resistance terms HM excluding Karpov correction

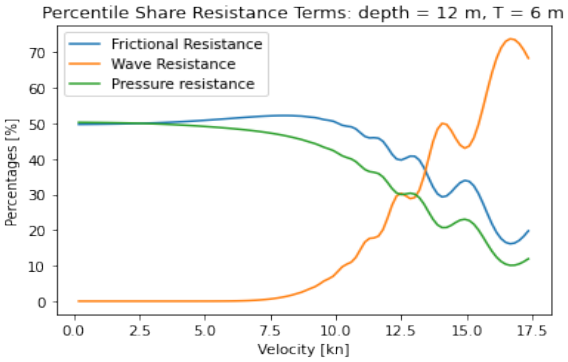

(a) Shallow depth HM including Karpov correction

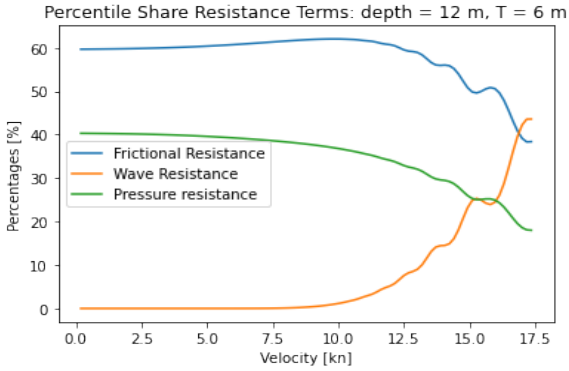

(b) Deep depth HM including Karpov correction

Figure 3.4: Distribution of resistance terms HM including Karpov correction

3.2 Estimation Simulation

In this section the proposed estimation method of Holtrop & Mennen (HM) is simulated by means of the software OpenCLSim. The goal of the simulation is to see what the required power and energy consumption is according to the modified HM method for various values of parameters as input. However, the simulation tool also enables the user to retrieve the velocity of the vessel for a given power. In this way, the tool is able to calculate the required power for free sailing at a certain speed or, vice-versa, calculate the vessel speed for a certain power. Note that the simulation of the estimation method of modified HM is an estimation method for free sailing only. After giving an overview of the estimation simulation, the current estimation method of Van Oord and the modified HM method are compared to each other and certain advantages and disadvantages are highlighted.

3.2.1 Simulation Modified Holtrop & Mennen

According to IHC (2001), the propulsion power of the TSHD consists of a portside propeller and a starboard propeller. Both propeller systems have a maximum power of 12,600 kW, which results in a maximum propeller power of:

$$P_{prop} = P_{ps} + P_{sb} = 10000 + 10000 = 20000 \text{ kW} \tag{3.53}$$

In the simulation the estimated power that is used by the board net of the vessel is estimated to be 10% of the max installed power. This results in the following maximum power for carrying out a free sailing stage according to Holtrop & Mennen (1982):

$$P_{max} = P_{prop} + P_{board} = P_{prop} + 0.1 * P_{inst} = 20000 + 0.1 * 25000 = 22500 \text{ kW} \tag{3.54}$$

With the calculated value of the available power, the simulation model is able to calculate the vessel speed for all velocities. In Figure 3.5 the required power according to modified HM is shown for varying input for the vessel speed.

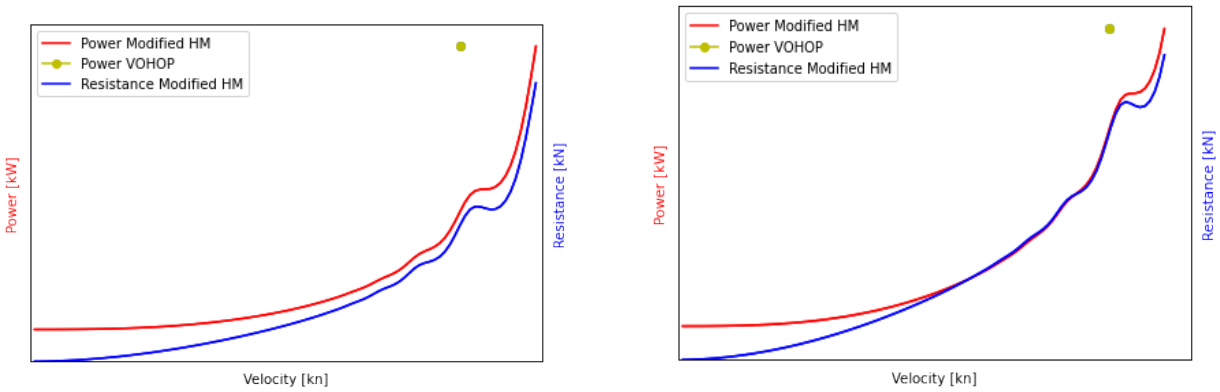

(a) Power and resistance as function of velocity (sailing empty)

(b) Power and resistance as function of velocity (sailing full)

Figure 3.5: Power and resistance as function of velocity TSHD

On the right axis of the figure, the corresponding resistance is given, while on the left side of the figure the corresponding power is given. Note that the value for the power does not start at zero due to the board net that always requires the same amount of power during sailing. In the figure, the yellow dot represents the estimation value according to VOHOP for maximum velocity.

Humps and Hollows

Figure 3.5 shows the relation of the required power and resistance to the velocity of the vessel. However at v $\approx$ 17, the graphs show a 'bump'. This phenomenon is called a 'hump' and a 'hollow'. In order to understand why this bump is situated on the graph, the concept of 'humps' and 'hollows' is explained. During movement of the vessel, waves are created due to varying pressure fields around the bow and the stern. These waves are either caused due to a moving pressure field which is created near the bow of the ship, or a moving suction field, which is situated near the stern of the ship (MC, 2021). Both the pressure field and the suction field create a system of waves. The effects that these waves have on the moving vessel are called interference effects (MC, 2021). The transverse waves, waves that oscillate in perpendicular direction relative to the direction they advance (Russel, 2015), travel from the bow in the direction of the hindside of the vessel. At a certain point, the bow-generated waves reach the stern-generated waves and this causes interaction of the waves. At a certain velocity, the crest of a bow-generated wave precisely coincides with the crest of the stern-generated waves, which results in a combined wave with greater magnitude due to the combination of the waves. On the other side, if a crest of one wave system is combined with the through of another system, the wave energy will be less (MC, 2021). The result of the combined wave systems is a higher or lower resistance acting on the vessel, dependent on the type of combination. However, it is important to notice that the phenomenon only occurs at certain velocities at which the wavelengths are such, that the combination of a crest with another crest can be made or a crest with a through. The result of these interference effects are the so called 'humps' and 'hollows' in the graph, where the hump is the small increase in required power and the hollow is the small decrease in required power (MC, 2021).

To specify some more: the effect of the interference effects is decreased by the bulbous bow that is situated at the bow of the TSHD. The bulbous bow modifies the way the water that flows around the hull of the vessel in order to reduce the wave resistance acting on the vessel. Figure 3.6 shows the same situation for the TSHD but without bulbous bow. It can be seen that the interference effects are more significant. Moreover, the maximum velocity that can be reached is slightly lower than for the TSHD with a bulbous bow due to the higher resulting resistance on the vessel.

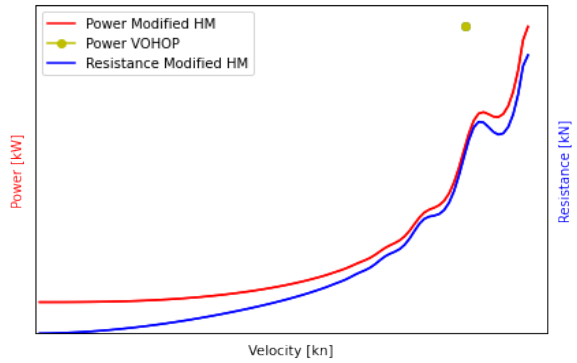

(a) Power and resistance, no bulbous bow (sailing empty)

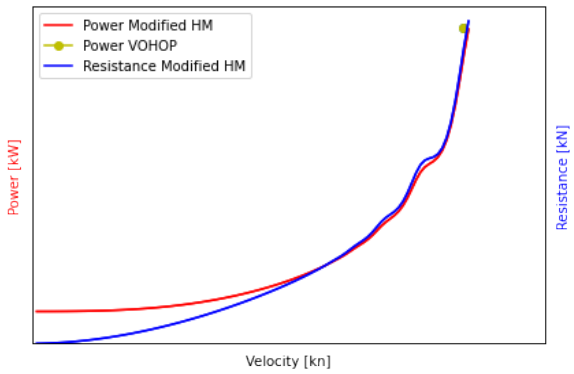

(b) Power and resistance, no bulbous bow (sailing full)

Figure 3.6: TSHD without bulbous bow

3.2.2 Base Case Comparison

In this section the results of the OpenCLSim module for the modified HM estimation method is shown for a base case. After the results are given, the results of the current estimation method VOHOP are also shown for the same situation. A short analysis is done where the two methods are compared

The base case comparison takes into account certain vessel properties that play a role when estimating the energy consumption during the sailing stages. The parameters are shown in Table 3.2. Where:

s_{sail} = sailing distance in nautical miles

d = water depth [m]

L_{wl} = length at waterline [m]

B = width of the vessel [m]

ρ_w = density of water $[kg/m^3]$

Parameter	Base Case Value
s_{sail} [nm]	10
d [m]	70
L_{wl} [m]	191
B [m]	38
$\rho_w[kg/m3]$	1025

Table 3.2: Vessel properties base case

All vessel properties are based on data provided by Van Oord. The distance and the depth are chosen to be large enough so that there is no external influence on the required power for a certain velocity due to a too small depth or too short distance.

The analysis is done for both sailing empty as for sailing full, where different parameters are used for both stages. Note that in Table 3.3 the values used for the Holtrop & Mennen analysis are referred to as HM, and the current estimation method is referred to as VOHOP.

Parameter	Mod HM Empty	Mod HM Full	VOHOP Empty	VOHOP Full
P_max [kW]	22500	22500	31700	31700
v_max [knots]	23.8	22.4	20.16	18.48
T [m]	7.0	15.6	7.0	15.6
d [m]	70	70	70	70

Table 3.3: Phase related parameters

Where:

P_{max} = maximum power [kW]

v_{max} = maximum speed [kn]

T = vessel draught [m]

d = water depth [m]

The maximum power and maximum velocity for modified (Mod) HM Empty and HM Full are calculated by means of the OpenCLSim module with as input the modified Holtrop & Mennen approach. First the results of the energy estimation for the sailing stages is given for VOHOP. Subsequently, the estimation results of the method are given.

VOHOP Results

The energy estimation according to VOHOP is done by means of equation 2.32:

$$E_{empty} = (P_{prop,SU} * t_{SU} + P_{prop,SD} * t_{SD} + P_{board} * t_{tot} + P_{prop,free} * (t_{tot} - t_{SD} - t_{SU}))/60 \tag{3.55}$$

$$E_{empty} = (18900 * 8.4 + 7560 * 7.4 + 1460 * 43.2 + 22500 * (43.2 - 7.4 - 8.4))/60 = 14905 \text{ kWh} \tag{3.56}$$

Note that the required power for a certain action is determined by the P% values for either speeding up, free sailing or deceleration. The total energy consumption is then calculated by multiplying the used power with the time needed for the action (Equation (2.5)). Equation 2.32 is also used for the sailing full stage estimation, where different values for certain parameters are used. This leads to the following results:

$$E_{full} = (P_{prop,SU} * t_{SU} + P_{prop,SD} * t_{SD} + P_{board} * t_{tot} + P_{prop,free} * (t_{tot} - t_{SD} - t_{SU}))/60 \tag{3.57}$$

$$E_{full} = (18900 * 8.93 + 7560 * 10.27 + 1460 * 48 + 22500 * (48 - 10.27 - 8.93))/60 = 16075 \text{ kWh} \tag{3.58}$$

The exact calculations for t_{SU}, t_{tot} and t_{SD} can be found in Chapter 2.

Holtrop & Mennen Results

The energy estimation according to the approach of Holtrop & Mennen is calculated by means of the OpenClSim module. The values of certain parameters are set as input in the model according to Table 3.2 and Table 3.3. The method is described in Section 3.1. With the base case parameters the results are:

$$E_{empty} = P_{empty} * t_{empty} = 22500 * 30.38/60 = 11393 \text{ kWh} \tag{3.59}$$

$$E_{full} = P_{full} * t_{full} = 22500 * 32.15/60 = 12056 \text{ kWh} \tag{3.60}$$

The simulation output of the OpenCLSim module, shown in Figure 3.7, gives an overview of the dredging cycle that is performed during the project, where a time of one hour is assumed for dredging and disposing to give a more realistic view. The results of both methods for energy consumption are shown in Table 3.4.

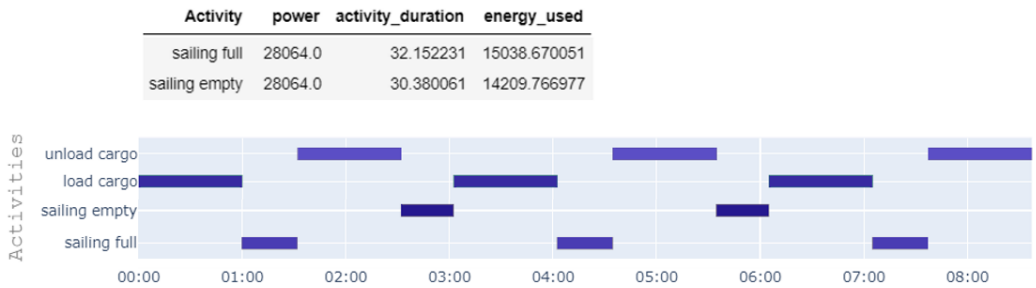

Figure 3.7: Gant chart dredging cycle

	Mod HM Empty	VOHOP Empty	Mod HM Full	VOHOP Full
Energy [kWh]	11393	14905	12056	16075

Table 3.4: Base case results

The resulting energy consumption according to the VOHOP calculation are higher than the one from modified HM. The reason for this difference can be found when analyzing both methods and concluding the difference between them. First, a possible reason for the higher outcome of the VOHOP calculation could be that the VOHOP calculation is based on empirical data, where the method proposed by Holtrop & Mennen is based on

both physics and empirical data. The difference between these two approaches is that the latter one enables the user to calculate (on a theoretical level) the required power necessary for a vessel to sail at a certain speed and to overcome a certain resistance. The VOHOP approach is based on how much power is used in historical projects carried out by vessels. A possible difference in the calculation outcome is for example a difference in required power versus used power. Another example of extra power usage that VOHOP possibly takes into account in the empirical factors it uses is influence of external factors that play role during the execution of dredging activities. For instance the influence of currents or air resistance might be taken into account in the empirical factors of VOHOP.

3.3 Conclusion

The estimation analysis conducted in this chapter has shown an elaborate analysis of both the current estimation method used by Van Oord, VOHOP, and an alternative estimation method according to Holtrop & Mennen. First the modified Holtrop & Mennen approach is discussed in more detail where the different types of resistance, frictional, wave and pressure resistance, are named that are taken into account. It is emphasized that the modified Holtrop & Mennen approach calculates the required power for a vessel to move as function of its speed. The dimensions of the vessel have influence on the resistance that is acting on the vessel. It is important to notice that the modified Holtrop & Mennen approach that is reviewed in this section only takes into account free sailing, where the method proposed by Van Oord takes acceleration and deceleration into account.

The simulation in OpenCLSim of the modified Holtrop & Mennen approach has shown the progression of the total required power that the vessel needs to deliver to sail at a certain speed and to overcome a certain resistance. A clear bump depicted the phenomenon of humps and hollows. These interference effect cause a slightly higher or lower wave resistance on the vessel for the hump and the hollow respectively. However, due to the bulbous bow of the TSHD, the effect of the interference effects is slightly flattened out.

In the last section of this chapter, an energy estimation is done for a base case. Table 3.4 shows the different results that are the output from both estimation models. It can be seen that the estimated energy according to VOHOP is considered to be higher than the method proposed by Holtrop & Mennen. This chapter answers the third sub-question partially by showing how the OpenCLSim module works and creating the option to have a base case study as input in the model, with an energy estimation as result. However, the results that come from this base case comparison need to be verified on behalf of actual data, which is done in the next two chapters. This verification will give an answer to the other part of the third sub-question.

4 | Historical Data Analysis

In this chapter an analysis is carried out on the historical data, also called actual data, that is retrieved from sensordata from the TSHD. First, the process of gathering data is described followed by an example of what the data looks like. After this some parameters are named that are important to analyse in the actual data followed by the actual analysis. Parameters are defined and are compared for different circumstances. At last, three projects are selected to be representative for comparison with the estimation module. The actual data is used to validate whether the created estimation method is correct or not. Therefore this chapter contributes to answering sub-question four.

(iv.) How to develop and validate a model to evaluate and improve the estimation of energy consumption?

4.1 Description of Analysis

In the actual analysis, the data that is observed is retrieved from sensor-data. Since 2012 Van Oord uses sensors that measure various signals during the cycle of a dredging project. The sensors can be observed as the senses of the vessel. There are numerous signals that can be measured and interpreted by the sensors and their processors. For this research the focus is on three signals only: movement, depth and power. Each one of them is shortly described underneath to give some understanding to the data that is treated in this chapter.

First the movement sensors are treated. These sensors are capable of detecting the movement of the vessel in either x-direction or y-direction. In this way the position of the vessel can be determined over time and this can be expressed as the movement of the vessel. The x,y coordinates can be measured in two ways: by GPS data and RTK data. GPS (Global Positioning System) uses satellite connection to determine the position of the vessel (Ranek, 2022). The advantage of GPS is that due to the connection with satellites, the position of the vessel can be determined wherever the vessel is. A disadvantage is the accuracy of GPS as it is determined more globally than RTK. RTK (Real Time Kinetics) is a more local approach of determining position and movement (NovAtel, 2022). It is more accurate than GPS, but has its limits. The RTK function shows its limits for vessels that are located far away from the shore, as the wave signals that are used for this method cannot reach the vessel anymore. Both methods are used when determining the movement of the vessel, depending on the situation that occurs (far away located vessels use GPS and closer vessels use RTK).

The second sensor that is used considers the depth-sensor. This sensor uses pressure differences to determine the bottom depth at which the vessel is located (Grosse, 2010). The sensor makes use of a diaphragm that detects the water pressure by means of a piezoelectric element. This method is considered to be accurate and does not have many limitations besides the small chance of a clogged entry in the piezoelectric element.

The last sensor is used to determine the power and is divided into two elements: the measurement of the torque and the measurement of the rounds per minute (rpm). The rpm is measured by means of induction. A small magnet is used to measure the amount of rounds that are made by the engine per minute. The measurement is done by applying a small magnetic coat in the engine that sends off a signal everytime it is connected to the attached magnet. The torque of the engine is determined by means of so called 'strain gauges' that are made of steel (Althens, 2022). However, this method is considered highly sensitive for mismatches. The system measures the amount of torque that is applied on the stroke and, due to the characteristic of steel, the resistance of the steel will change. Based on this difference, the torque can be determined. However due to aging of the steel, the strokes detect a different value than the actual value. This leads to miscalculations and can be prevented by regularly calibrating the strokes. The sensors send their data to the processor which in its way converts it into data that is readable and understandable for humans.

Due to large set of data (20+ projects), some filters are applied in order to create only representative data and to filter out unrepresentative data. The filters increase the generality of the data, which has as consequence

that the uncertainty and sensibility increases. At first it is key to observe the data of the TSHD, only when the vessel is actually performing a dredging activity. This is verified by project data from Van Oord. After this, the data set is shortened to only the sailing stages (leaving out the dredging and disposing stage) and a set of multiple trips is selected. However as the sensor-data does have some issues with collecting data, there are various data extractions that result in a mismatch. A view of what the mismatched data then looks like is shown in Figure 4.1, where a too large time step, extra data interpretation of the next cycle and missing sensor-data cause a mismatch of sensor-data in Figure a,b and c respectively.

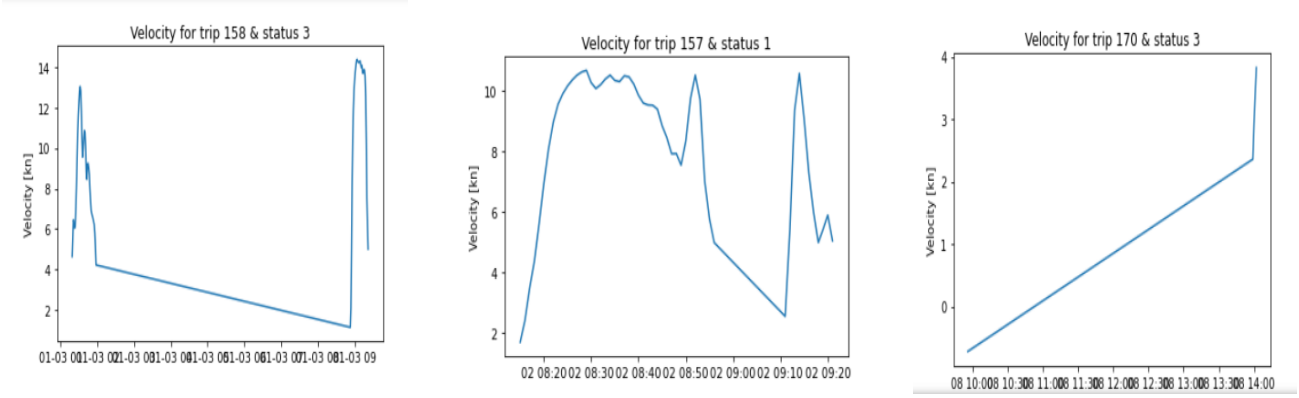

(a) Large time step (b) Extra data (c) Missing data

Figure 4.1: Unrealistic data

In order to retrieve reliable data, some requirements are set to the data that is extracted. The requirements are listed underneath:

- **Zero-valued sensor-data is filtered out**
  In order to filter out misleading sensor-data such as zero-values, all zero-values are filtered out. The reason for zero-valued data (also known as nan-data) is various, an example is the extraction of data in the middle of a trip, where the trip number will then give nan (not a number) as result as the trip is not complete.

- **Filtering of phases of the dredging cycle**
  The dredging stage and disposing stage are not inside the scope of this research and therefore left out of the analysis. The data that is left consists of the phases sailing empty and sailing full.

- **Filter miss-interpreted data**
  This filtering is done to prevent mismatches such as shown in Figure 4.1a, where the time-step that is interpreted is too large. This filter is needed to make sure that further filters are applied on a data set with only valuable data. Before the filtering is done the miss-interpretations must be identified in order to understand in what way the filtering needs to take place. An example of the identification of the data is shown in Figure 4.2. The figure shows the distribution of the duration of trips for a certain project according to actual data. According to (Jajodia, 2017), the usage of the standard deviation and the mean value of the data set can deliver a potential reliable result that covers 95% of the data, this is further explained in the next bullet. However, this approach is only viable if it is used for a normal distribution. Therefore the non-valuable data that is inside the distribution needs to be filtered out first. For example, a duration over 500 minutes is an example of miss-data as presented in Figure 4.1a. If the standard deviation method would have been used in this situation, the red line represents the value that is the boundary of cut out, see Figure 4.2. However, based on visual observation and conducting an iterative research, the green line shows a much more reliable result. Therefore the data that lies to the right of the green line is removed from the used data-set.

- **Outliers in trip duration are filtered out**
  This filtering is done to select the trips that are most common for the dredging activity and to remove outliers that decrease the viability of the data. In order to define the outliers, one first has to determine the mean duration of all trips. Subsequently, the standard deviation can be determined based on the variation of the data as the distribution of time duration is considered to be normal. Standard deviation is a metric of variance i.e. how much the individual data points are spread out from the mean (Jajodia, 2017). The value of one standard deviation is considered to cover 68% of the values drawn from the mean value, where two times the standard deviation is considered to cover 95% and three times covers 99.7%, also the 68-95-99.7 rule (see Figure 4.3). In order to cut out outliers, all values that are situated outside the (mean +- 2std) boundary are not taken into consideration (Jajodia, 2017).

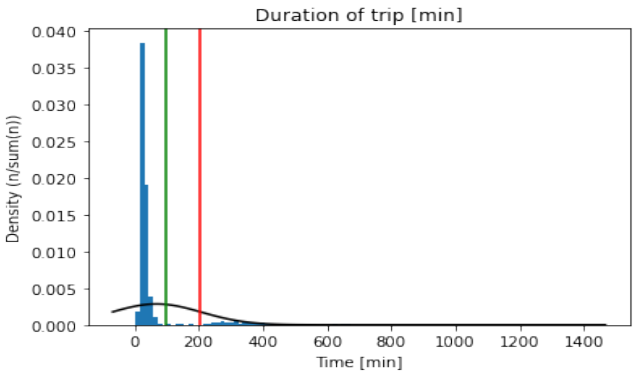

Figure 4.2: Histogram distribution of trip duration

- **Outliers in mean velocity are filtered out**
  This filtering is done to prevent unrepresentative data, such as too low velocity profile, from being used in the analysis. The outliers are determined the same way as the duration outliers are determined, by determining the standard deviation and cutting out all values that lay outside the boundary of (mean +- 2std).

- **Pitched trips are filtered out**
  If a pitch is applied on the maximum propulsion power when accelerating, the trip is filtered out to retrieve a consequent power pattern, as pitching situations deviate from the commonly used non-pitched situation. The exact definition of pitch is described in a further paragraph.

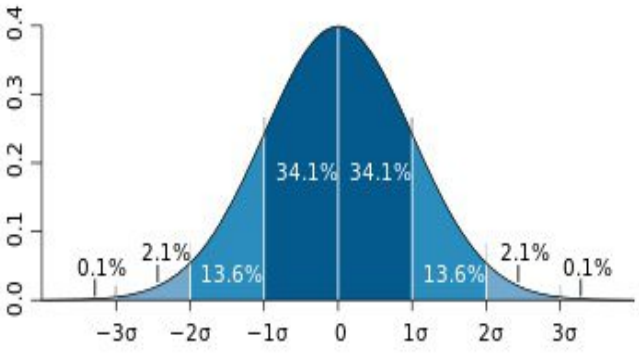

Figure 4.3: Standard deviation

This results in a data pattern for a single trip, where an example is shown in Figure 4.4a. Now that the data that is retrieved is considered representative, the actual analysis is carried out. The analysis has multiple results as output. Firstly, after analyzing the data, a representative value for acceleration can be defined that can be used inside the estimation model discussed in the previous chapter. Subsequently, the same procedure is done in order to define an appropriate value for deceleration that can be used in the estimation tool as well. After this, the velocity during free sailing is defined for multiple situations in order to compare it to the estimation method. At last the required power pattern that is linked to the data is calculated so that it can be compared to the estimation data. This is done on behalf of a selection of projects, however this will be treated later in this chapter. The parameters depth and distance are observed in order to validate whether there is a relation between the amount of energy consumed and the value of these parameters. For this research, the observed data ranged from a depth of -60 m to -8 m, therefore these type of depths are considered as deep and shallow respectively, where in the marine world a depth of -60 m is still observed as limited depth (Bianconi, 2002).

4.2 Analysis of Historical Data

In this section the actual data is used to define a representative value for acceleration, deceleration and free sailing. This analysis is done for multiple projects each consisting of multiple trips. After analysing, distinctions are made between depth and distance and differences in outcome are discussed and applied in further definition of value.

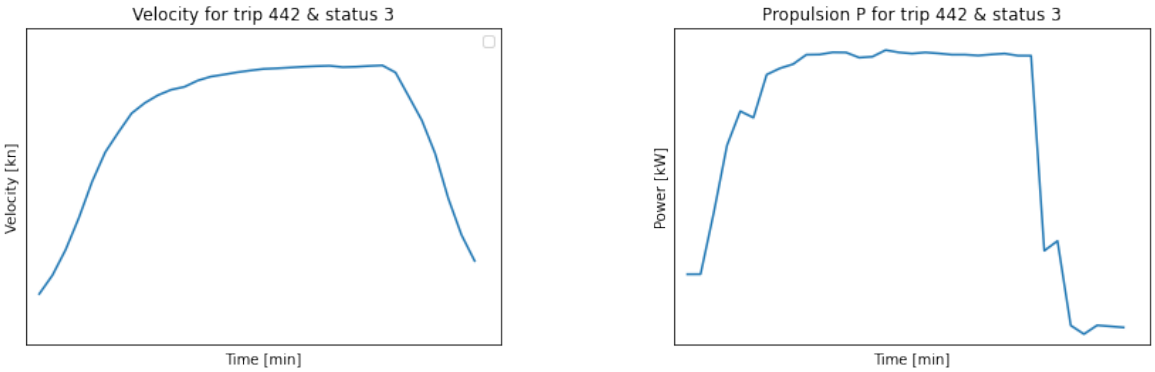

(a) Representative data pattern velocity

(b) Representative data pattern propulsion

Figure 4.4: Representative trip profile

4.2.1 Acceleration

In order to define the acceleration per trip, the pattern of acceleration has to be defined first. After visualizing the actual data, some requirements are set that have to be fulfilled in order to take a certain period of time of sailing into account as acceleration. The requirements consist of:

- **Value of acceleration $>$ 0.5 [kn/min]**
  After analysing acceleration patterns, this value is selected to be appropriate as boundary. The analysis is based on visualising the area of acceleration for different interpretations of acceleration. Figure 4.5 shows a representative view of the different area of acceleration for different values of acceleration. As the results do not differ for definitions below 0.5 knots/min, this value is chosen as definition of acceleration for this research. However, keep in mind that this assumption of the definition of acceleration can lead to different results than for taking into account another definition of acceleration.
- **A fitting line is drawn in between all points inside the acceleration curve $>$ 0.5 [kn/min]** using the values of the fitting line gives a more representative average result of the acceleration as deviating data is compensated by the fitting.

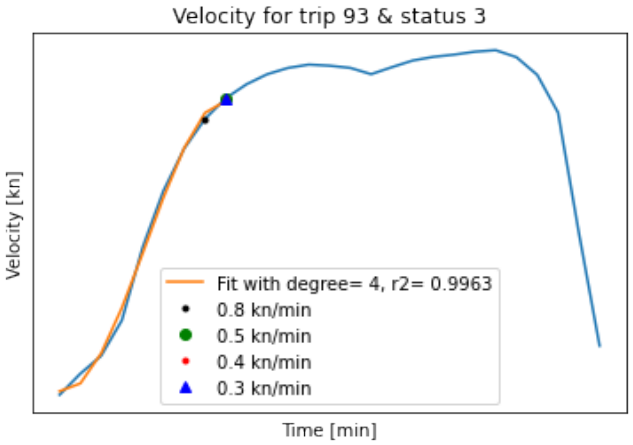

Figure 4.5: Different definitions of acceleration

The fitting consists of a polynomial fitting. The degree of the fitting is determined by which degree of fitting has the best R-value. This leads to Figure 4.6, where the blue dot and red dot represent the start- and endpoint of the fitting line of acceleration respectively. The R-squared method, or coefficient of determination, is a statistical measure that defines the variance of a dependant variable, that can be explained by the independent variable. Simply explained, the r-squared shows the goodness of the fit (CFI, 2022). R2 can have a value between 0 and 1. To explain the R2 value some more: if the R2 value is 0.6 for example, about 60% of the observed variation can be explained by input of the model (Data Science Team, 2020). Therefore a value of 1.0, means that all of the observed variation data can be explained by the model inputs. In this research, the fitting line is drawn between the defined acceleration, free sailing and deceleration area. After that, the goodness of the fit is determined by means of the R2 method, where it is measured for a 1st degree, 2nd degree, 3rd degree and 4th degree polynomial. At the end the fitting which has the highest R2 value is used. The result of this analysis

is to have all acceleration data defined. The next step is to plot the acceleration data against the modified HM approach and determine the difference. However, first deceleration and free sailing is defined as for these phases the same procedure is used.

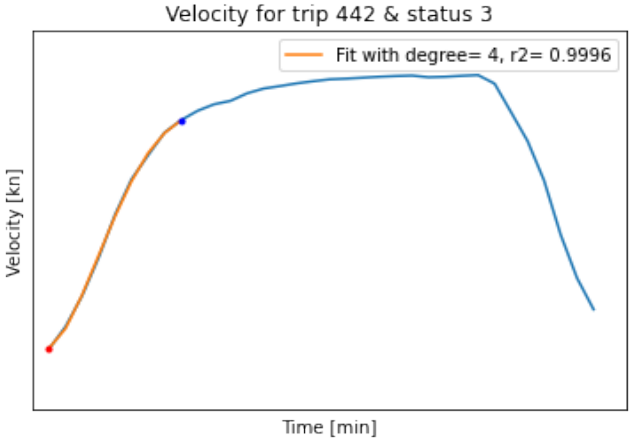

Figure 4.6: Period of acceleration

4.2.2 Free Sailing

For the free sailing part, it is important to determine the reached velocity during free sailing and the corresponding depth and distance of the total trip. First, the period of free sailing has to be defined. The requirements of free sailing are listed underneath:

- **Value of acceleration has to fulfill both requirements: acc $<$ 0.5 [kn/min] & acc $>$ -0.5 [kn/min]**
  After analysing acceleration and deceleration patterns, these values are selected to be appropriate as a boundaries. The method for determination is described in the previous paragraph for acceleration and in the next paragraph for deceleration

- **A fitting line is drawn in between all points inside the free sailing curve**
  the fitting line gives a more representative average result of the speed of free sailing. Moreover, deviating data is not taken into account by using a correct fitting. The R2 method as described earlier is used to determine the goodness of the fit.

A filter on maximum velocity could also be implemented on the free sailing profile, as reaching a certain velocity could provide useful information for analysing the data. However, in this research this filter of minimum reached velocity is left out due to the already relatively small sample size that is used. Applying the filter would decrease the sample size even more. An example of how the free sailing phase is visualised is shown in Figure 4.7. Notice that there is still some acceleration or deceleration in the free sailing phase, however for this research the definition of free sailing is considered as described earlier.

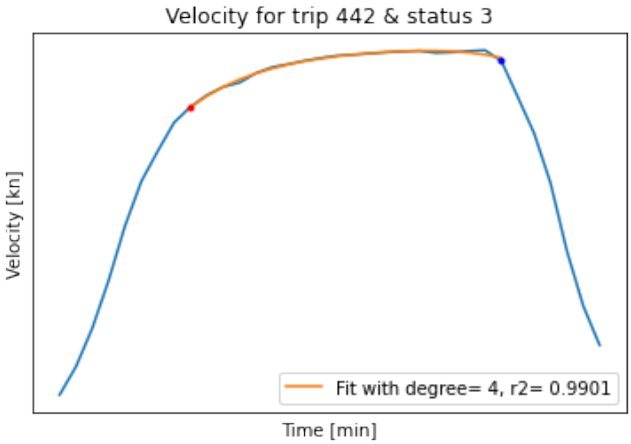

Figure 4.7: Period of free sailing

4.2.3 Deceleration

At last the deceleration part of the actual data is defined. This is done in order to find a representative value for deceleration to use in the estimation model during the sailing stages of a dredging cycle. First, out of all representative trips, the period of deceleration has to be defined. The requirements are listed underneath:

- **Value of deceleration < -0.5 [kn/min]**
  After analysing deceleration patterns, this value is selected to be appropriate as a boundary. The same method is used as for acceleration, with the same value as resulting definition of deceleration. It is important to notice that this definition of deceleration is based on visual observation. Other situations could result in a different value of deceleration, which must be taken into account.
- **A fitting line is drawn in between all points inside the deceleration curve < -0.5 [kn/min]** taking the derivative of the fitting line gives a more representative average result of the acceleration. Moreover, deviating data is not taken into account by using a correct fitting. The goodness of the fit is determined by the R2 method that is described earlier.

A representative period of deceleration, with the corresponding fitting, is shown in Figure 4.8.

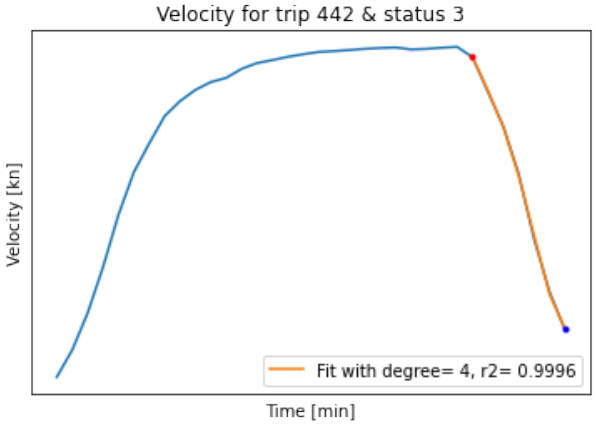

Figure 4.8: Period of deceleration

4.3 Project Analysis

Now that the three phases of a trip have been defined as acceleration, free sailing and deceleration, and their boundaries have been mentioned, the actual data can be retrieved. In this section the described way of extracting representative data is carried out on three historical projects carried out by Van Oord. The filters are applied and the outcome of the data is shown. The purpose of this section is to give a view on what the data results look like that will be used for comparison with estimation data and to define a representative value for acceleration and deceleration inside the estimation model based on actual data.

For the analysis, a selection of 12 years of sensordata for the TSHD is gathered. In this selection, 23 different dredging projects are distinguished, each of them their data is retrieved. After analyzing all projects in the dataset of Van Oord a selection is made to decide which projects are used to compare the actual data with the estimation model. Besides, the selection of these projects is also based on the difference in distance and depth in order to carry out a good comparison after the analysis. Based on whether sufficient amount of data was available and the workability of the data the selected projects consist of:

- Project A: (+-800 trips, 710 after filtering)
- Project B Reclamation: (+-130 trips, 108 after filtering)
- Project C: (+- 500 trips, 470 trips after filtering)

Keep in mind that the amount of trips in the above mentioned bullets consist of either sailing empty or sailing full. So the total amount of trips that contribute to sailing empty is half the the total amount of trips as the other half is sailing full (Example: Project A consists of 710 trips, 355 sailing empty and 355 sailing full).

In order to give a view of what the data looks like, each phase (acceleration, free sailing and deceleration) is treated separately first. Subsequently a representative value for acceleration and deceleration is determined based on the extracted data. It is important to notice that for each project the amount of trips/data differs.

Project Acceleration

In this section an overview of the extracted data of each project is given based on the acceleration filters that are mentioned in Paragraph 4.2.1. The graphs shown in Figure 4.9 give a view on the mean acceleration where each dot represents a single trip, during a single status (in the figures shown sailing empty). The mean acceleration is plotted against the mean depth and mean propulsion power used over the same period. In order to find the representative value for acceleration based on depth, a fitting curve is drawn in between the lines. At last, the plotted values are set into a histogram to give a view on what value of acceleration is most common for this particular project. The histogram shows the acceleration profile for each project with on the x-axis the acceleration and on the y-axis the density of the corresponding acceleration. This means the amount of times that a certain acceleration value is extracted divided by the total amount of extracted data for that particular project.

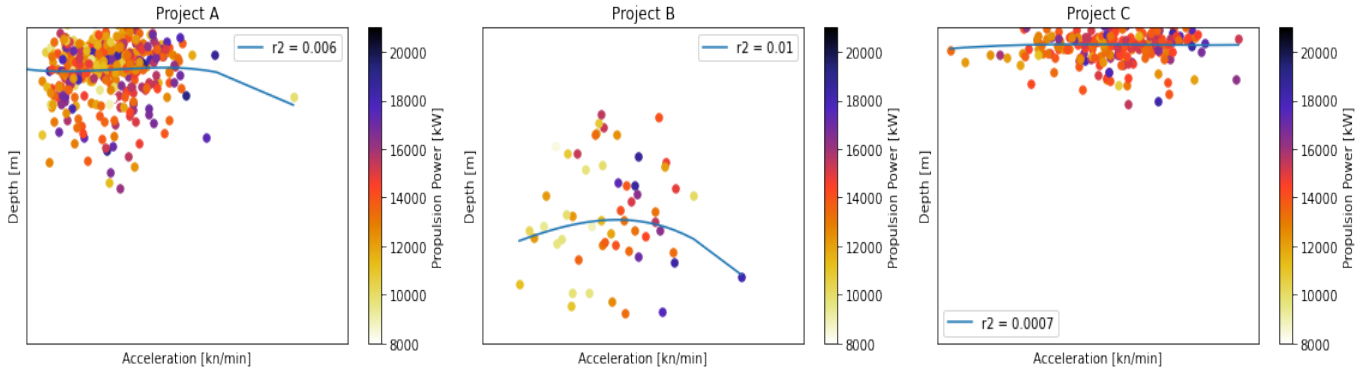

(a) Acceleration and depth Project A (b) Acceleration and depth Project B (c) Acceleration and depth Project C

Figure 4.9: Acceleration depth and power relation

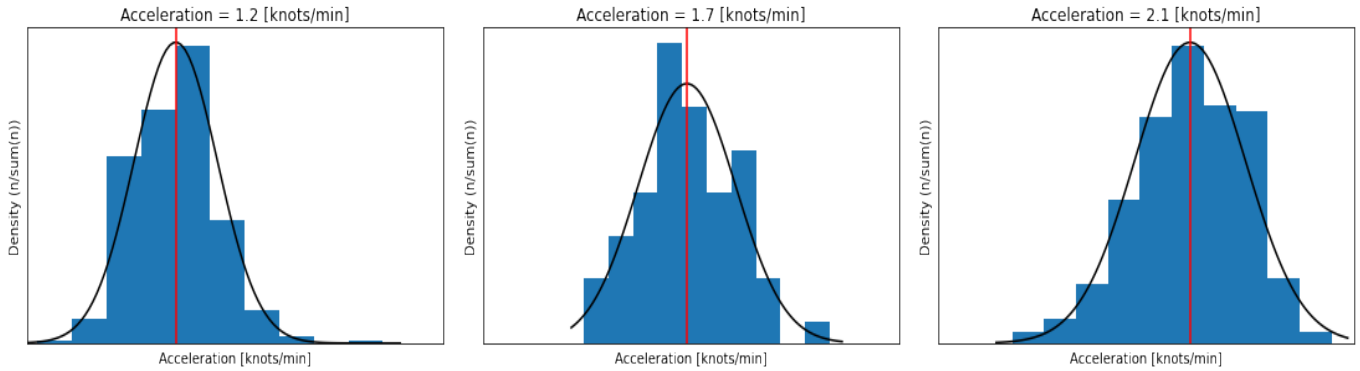

(a) Acceleration distribution Project A (b) Acceleration distribution Project B (c) Acceleration distribution Project C

Figure 4.10: Acceleration distributions

Project Free Sailing

An overview of the extracted data for the three selected projects is also given for the free sailing stage. The same type of graphs are plotted as shown before. However, for free sailing, it is important to not only take into account variations in depth, but also variations in distance. This is important because for situations that have a small distance to cover, the circumstances might lead to the vessel not having enough time to reach its maximum velocity as it already needs to decelerate before reaching the maximum velocity. Keep in mind that the depth is assumed to remain constant over the whole trip. The vessel does not have to take into account that a descending profile is ahead and that the deceleration process can be started at a later moment (due to more friction at lower depths and thus less time needed for decelerating the vessel). Underneath the data profiles for free sailing is given.

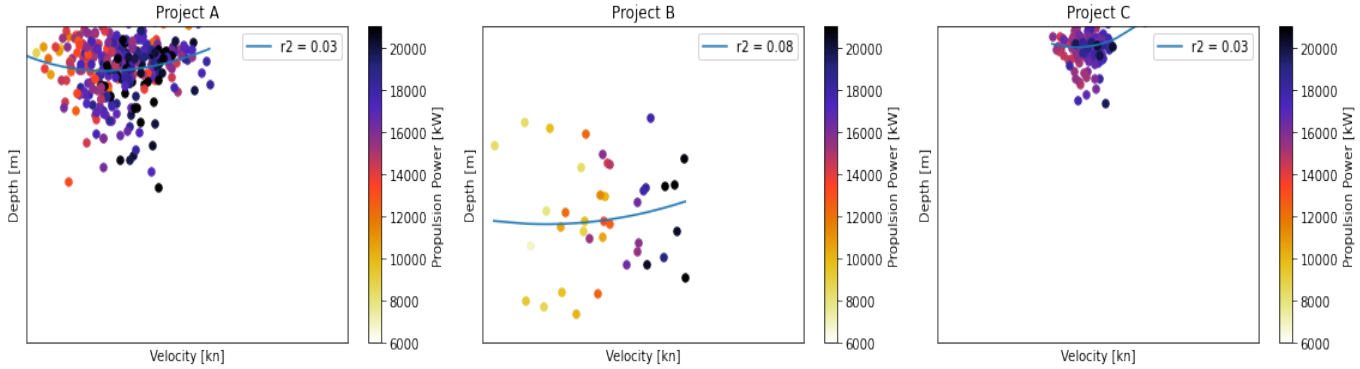

(a) Velocity and depth Project A (b) Velocity and depth Project B (c) Velocity and depth Project C

Figure 4.11: Velocity, depth and power relation

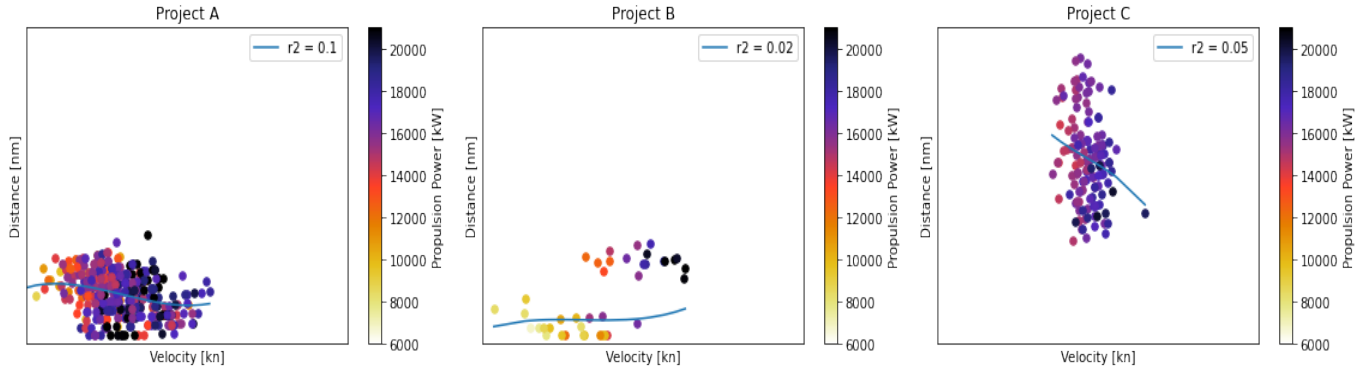

(a) Velocity and distance Project A (b) Velocity and distance Project B (c) Velocity and distance Project C

Figure 4.12: Velocity, distance and power relation

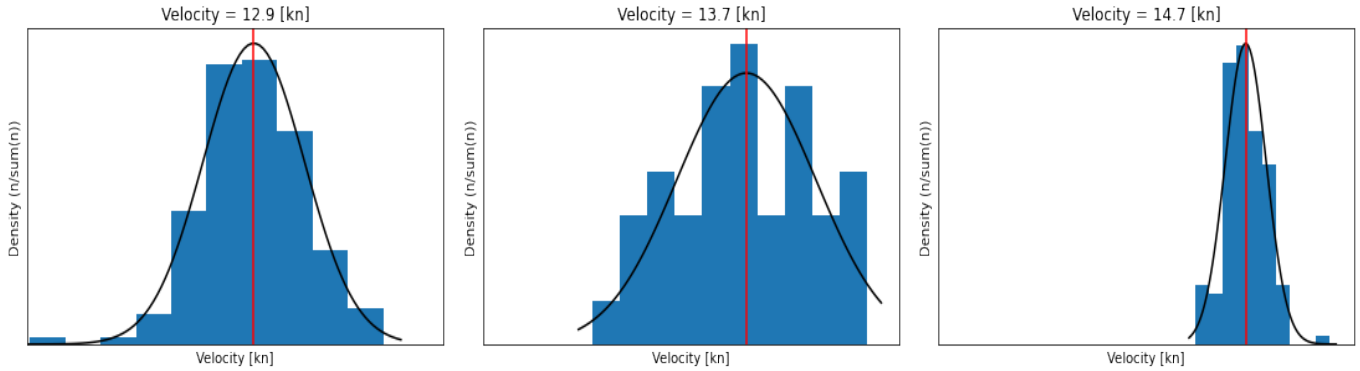

(a) Velocity distribution Project A (b) Velocity distribution Project B (c) Velocity distribution Project C

Figure 4.13: Velocity distribution Histograms

Project Deceleration

For the deceleration part, the same procedure is carried out as done for the acceleration part. This gives an overview of what the deceleration data looks like based on the filters applied that are mentioned earlier. The examples shown underneath only show the data for the sailing empty phase, however same procedure is carried out for the sailing full phase.

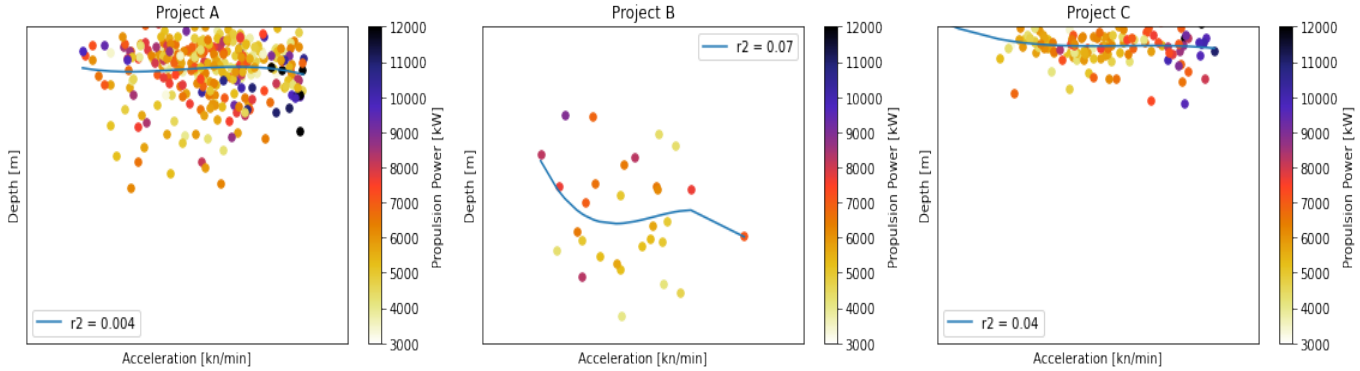

(a) Deceleration and depth Project A (b) Deceleration and depth Project B (c) Deceleration and depth Project C

Figure 4.14: Deceleration, depth and power relation

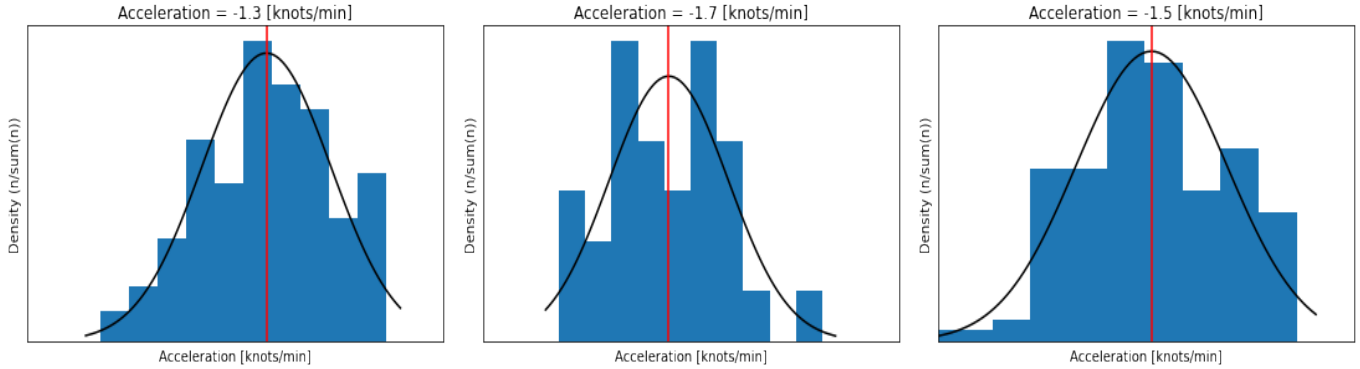

(a) Deceleration distribution Project A (b) Deceleration distribution Project B (c) Deceleration distribution Project C

Figure 4.15: Deceleration distributions

4.4 Conclusion

The analysis of the actual data has given a view of what the actual data, provided by Van Oord, looks like. First a description is given on how the actual data is retrieved in the real world situation. What equipment is needed in order to extract reliable data form a vessel. Moreover, what are possible problems that might occur when using the sensor equipment, and what are the possible results of these problems. It is important to notice these risks as they have to be taken into account before analysing the data. Knowing the possible risks provides a better view on whether data is reliable or if a possible miss-match is the outcome. After defining the method of retrieving data, some examples are given of miss-matches such as: too large time step, extra data from the next trip or missing data. Therefore sufficient amount of effective filters must be applied to the dataset in order to make the data reliable. After application of the filters, the dataset is considered to give a representative results for the trips that are actually carried out. However, applying the filters also increases the uncertainty of the data analysis.

After the analysis description is given and the filters are applied, the data is analysed. The purpose of analysing the data is to get a better understanding of what the extracted data looks like and to select data that is useful for comparing with the estimation model in order to improve the estimation model eventually. The data is analysed per phase of a trip consisting of: acceleration, free sailing and deceleration. The period of acceleration, free sailing and deceleration is defined and by plotting a fitting curve through the data, workable data is identified. The reliability of the filters is identified and the used data is made less sensitive, but more uncertain, which is a consequence of applying filters.

The last part of the actual data analysis is selecting the historical projects that are compared with the estimation model in order to evaluate the accuracy of the estimation model. Multiple projects were analysed and three projects were selected that were considered to give the most suitable data outcome to be used. Per phase of the trip, the data for each project is shown in a graph to give a view on what the results look like. The relation of acceleration, free sailing velocity and deceleration with depth and distance is shown by means of multiple graphs for each project. It is observed that the amount of data per project differs significantly which may lead to more uncertainty for certain projects, which is important to keep in mind when analyzing the data and drawing conclusions. Analysing the actual data and preparing a data selection that is suitable to compare with the estimation model is part of answering sub-question (iv.): How to **develop** and validate a model to evaluate and improve the estimation of energy consumption. The actual data that is selected is, based on common practice dredging methods, considered suitable to compare with the estimation model so that an evaluation can be done, after which improvements can be made (Van Oord, 2022). The next step is to compare the plotted outcome of the actual data with the estimation model for the same input variables. This will be done in the next chapter.

5 | Application and Results

In this chapter the modified estimation of Holtrop & Mennen is compared to the actual data. The correlation between different depth is analysed as well as the correlation of different sailing distances. After comparing the estimation method with the actual data, the results are mentioned. If needed, possible corrections are created and applied in order to improve the estimation method. This chapter answers sub-question four:

(iv.) How to develop and validate a model to evaluate and improve the estimation of energy consumption?

5.1 Estimation Evaluation Method

The estimation model based on Holtrop & Mennen is only tested with base case input parameters in OpenCLSim at the moment. However in order to evaluate the estimation model, the model is compared to the selection of projects as mentioned in Chapter 4. Before the comparison and evaluation is done, it is important know how the evaluation is done exactly and what the current expectations are. The estimation model its input values are set to be the same as for the actual data. For each phase the evaluation is done separately. Where first free sailing is treated, followed by acceleration and at last deceleration. The reason to treat acceleration after free sailing is because the approach of acceleration is similar to deceleration. The combined situation of the three phases is the outcome of the total evaluation. The comparison is done by comparing the relation between velocity and depth and distance of the estimation model for different values of power. To point out what the expectations are, two different scenario's are thought of that are described underneath:

- **EST $\approx$ ACT**
  If the estimation model has similarities to the actual data, some adjustments are made to the estimation model in order to have an improvement as output. The criteria for a situation to fall into this scenario is for the EST output to have a deviation of maximum 20% (Van Oord, 2022).

- **EST $\neq$ ACT**
  If the estimation model does not correspond to the actual data the reason behind the miss-match must be found in order to set some changes and validate the evaluation or to conclude whether the estimation model proposed by Holtrop & Mennen including modifications is not suitable. The criteria for this scenario is if the EST output has larger deviations than 20% of the ACT output (Van Oord, 2022).

To elaborate on each expectation scenario, a brief explanation is given. For the scenario where the estimation model does have some similarities to the actual data, but is not exactly equal (EST $\approx$ ACT), it is important to find out why there is a small miss-match. The reason might consist of small errors such as wrong assumptions, wrong filters used in extracting the data or the fault could be dependant on one or more parameters that are not taken into account. An improvement might consist of applying a correction factor that leads to an improved result.
At last, if the estimation model does not have similarities with the actual data, the reason behind the miss-match must be found. This can be due to the estimation model proposed by modified Holtrop & Mennen or by the selection of actual data. A possible reason could be that the filters used for retrieving the actual data are not suitable and lead to the miss-matches, or other assumptions or parameters that are left out could be the possible reason for non-similarities. For this scenario, the method that is used to improve the estimation is decided based on the reason of miss-match between EST and ACT.

5.1.1 Model Comparison

In this section the estimation model is set up in a way so that it is compatible for comparison with the actual data. This consists of comparing different parameters per phase of the trip. Where each phase, acceleration free sailing and deceleration, will be treated separately. However, first an overview of what the comparison looks like is shown in Figure 5.1. Notice that this is an example for a sailing empty phase (Figure 5.1a) and sailing

full phase (Figure 5.1b) for a certain project for one trip. However, in the research this comparison is carried out for not only one trip, but for all trips. In the figure the yellow dots represent the acceleration part of the actual data, where the power is plotted for each minute against the velocity that is reached in that minute. The same is done for the free sailing part (red dots) and the declaration part (green dots). The blue line is the power reached when implementing a certain velocity for the modified HM approach. The figure shows the actual data and modified HM approach for a certain depth (consisting of the draught of the vessel + the underkeel clearance) and the draught of the vessel as input parameters. Keep in mind that during free sailing, the vessel is considered to have minimal deviations in power usage and velocity. Therefore, in the figures the number of red dots occasionally falls on the same spot as the previous measurement, showing only little amount of dots, where in reality multiple dots are plotted (covering a long duration). Figure 5.2 shows the velocity, time profile for the same trip as Figure 5.1b. It is observed that the number of red dots is higher in reality than can be visualised in Figure 5.1b.

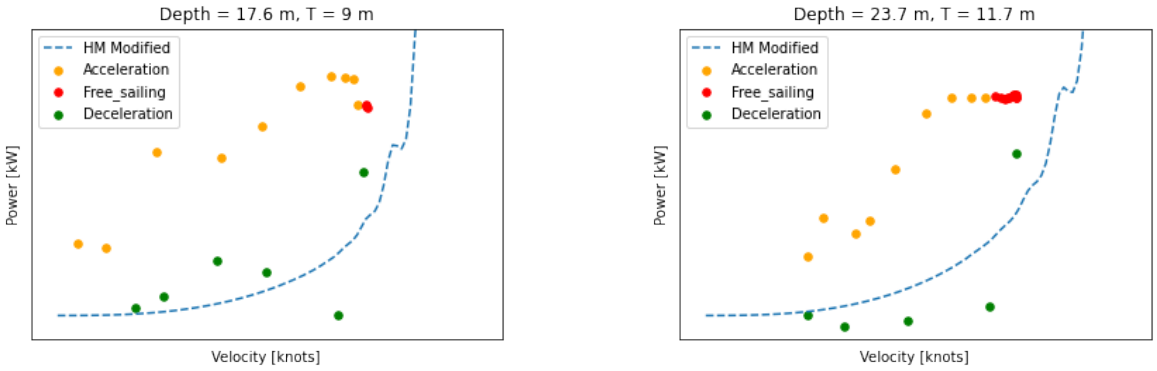

(a) Trip comparison sailing empty

(b) Trip comparison sailing full

Figure 5.1: Estimation vs actual data

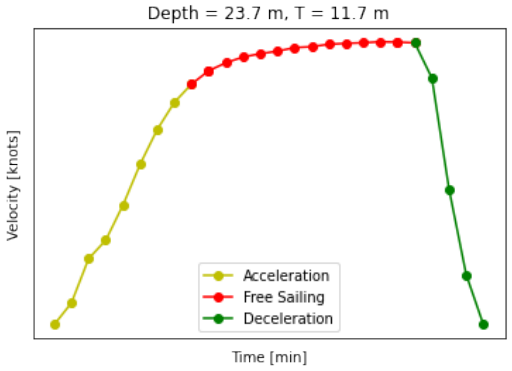

Figure 5.2: V,t diagram

5.1.2 Free Sailing Comparison

For the free sailing part different depths are compared to each other and the estimation is compared with the actual data. The analysis for different depth shows different results for more shallow depths versus deeper depths. This is shown in Figure 5.3.

The figure show that the estimation method is more accurate for more shallow depths and starts deviating from actual data for deeper depths. For more shallow results, the EST output shows a small deviation (less than 20%), therefore for the more shallow results, the scenario EST $\approx$ ACT is considered, where for deeper depths scenario EST $\neq$ ACT is considered. It is key to analyse the estimation method in order to find the reason behind the inaccurate estimation for an increasing depth and to eventually consider actions to improve the estimation.

Comparing the contribution of each type of resistance to the total resistance for the different depth inputs gives an indication on where the difference in the estimation method is based on. This will give a view on where the inaccuracy of the estimation is situated. The resulting resistance terms for the different depth while reaching the same velocity are shown in Table 5.1. The table shows that for increasing depth, the main factor that decreases the most is the wave resistance term, resulting in a too low estimation for deeper depths. From this analysis it is concluded that the inaccuracy for deeper depths is due to the calculation for wave resistance for

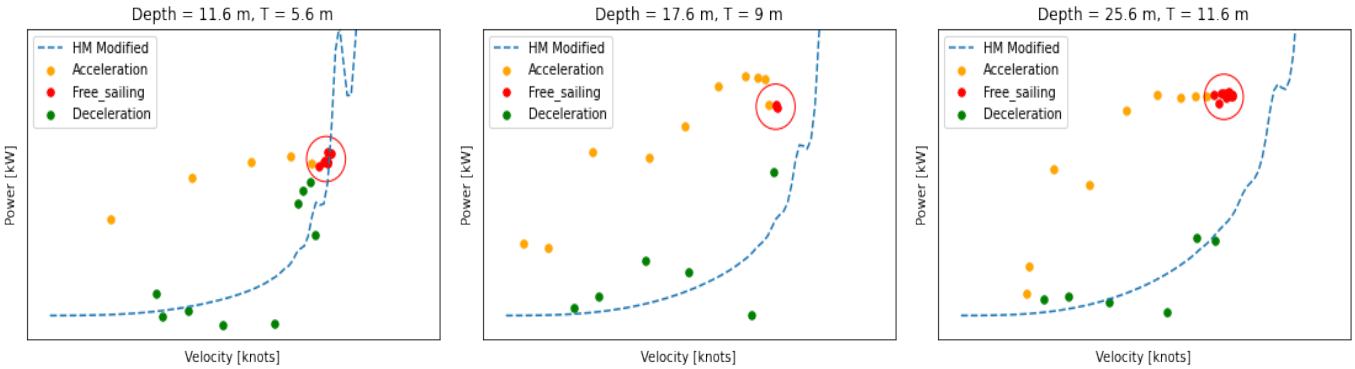

(a) Lower depth comparison (b) Moderate depth comparison (c) Higher depth comparison

Figure 5.3: Comparison for varying depths

deeper depths. It is key to find the reason of this difference in estimation for wave resistance.

Resistance [kN]	**Depth = 11 m**	**Depth = 25 m**	**Diff d11/d25**
Rf	333	324	1.02
Rapp	59	57	1.04
Rw	706	84	8.40
Rb	30	22	1.36
Rtr	155	115	1.35
Ra	108	65	1.66
Rtot	1392	668	2.08

Table 5.1: Resistance terms for varying depths

As mentioned earlier, the original method to estimate energy consumption proposed by Holtrop & Mennen is modified in different parts (Zeng and Karpov). The modification that is applied by Karpov is the correction on the velocity that accounts for limited water depth. The velocity is corrected to V2. This V2 term is then implemented into the wave resistance and the residual resistance terms. The shallower the input parameters, the more enhancing the modification of Karpov is. The input velocity is modified by a factor α, which is based on the relation between the depth and the draught of the vessel. Subsequently it calculates the value for α based on the Froude number that is depth related:

$$F_{nh} = V_0/\sqrt{g * d} \tag{5.1}$$

A higher Froude number leads to a lower value for α. As the relation of V2 against V0 is based on equation (5.2), the modification leads to the enhancing effect for decreasing depths, which in its places leads to a higher wave resistance as the wave resistance is dependant on the velocity (a higher velocity leads to a higher wave resistance).

$$V_2 = V_0/\alpha \tag{5.2}$$

Concluding from the evaluation analysis, a correction factor is needed for the wave resistance for deeper situations. Therefore, despite that for deeper situations the estimation output is considered to fall into scenario EST $\neq$ ACT, a correction factor is still suitable after analysing the reason of miss-estimation. However, first the region where this correction factor must be applied is determined, after that, the actual correction factor is created and implemented.

5.1.3 Free Sailing Improvement

According to the evaluation, as described in the previous paragraph, the modified HM approach is considered to be more accurate for limited depths and starts deviating from the actual data for increasing depth. However, first the reason for this deviation is identified. According to the modified HM method, the wave resistance is calculated based on the relation between the draught, T, and the water depth, d. Some large deviations occur because of the discrete variables that Karpov uses in the modification. The factor α, as mentioned in the previous paragraph is based on the following relation shown in Table 5.2. The exact discrete distribution of Karpov is shown in Appendix A.1. Table 5.2 shows an example for a situation where the draught T = 6 m. The table shows that the difference in wave resistance increases significantly for small differences (12 vs 13 m), where it stays constant for the same difference in depth (13 vs 14 m). These significant instant increases lead to the

d [m]	d/T	α	F_nh [-]	Rw [kN]
12	2	0.76	0.66	769
13	2.17	0.80	0.64	494
14	2.33	0.86	0.61	493
15	2.5	0.88	0.59	323

Table 5.2: Wave resistance for varying depths, T = 6 m, v = 14 kn

profile of power consumption that the modified HM approach shows. The actual data and the corresponding values for certain parameters are shown in Table 5.3. It can be seen that for increasing power, the parameter of draught corresponds to increasing power, where the other parameters do not respond the same way.

P [kW]	T [m]	d [m]	V [kn]
12000	**5.75**	12.65	12.65
14000	**8**	34	12.5
18000	**9**	17.6	14
21000	**13.85**	28	13.8

Table 5.3: Parameter relation to power

As Table 5.1 shows, the frictional resistance only shows a slight change for different depths. Now to see the correction that is needed based on different draughts and power, Figure 5.4 shows the relation between the total resistance calculated by the modified HM approach, and the total resistance as calculated from the actual data (where frictional resistance is considered to stay almost constant during increase of power). The orange line in Figure 5.4 represents the wave resistance acting on the vessel for a certain draught according to actual data. After extracting this information for multiple projects, the orange line is created (all for same reached velocity). The blue line is created by inserting the same input parameters as used for the actual data. The figure shows that the modified HM approach only shows realistic results for a small range of low drafts and a small deviation of draft causes a drastic increase (just as the previous figures showed), but for larger drafts, the modified HM approach estimates the resistance lower than the actual results. Therefore the correction factor that is needed is a correction on the modified HM results (blue line), to convert it into the actual data (orange line). This is done by an iterative process, creating a formula where the wave resistance is dependent on the draught.

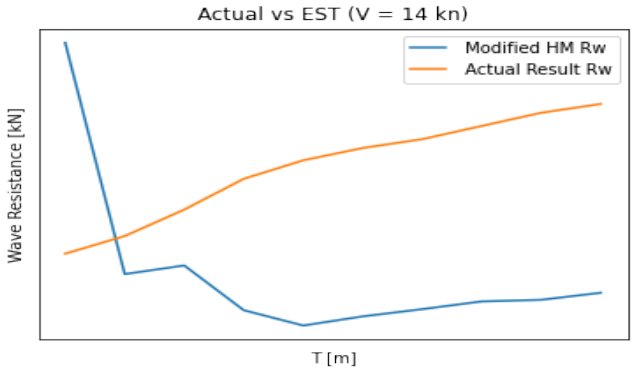

Figure 5.4: Power as function of draught (v = 14 knots)

T [m]	d [m]	Rw [kN] (EST)	Rw [kN] (ACT)
5	9	2398	1175
5.8	10.4	1189	1200
7.4	12.9	1261	1350
8	13.3	835	1600

Table 5.4: Corresponding draught and depth for wave resistance

In order to verify whether the created formula is correct, new projects (other than the already used actual data) are checked with the new correction on wave resistance applied. The following figures show the result of the new proposed HM approach where wave resistance is corrected based on draught. The new situations that are tested for the new proposed HM approach are for both small draught and large draught, combined with small depth and larger depth.

The results show that for the proposed estimation method, the estimation improved with respect to the

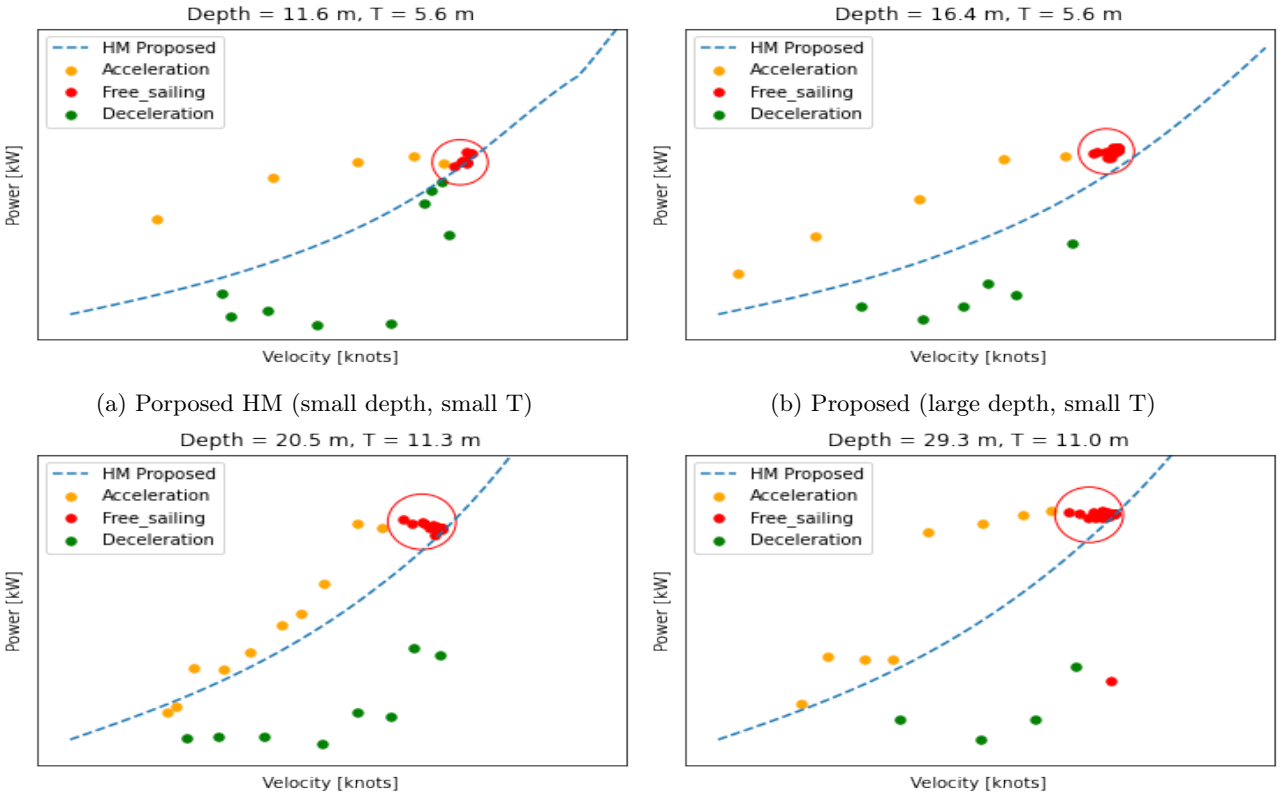

(a) Porposed HM (small depth, small T)

(b) Proposed (large depth, small T)

(c) Porposed HM (small depth, large T)

(d) Proposed HM (large depth, large T)

Figure 5.5: Validation of proposed HM for different depth and draught

former modified HM approach. Another advantage of the correction method is that, if the estimation is not exactly accurate but has a small deviation, the resulting calculated power does not deviate much from the actual results, where for the modified HM approach, the results deviated significantly due to the instant increase in power. Also there is no use of discrete variables, but the wave resistance is now dependent in a continuous way on the draught. This will prevent the sudden increases in wave resistance to occur. Keep in mind that the estimation does not show accurate results for the acceleration phase (value for low velocity). However, in this evaluation and improvement the research only observed the free sailing phase, for which the correction has improved accuracy. The created formula that shows the corrected results is thus based on the draught of the ship. The resulting formula is:

$$R_W = -4.8356 * T^2 + 178.9 * T + 45.56 \tag{5.3}$$

Despite that the formula shows accurate results for the tested situations (50+ trips, 3 projects), this results is only based on the little amount of data that is used and only tested on these particular situations. A follow-up study is needed to validate whether the correction is applicable for all situations. More data is needed to test this and more different situations on which the correction can be tested.

5.1.4 Acceleration Comparison

For the acceleration part the actual data consists of the yellow dots in Figure 5.1. Compared to the modified HM pattern, the actual power pattern uses a significantly higher power to reach a certain velocity. Therefore this can be seen as the EST $\neq$ ACT scenario. The actual data is analyzed in order to find the reason of the mismatch between the estimation method and the actual data.
When looking at the power pattern and the velocity pattern of the actual data, the mismatch between modified HM and the actual data becomes clear. Figure 5.6 shows the power pattern (Figure 5.6a) and velocity pattern (Figure 5.6b). The power setting, adjusted by the captain of the vessel, is instantly set from a value of +- 5,000 kW to a value of +- 20,000 kW. The few moments after that, the power setting stays on 20,000 kW. The start- and endpoint of the acceleration is shown by the red and blue dot respectively. The figure shows, that even though the power already reached 20,000 kW, the acceleration part has not ended yet, only for a few moments later when the blue dot is met. To dive into it a bit deeper, Figure 5.6b shows the corresponding velocity profile. It shows that even though the power is increased instantly from 5,000 to 20,000, the velocity does not increase in the same way. From this it can be concluded that: where the modified HM method calculates the **required**

power for a vessel to sail at a certain speed, the actual data shows the **used** power that the vessel uses in reality, which is significantly more power to reach that same velocity.

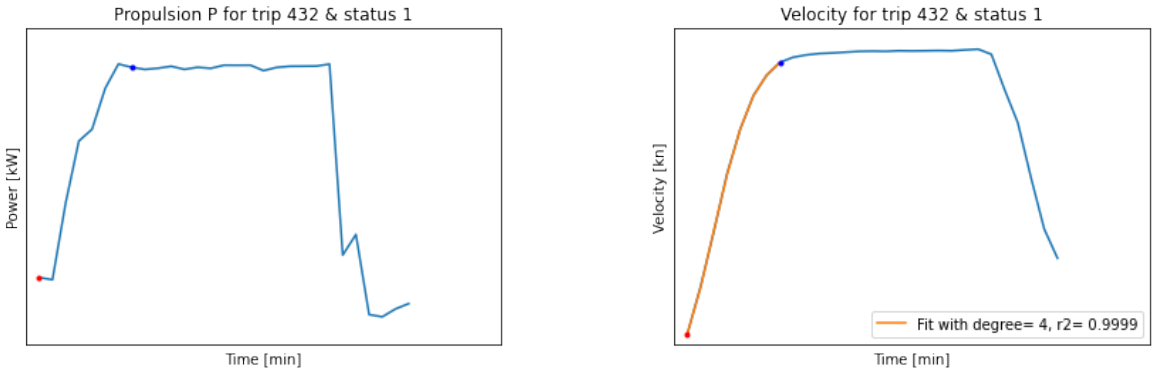

(a) Non-pitched power pattern

(b) Non-pitched velocity pattern

Figure 5.6: Non-pitched power and velocity pattern

Propeller Slip

A clarification of this phenomenon in order to understand what is happening: The instant increase in power causes a slip of the propeller through the water that directly affects the performance of the vessel. The propeller can be compared to a screw. Each complete turn of the screw into the wood, it has completed a so-called "pitch". It is the distance the screw traveled during this complete turn and is adjusted by tilting the propeller blades (Panagiotopoulos, 2022). For a propeller the same performance occurs, however it is situated underwater which causes a drag force to act on the vessel and the propeller. Therefore the propeller never actually reaches the full pitch. The difference between the theoretically reached distance and the actually reached distance is called slip. Reducing the slip results in more fuel efficiency and vessel performance. A schematising of the slip principle is shown in Figure 5.7. The slip is related to the level of pitch that is used where the lower the pitch, the lower the slip. In the situation where the power increases instantly, the pitch value is set at a high percentage instantly as well. This causes the difference in required power and used power for reaching the same velocity.

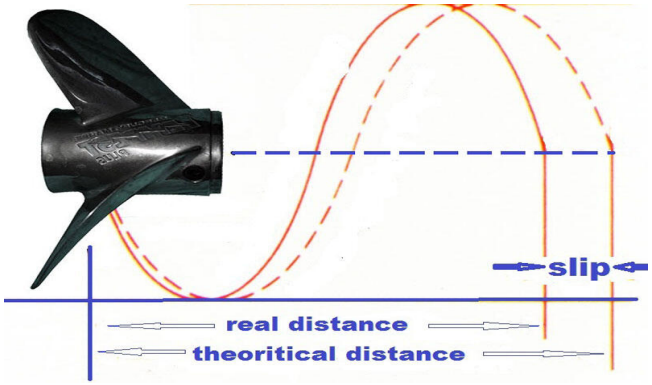

Figure 5.7: Slip principle vessel

It seems unlogical to compare the required power calculated by the modified HM approach with the used power from the actual data, as this used power is not the efficient way of using the vessel power. However, there are situations in which the captain set the pitch value a certain value that increases incrementally with the velocity of the vessel. An example of this situation is shown in Figure 5.8. The figures show that for incrementally increasing the power, and thus saving power usage compared to the instant increasing power situation, the velocity is not increasing incrementally, but shows similar increase profile as for instant power increase.

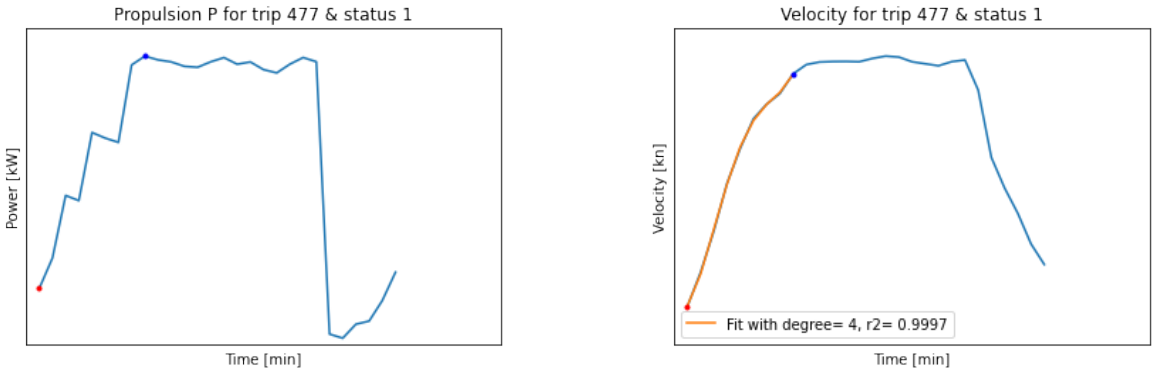

(a) Pitched power pattern

(b) Pitched velocity pattern

Figure 5.8: Pitched power and velocity pattern

Pitched versus Non-pitched

It is useful to gain more insight in the difference between the situation described in Figure 5.8, which is described as the "pitched "situation and the situation described in Figure 5.6, which is described as the "non-pitched" situation in this research. First of all, it is important to mention that in reality, according to the actual data, the pitched situation occurs significantly lower amount of times. For example for the Project C project, the amount of pitched trips after applying filters, is a percentage of 1.1% out of all trips. Figure 5.9 shows the energy consumption for a pitched situation and for a non-pitched situation of actual data. The green area represents the modified HM estimation, which is significantly lower than the actual data results due to the difference in required power and used power. However, the figure shows the effect of pitching. the area where the blue area is greater than the orange area can be considered as energy loss due to non-pitched situation. The expectation is that the pitched situation is a more sustainable solution. Nonetheless, the figure shows that the duration of the pitched situation is longer (4.83 min) than for the non-pitched situation (4 min), which leads to extra energy consumption. Moreover, calculating the area underneath the graph, the energy consumption for the non pitched situation is 899 kWh, while it is 1,000 kWh for the pitched situation. This means it is not always effective to use pitched settings. Keep in mind that this conclusion is based on little amount of research as there is a little amount of data that represents the pitched situation. The comparison between pitched situation and non-pitched should be explored further with more data available in order to be able to conclude the effect of pitch.

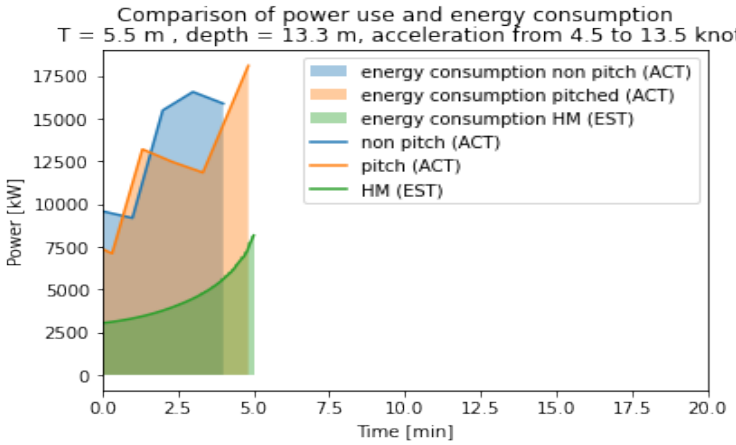

Figure 5.9: schematisation pitch, non-pitch and modified HM

	Pitched	Non-pitched	Modified HM
t [min]	4.83	4	5.01
E [kWh]	1,000	899	366

Table 5.5: Comparison pitch, non-pitch and modified HM

Despite the inefficiency of the pitched situation that is found by analysing actual data, one can imagine that if the pitching is used in such a way that it corresponds exactly (or similarly close) to the required power e.g. the modified HM pattern, the energy that is consumed can be reduced significantly. From Table 5.5 the difference in energy consumption can be found: 899 kWh - 366 kWh = 533 kWh reduction. However, the decision of using pitch and accepting a larger duration for less energy consumption against consuming more energy and conducting a dredging project within the least amount if time is a difficult decision. At the moment the costs of hiring/using a TSHD are significantly higher than the costs that are made for fuel consumption. Therefore nowadays, only a small part of the trips is carried out with pitch installed. However, in the future this might become more important as certain emission taxes could play a role in the use of pitch. Moreover, there are already advantages when proposing to carry out a tender in a climate friendly manner, which might become leading at a certain moment in the future.

5.1.5 Acceleration Improvement of Estimation

Concluding from the evaluation of the actual data of acceleration, this research only concerns the non-pitched situation as the amount of data of the pitched situation is too little to do research on. As comparing the estimation method with the non-pitched situation seems unlogical due to the difference in required power and used power, another method is chosen in order to estimate the energy consumption during acceleration. The method proposed consists of finding the most common power versus time fit for varying depths and distances. To give a better view on the method Figure 5.10 gives a schematization of the expectation of the power fits.

Notice that the horizontal part of the schematization is also part of the acceleration, as the vessel is sailing on maximum power earlier than reaching its maximum velocity. The eventual result of the fit is to create an estimation method that is capable of estimating the power fit based on a certain depth, and a reached velocity after accelerating. This reached velocity is in its way determined by the total distance of the trip, which will be explained later in this paragraph.

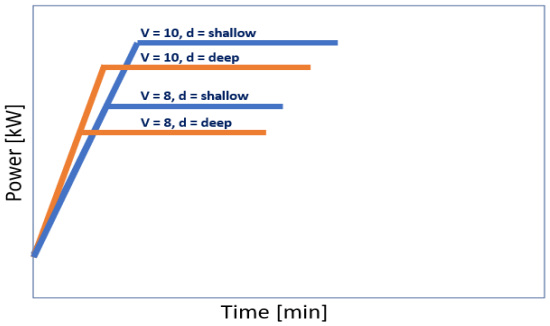

Figure 5.10: Schematisation of power fit acceleration

The fit is used to know on beforehand what the used power will be of a certain project. To distinguish certain fits, it is key to distinguish different type of depths. In this way each type of depth will have its own power fit. It is important to notice that the depths that are presented consider the depth to stay constant during the whole acceleration phase. Therefore the average depth is used as depth per trip. Figure 5.11 shows the depth distribution for the three selected projects for the sailing empty (SE) phase only. Keep in mind that the same procedure is used for determining the depth regions of the sailing full (SF) stage. From the figures, the depth region to be observed is determined at:

- Depth = -8 m to -14 m (Project C)
- Depth = -14 m to -19 m (Project C)
- Depth = -19 m to -29 m (Project A)
- Depth = -29 m to -59 m (Project B)

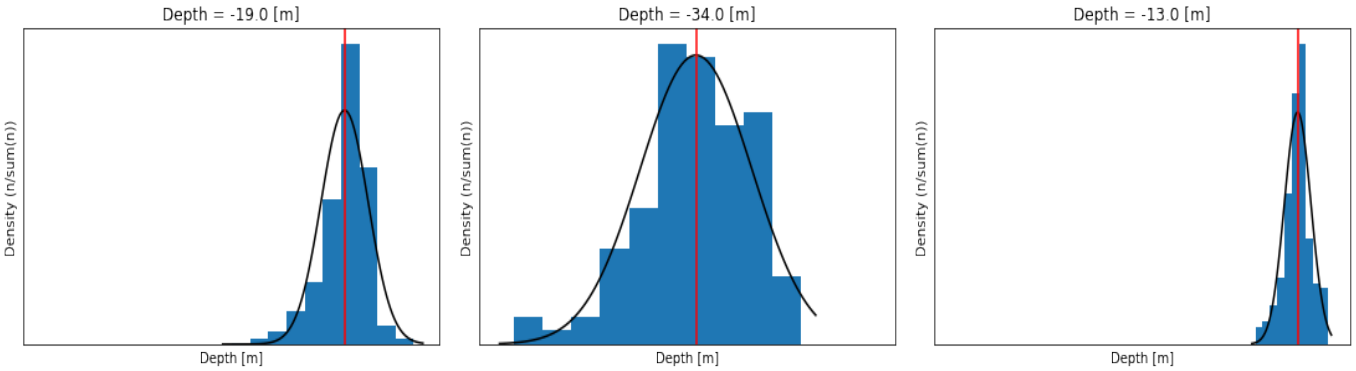

(a) Project A depth distribution (SE) (b) Project B depth distribution (SE) (c) Project C depth distribution (SE)

Figure 5.11: Depth distributions (SE)

Now that the regions of depth are determined, it is key to find the common sailing distance for the same regions. The total sailing distance is observed as this is expected to influence the reached velocity of the vessel. This expectation is based on the given that a vessel cannot reach its maximum velocity if the sailing distance is too short to accelerate up until the point of maximum velocity. In that case the vessel already has to start decelerating before the max velocity is reached. The relation between reached velocity and the total sailing distance of a project is shown in Figure 5.12. When observing the graph it becomes clear that for the selected data that is observed, there is a distinction in sailing distance that divides the data into a sailing distance < 5 nautical miles and a sailing distance > 5 nautical miles.

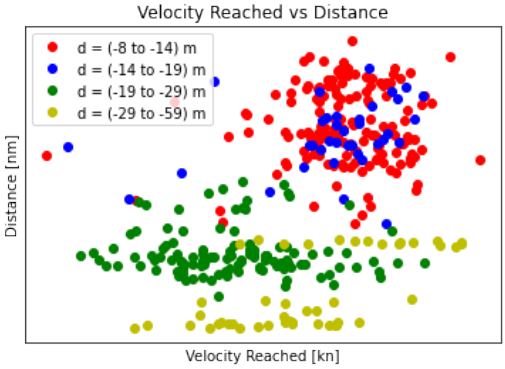

Figure 5.12: Reached velocity relation to sailing distance (SE)

Figure 5.12 gives a representation of the sailed distance versus the velocity that is reached. It clearly indicates that there is a s relation between these two parameters as this example shows that for higher sailing distances, as expected, a higher velocity is reached. For lower sailing distances it is the other way around. However, due to the little amount of data that is observed in this research, the figure only shows the relation for two particular situations: small sailing distance combined with relatively low reached velocity & large sailing distance combined with relatively high reached velocity. The situations that lay in between these two are not observed. This must be taken into account when creating certain power fits and results. Therefore the power fit will only be created for the two mentioned situations. If a situation lays in between these regions, the power fit is assumed to be corresponding to the observed area's.

Power fit Acceleration

The next step to be taken is to observe the power fit of the actual data for a certain region of depth and a certain reached velocity. The data for which a power fit is observed is listed underneath:

- Depth = -8 m to -14 m & Reached Velocity = 13.8 to 14.6 kn & Distance $>$ 5 nm
- Depth = -14 m to -19 m & Reached Velocity = 13.8 to 14.6 kn & Distance $>$ 5 nm
- Depth = -19 m to -29 m & Reached Velocity = 11.7 to 13.3 kn & Distance $<$ 5 nm
- Depth = -29 m to -59 m & Reached Velocity = 11.7 to 13.3 kn & Distance $<$ 5 nm

After defining the data to be observed according to the list shown above, the propulsion power is plotted against the time required to reach the certain velocity. Where this is done for every region, an example of what the data looks like is given for the first named region. For this research, the average power fit is used as the new fit to estimate acceleration. The blue line in Figure 5.13 shows the result. Notice that the line stops at t = 6. The reason for this is because in this research the assumption is made that if less than 25% of the data occurs at a certain moment of time, it is not taken into account anymore as this would give unrepresentative results (the line would stop at t = 9 only because one trip had an acceleration pattern that actually took 9 minutes).

After applying the same method for all regions, the outcome of the power fit is shown in Figure 5.14. Based on the power fit, a formula is created that has distance and depth as input in order to calculate the power profile corresponding to the power fit according to the actual data. The result of applying the formula is shown in the same figure representing the black round- or triangledotted line. The created formula for this situation is shown in Equation (5.4). The formulas for the other situations can be found in Appendix A.2 next to their schematisation of power fit. The use of the common fit does have some consequences as it makes the estimate less representative. This can be overcome by creating more depths regions that result in a more specific estimate for more situations.

$$Power = 51.65 * t^3 - 771.83 * t^2 + 3924 * t + 9323.8 \tag{5.4}$$

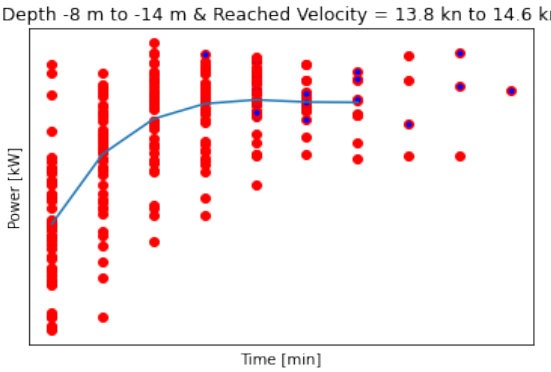

Figure 5.13: Power as function of time

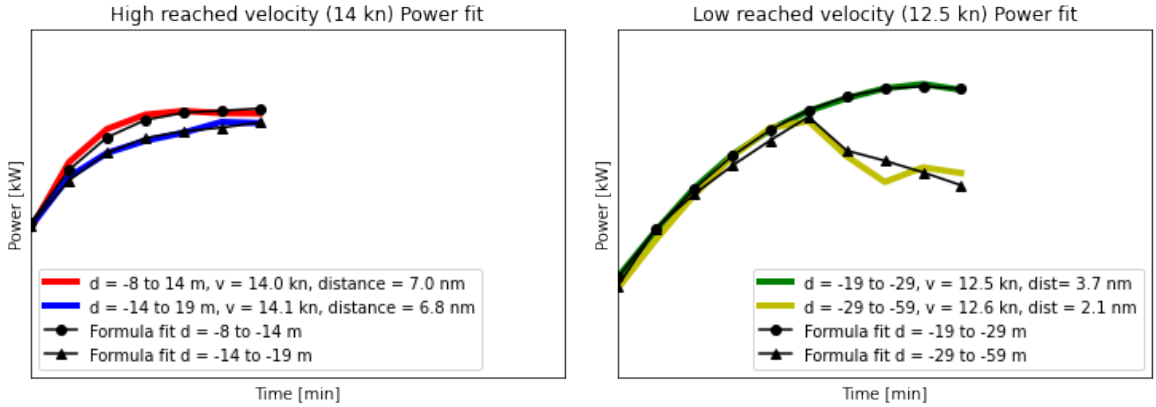

(a) Power fit for higher reached velocity (SE) (b) Power fit for lower reached velocity (SE)

Figure 5.14: Power fits acceleration (SE)

The result of this acceleration analysis is an estimation formula for used power against time based on depth and distance of actual data. Keep in mind that the shown examples are all for the sailing empty stage, The exact same procedure is done for sailing full. Before the power fit of the sailing full stage can be made, the different regions of depth need to be defined. Applying the same procedure as for sailing empty leads to the following chosen depth regions according to Figure 5.15:

- Depth = -20 m to -24 m (Project C)
- Depth = -24 m to -28 m (Project C)
- Depth = -28 m to -35 m (Project A)
- Depth = -35 m to -59 m (Project B)

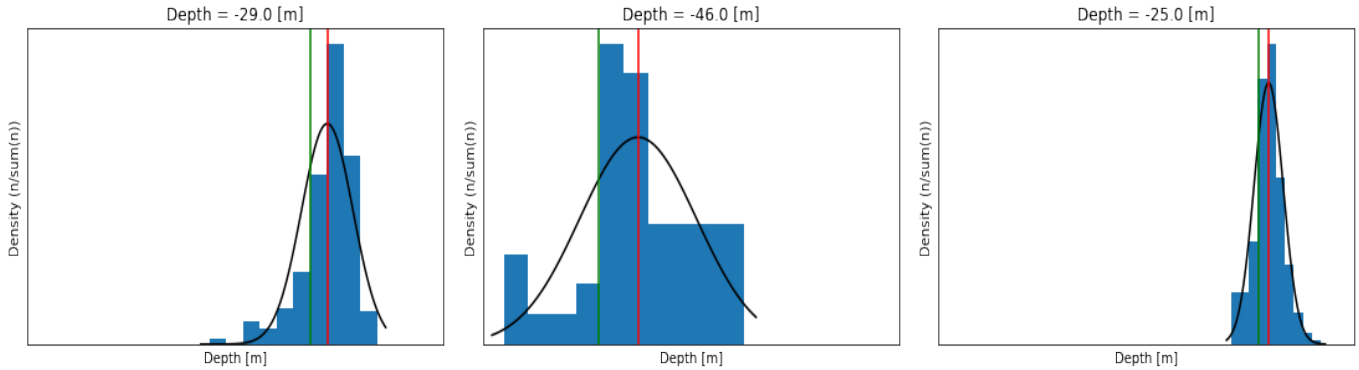

(a) Project A depth distribution (SF) (b) Project B depth distribution (SF) (c) Project C depth distribution (SF)

Figure 5.15: Depth distributions (SF)

Due to the difference in load on the vessel, the draught of the vessel also increases for a loaded vessel. The larger draught of the vessel might potentially lead to a longer sailing distance as certain areas might become unreachable. This leads to a different relation between reached velocity and sailed distance. The relation is shown in Figure 5.16, and the resulting reached velocity that is linked to the depth regions is:

- Depth = -20 m to -24 m & Reached Velocity = 11.8 to 13.5 kn & Distance > 5 nm
- Depth = -24 m to -28 m & Reached Velocity = 11.8 to 13.5 kn & Distance > 5 nm
- Depth = -28 m to -35 m & Reached Velocity = 10.5 to 12.5 kn & 3 nm < Distance < 5 nm
- Depth = -35 m to -59 m & Reached Velocity = 8.0 to 12.0 kn & Distance < 3 nm

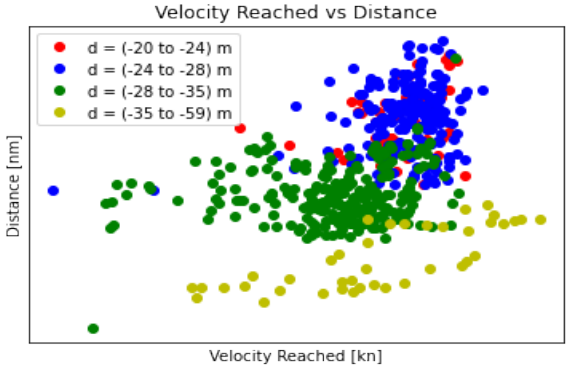

Figure 5.16: Reached velocity relation to sailing distance (SF)

After analyzing the resulting data for sailing empty, the power fit formula is created based on the power fits. The resulting power fits that are created based on the same procedure that is used for sailing empty are shown in Figure 5.17. The corresponding formulas for creating the estimation fit are stated in Appendix A.2.

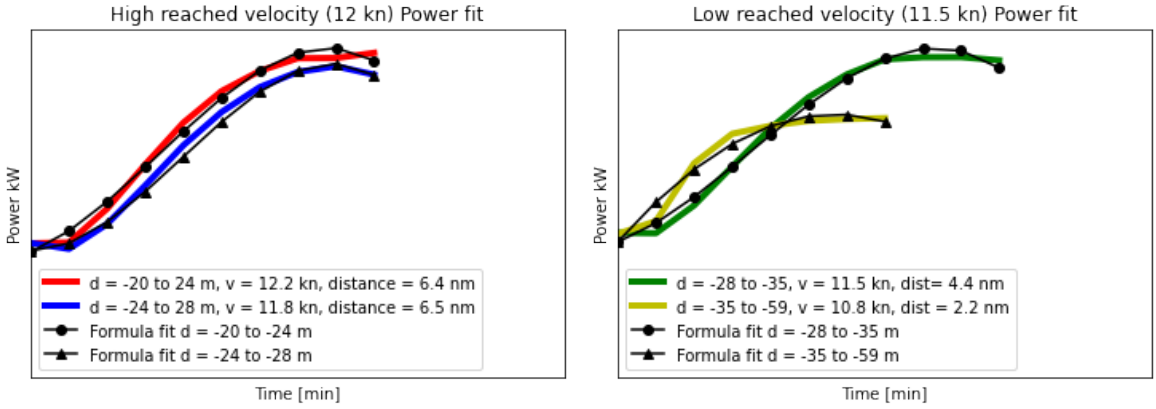

(a) Power fit for higher reached velocity (SF)

(b) Power fit for lower reached velocity (SF)

Figure 5.17: Power fits acceleration (SF)

5.1.6 Deceleration Comparison

The deceleration part consists of the green dots presented in Figure 5.1. From analyzing the deceleration data, the modified HM estimation shows fluctuation results. This is also observed in Figure 5.1. Therefore the resulting scenario is seen as EST $\neq$ ACT. The fluctuations that are observed in the actual data of deceleration can be related to variable reasons. For example external influence of traffic can influence the power usage of the vessel as it has to increase its manoeuvrability. Other factors that play a role are: velocity restrictions when sailing into destination sites, currents or in reality depths could be decreasing/increasing which could influence the used power for decelerating. Analyzing the deceleration fit shows that the setting of power is instantly dropped, leading to a large decrease of used power. An example is shown in Figure 5.18, where a certain drop of power is observed. However, the fluctuation at the end of the deceleration shows that the deceleration profile is difficult to predict as these kind of fluctuations are common for a deceleration fit. In order to visualize how common these fluctuations are and in order to predict the power fit during deceleration, despite the difficulty of estimating it, the same procedure of creating a power fit as in the acceleration phase is performed for the deceleration phase.

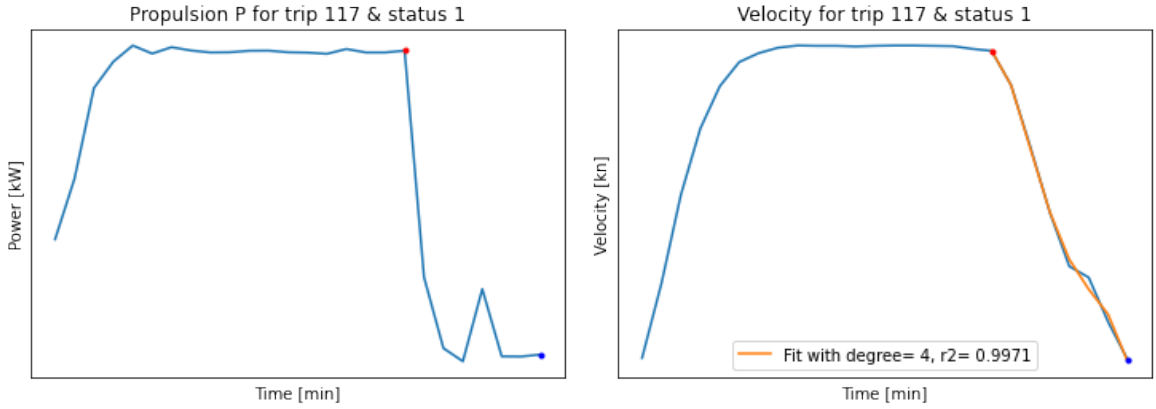

(a) Power profile deceleration

(b) Velocity profile deceleration

Figure 5.18: Deceleration profile

5.1.7 Deceleration Improvement of Estimation

The method proposed to estimate the deceleration power usage over time is the same as for acceleration. It is key to distinguish the power fit based on varying depth and distance. To give a better view on what the expectations are, Figure 5.19 shows the expected power fit without external influences included. Notice that the horizontal line in the figure represents the free sailing part, and is only shown to indicate the start velocity of which the deceleration has to start. The deceleration part itself starts at the drop of the line.

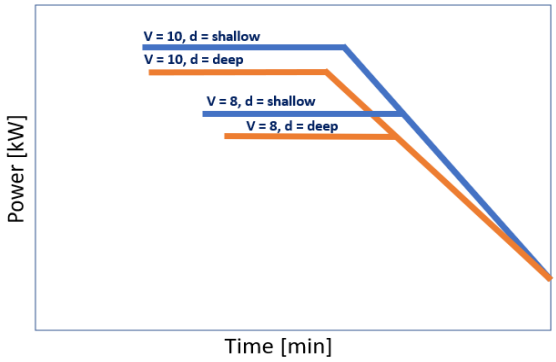

Figure 5.19: Schematization of power fit deceleration

The considered regions of depth and sailed distance are the same for deceleration as for acceleration (as the trips are exactly the same trips). Therefore for this phase, the relation between reached velocity and sailed distance can immediately be shown. Keep in mind that the results for sailing empty are shown, but the exact same procedure is done for sailing full in order to create an estimation for sailing full as well. Where the sailing distances have not changed for deceleration with respect to acceleration, the reached velocity points do have some adjusted values. The reason for this small difference can be explained by a slight acceleration during free sailing, that is not accounted for as acceleration. For example, if a trip is accelerating from 13 to 14 knots in 20

minutes of free sailing, the acceleration value during free sailing is < 0.001 [kn/min] which can be considered as free sailing as mentioned earlier when defining an appropriate value for the definition of acceleration and deceleration. Therefore the new regions that will be observed are:

- Depth = -8 m to -14 m & Reached Velocity = 13.8 to 15 kn & Distance $>$ 4.5 nm
- Depth = -14 m to -19 m & Reached Velocity = 13.8 to 15 kn & Distance $>$ 4.5 nm
- Depth = -19 m to -29 m & Reached Velocity = 12 to 13.5 kn & Distance $<$ 4.5 nm
- Depth = -29 m to -59 m & Reached Velocity = 12 to 13.5 kn & Distance $<$ 4.5 nm

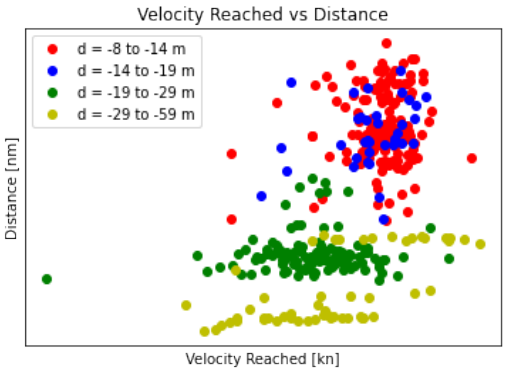

Figure 5.20: Reached velocity related to sailing distance (SE)

The next step is to plot the used propulsion power during deceleration against the time and draw a fit for the propulsion power based on the outcome. This procedure is done for every region listed above. The outcome of the average propulsion power per unit of time is shown in Figure 5.21 for every region. Added are the profile of the created formulas that are based on the actual power fit. From the power fit a formula is created where a distinction is made between depths and reached velocity, which is dependant on the sailing distance of the whole trip. The formula is found in Appendix A.2.

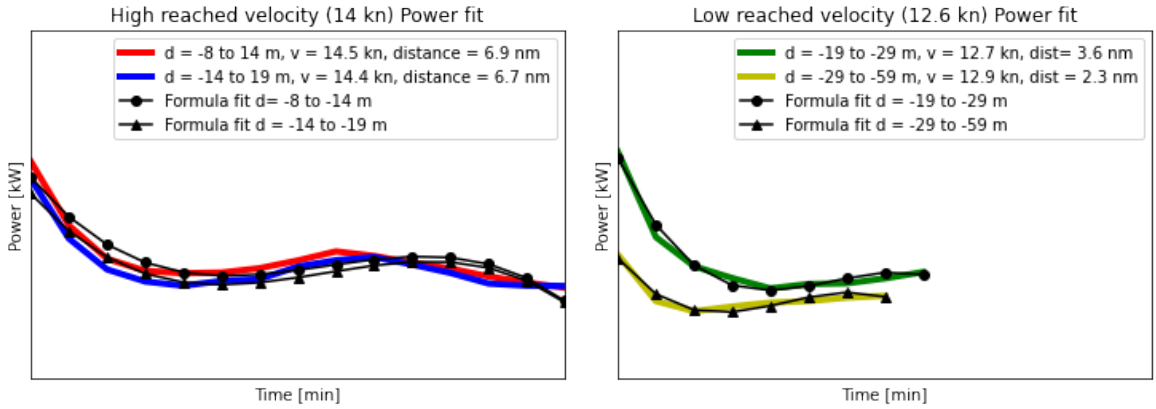

(a) Power fit for higher reached velocity (SE)

(b) Power fit for lower reached velocity (SE)

Figure 5.21: Power fits deceleration (SE)

The procedure of creating a power fit for the deceleration stage is also done for the sailing full stage, as above results only correspond to the sailing empty stage. The created formulas can be found in Appendix A.2. However, as also shown in the creation of the acceleration power fit, the reached velocities, sailing distances and depth regions of the sailing full stage might deviate from the sailing empty stage. With the depth regions for sailing full already mentioned in the acceleration part, the corresponding reached velocities and sailing distances for deceleration can be shown. From Figure 5.22 the following relation results:

- Depth = -20 m to -24 m & Reached Velocity = 12.5 to 15 kn & Distance $>$ 5.2 nm
- Depth = -24 m to -28 m & Reached Velocity = 12.5 to 15 kn & Distance $>$ 5.2 nm
- Depth = -28 m to -35 m & Reached Velocity = 11 to 13 kn & 3.2 nm $<$ Distance $<$ 4.5 nm
- Depth = -35 m to -59 m & Reached Velocity = 8 to 12.2 kn & Distance $<$ 3.2 nm

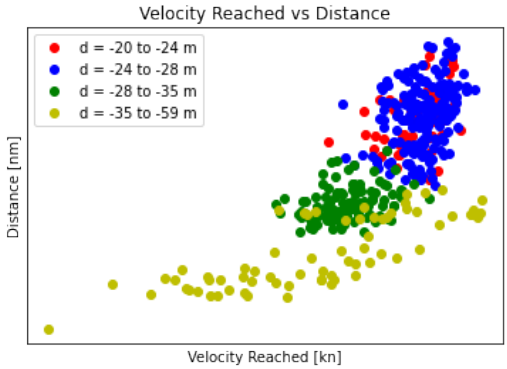

Figure 5.22: Reached velocity related to sailing distance (SF)

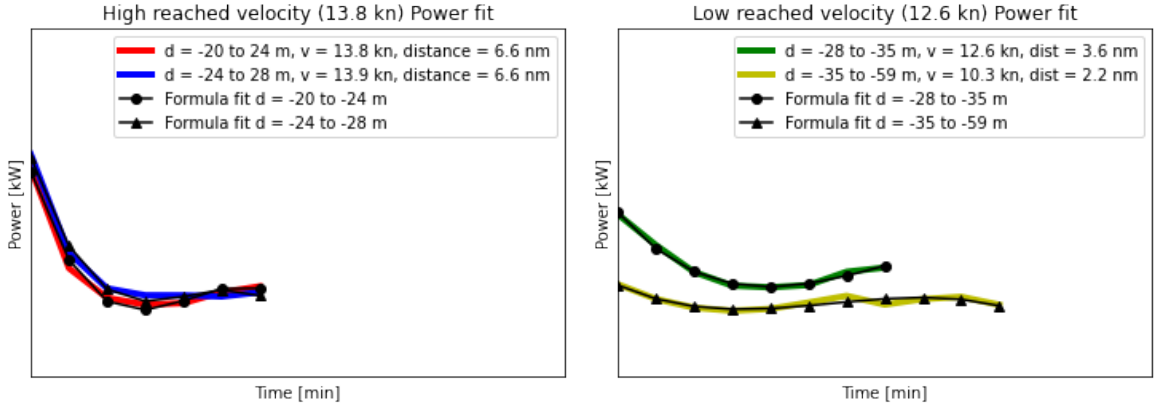

(a) Power fit for higher reached velocity (SF)

(b) Power fit for lower reached velocity (SF)

Figure 5.23: Power fits deceleration (SF)

5.2 Validation

In this section the results of the research are summed up and, eventually, added together. Before comparing the new estimation tool with VOHOP, the new estimation method is described in detail. In the comparison the energy consumption is calculated for a historical case study for three situations: the new estimation method itself, VOHOP and the actual data of the case study itself. An analysis on the energy consumption and the difference in results is shown for each phase apart consisting of acceleration, free sailing and deceleration after which the results are added to from the total trip. The result is an improved estimation tool that estimates energy consumption based on different depths and distances. To keep in mind, in this chapter, the created estimation method and the VOHOP method are compared to the actual data. The comparison shows the improvement of the newly created estimation method. All in all this method is stated as EST vs ACT = DIFF.

5.2.1 Case Studies

The resulting estimation tool consists of the three phases: acceleration, free sailing and deceleration. After analyzing the results, it is key that the results are linked together so that the eventual result shows a smooth curve corresponding to the actual data. To give a clear overview of what the resulting estimation tool looks like before diving into the different phases, Figure 5.24 shows an example of an estimated situation by means of the new estimation tool, where the estimation tool consists of applying the proposed HM method for free sailing and the power fits for acceleration and deceleration as described in previous paragraphs.

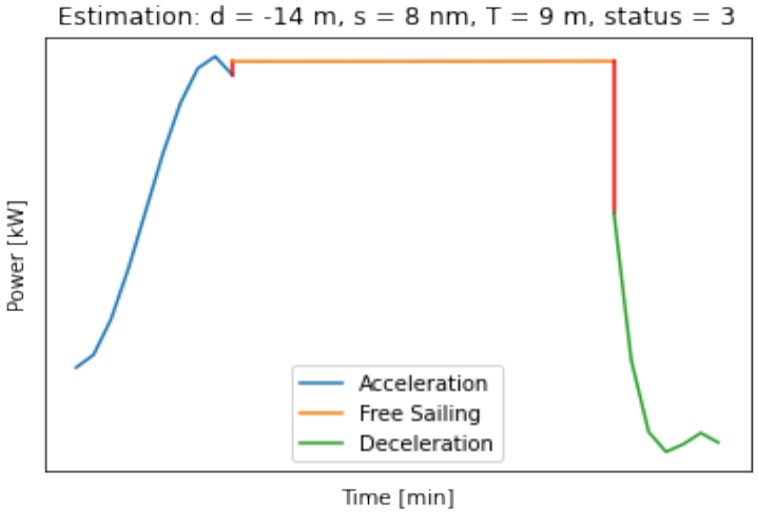

Figure 5.24: Estimation tool overview

The figure shows the estimated power usage for a certain period of time according to four input parameters: depth, distance, draught and the status of the vessel (sailing empty or sailing full). The estimated acceleration does not fit exactly on the estimated power usage according to free sailing, as shown in the figure. The two phases (where the same situation appears for deceleration) are connected through the red line. To define this red line, defined as connective area, it is the minute (the time step taken in the data) that exists between the definition of, for example, free sailing and deceleration. Imagine assigning this minute to either free sailing or deceleration, this would propose that either the deceleration starts at a velocity that is exactly the velocity as free sailing (the black dot in Figure 5.25), where this this moment is also already considered as free sailing. On the other side, considering the very next moment (the blue dot in Figure 5.25) as deceleration would propose that the region in between is considered as free sailing. However, there is a clear decrease in velocity in between that region, which is considered to be taken into account as deceleration. Therefore this red region is not taken into account for as any of the phases, as the phases are only connected by the lines. Now that the estimation tool is observed, the new estimation tool is compared to VOHOP based on a trips extracted from actual data. The comparison is done for four different situations, where the emphasize is on testing whether different distance and depth situations are correctly estimated. Therefore the tested cases consist of the cases as described in Paragraph 5.1.5 where a distinction is made between sailing empty and sailing full. For sailing empty the test cases are:

- **Case 1:** depth = -8 m to -14 m & Reached Velocity = 13.8 to 14.6 kn & Distance $>$ 5 nm
- **Case 2:** depth = -14 m to -19 m & Reached Velocity = 13.8 to 14.6 kn & Distance $>$ 5 nm
- **Case 3:** depth = -19 m to -29 m & Reached Velocity = 11.7 to 13.3 kn & Distance $<$ 5 nm

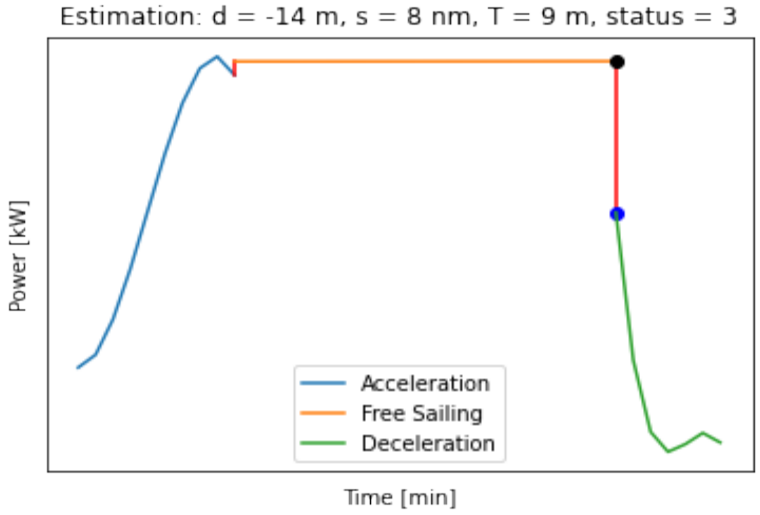

Figure 5.25: Connective area

- **Case 4:** depth = -29 m to -59 m & Reached Velocity = 11.7 to 13.3 kn & Distance $<$ 5 nm

Where for the sailing full situation, the following cases are treated:

- **Case 5:** depth = -20 m to -24 m & Reached Velocity = 11.8 to 13.5 kn & Distance $>$ 5.2 nm
- **Case 6:** depth = -24 m to -28 m & Reached Velocity = 11.8 to 13.5 kn & Distance $>$ 5.2 nm
- **Case 7:** depth = -28 m to -35 m & Reached Velocity = 10.5 to 12.5 kn & 3.2 nm $<$ Distance $<$ 5.2 nm
- **Case 8:** depth = -35 m to -59 m & Reached Velocity = 8.0 to 12.0 kn & Distance $<$ 3.2 nm

The comparison is done by first selecting a trip that suffices the requirements of the case, and calculating the energy consumption by determining the area under the power vs time graph. Subsequently, the variables depth and distance are used to estimate the energy consumption with both the VOHOP method as the new estimation tool, where E_{acc}, E_{free}, E_{dec} and E_{tot} stand for energy during acceleration, free sailing, deceleration and total energy respectively. The results are thus shown for each phase separately and at last added together to show the result of the complete trip. Hereafter, the difference between the VOHOP estimation and the difference between the estimation tool is given compared to the actual data, with subsequently the improvement/reduction shown in green or red.

Sailing Empty: Case 1 (d = -8 m to -14 m, s $>$ 5 nm & v = 13.8 kn to 14.6 kn)

The results for the comparison of Case 1 are shown in Figure 5.26 and Table 5.6. Analyzing the results per phase shows that for this case, the acceleration estimation has improvement as well as the free sailing part and its power usage during this phase, observed in Table 5.7. Only for deceleration, the new estimation tool has deteriorated. However for this example of Case 1, the total estimation of energy consumption has improved. In order to verify whether this improvement is actually occurring for every case, the subsequent paragraphs show the same procedure of comparison for the rest of the cases.

Case 1	VOHOP/ACT	EST/ACT	Improvement
$\mathbf{E}_{acc}$ [kWh]	2.05	1.30	+0.75
$\mathbf{E}_{free}$ [kWh]	1.26	0.98	+1.24
$\mathbf{E}_{dec}$ [kWh]	1.59	2.09	-0.50
$\mathbf{E}_{tot}$ [kWh]	1.45	1.18	+0.27

Table 5.6: Case 1 quantitative analysis

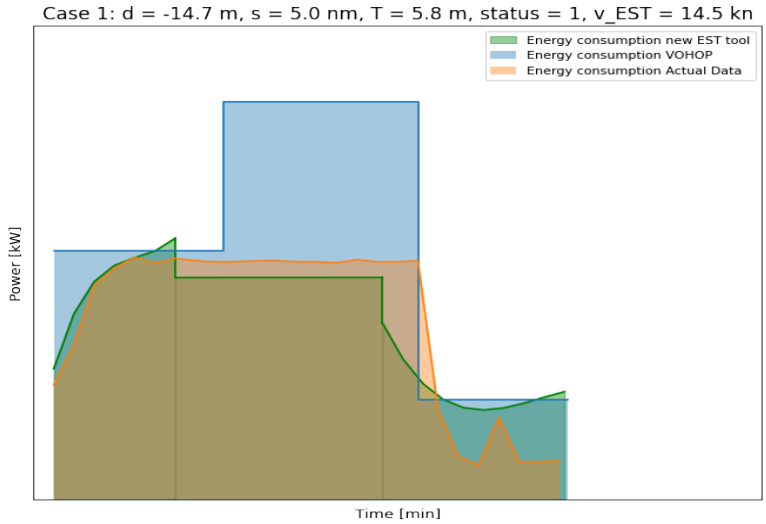

Figure 5.26: Case 1: Comparison improved estimation tool

Free Sailing	VOHOP/ACT	EST/ACT	Improvement
Power [kW]	**1.65**	**0.92**	+0.57

Table 5.7: Case 1: estimation of power

Sailing Empty: Case 2 (d = -14 m to -19 m, s > 5 nm & v = 13.8 kn to 14.6 kn)

The results for the estimation of energy consumption for Case 2 are shown in Figure 5.27 and Table 5.8. Analyzing the results per phase shows that for this case the results are the same as for Case 1: the acceleration estimation has improvement as well as the free sailing part and the power usage during free sailing according to Table 5.9. Only for deceleration, the new estimation tool has become less accurate. For this example of Case 2, the total estimation of energy consumption has improved.

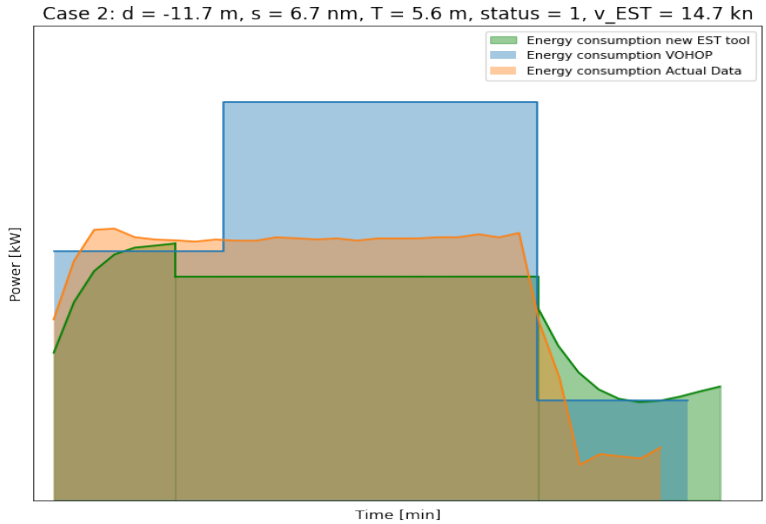

Figure 5.27: Case 2: Comparison improved estimation tool

Case 2	VOHOP/ACT	EST/ACT	Improvement
E_{acc} [kWh]	**2.08**	**1.34**	+0.74
E_{free} [kWh]	**1.24**	**0.80**	+0.04
E_{dec} [kWh]	**1.18**	**1.68**	-0.50
E_{tot} [kWh]	**1.36**	**0.97**	+0.33

Table 5.8: Case 2 quantitative analysis

Free Sailing	VOHOP/ACT	EST/ACT	Improvement
Power [kW]	1.51	0.85	+0.36

Table 5.9: Case 2: estimation of power

Sailing Empty: Case 3 (d = -19 m to -29 m, s < 5 nm & v = 11.7 kn to 13.3 kn)

The Case 3 results are shown in Figure 5.28 and Table 5.10. From the quantitative analysis, it is observed that for this case, the acceleration estimation has improved. However, the estimation for both deceleration and free sailing has deteriorated. The estimated power use of the free sailing part shows improvement, which indicates that the duration is miss-estimated as seen in Table 5.11. Where the increase of inaccuracy is small for deceleration, the free sailing part has significantly decreased in accuracy. The reason for this is the duration of the acceleration that is taken into count for in the estimation tool. The result is still a small improvement in estimation accuracy when looking at the total energy consumption. This is because the inaccuracy of the free sailing part, is taken into account for in the accelerating part.

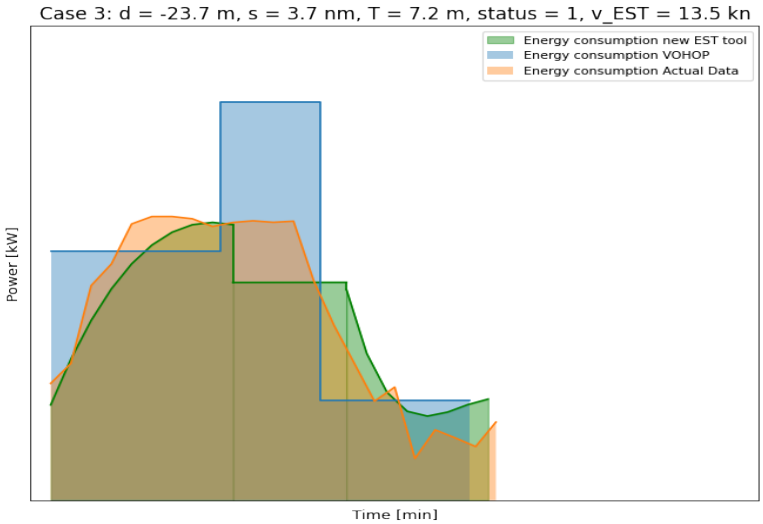

Figure 5.28: Case 3: Comparison improved estimation tool

Case 3	VOHOP/ACT	EST/ACT	Improvement
E_{acc} [kWh]	1.55	1.51	+0.04
E_{free} [kWh]	0.92	0.59	-0.33
E_{dec} [kWh]	1.05	1.09	-0.04
E_{tot} [kWh]	1.15	0.97	+0.12

Table 5.10: Case 3 quantitative analysis

Free Sailing	VOHOP/ACT	EST/ACT	Improvement
Power [kW]	1.42	0.77	+0.19

Table 5.11: Case 3: estimation of power

Sailing Empty: Case 4 (d = -29 m to -59 m, s < 5 nm & v = 11.7 kn to 13.3 kn)

The results of the Case 4 comparison are shown in Figure 5.29 and Table 5.12. The results show that for the short sailing distance, the VOHOP method and the estimation tool estimate the free sailing part to be non-existent, and the vessel is only accelerating and decelerating. The quantitative analysis shows an improvement of accuracy for the estimation tool of the acceleration phase, but a decrease in accuracy for the deceleration phase compared to VOHOP. Despite, the overall energy consumption estimation has a no improvement in accuracy. A reason for the varying results per phase is the difficulty in estimating the energy consumption for a short sailing distance. Small deviations can lead to a high percentile increase or decrease in energy usage. This can be seen in the figure by the orange curve, that shows large deflections. Moreover, the orange curve (that is defined to have a period of free sailing), does not visually show a free sailing part, this makes the estimation calculation more difficult as the actual data shows that using a fit for estimating energy consumption is not always representative.

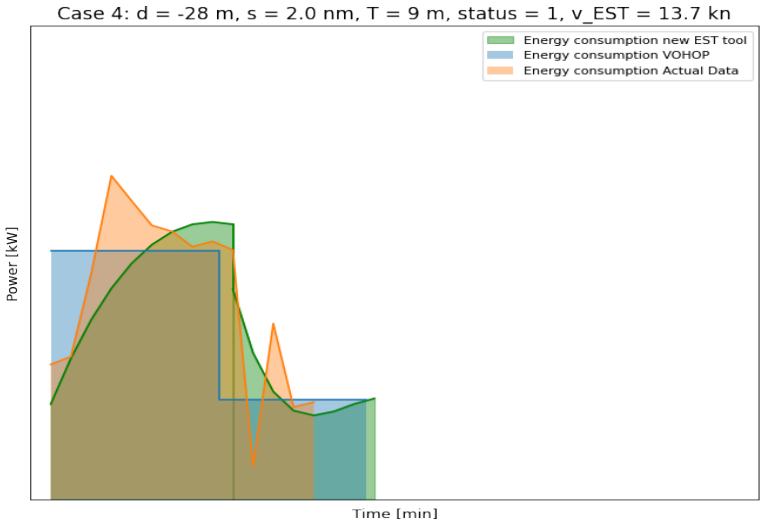

Figure 5.29: Case 4: Comparison improved estimation tool

Case 4	VOHOP/ACT	EST/ACT	Improvement
$\mathbf{E}_{acc}$ **[kWh]**	**1.41**	**1.38**	+0.03
$\mathbf{E}_{free}$ **[kWh]**	**0.00**	**0.00**	+0.00
$\mathbf{E}_{dec}$ **[kWh]**	**1.53**	**1.61**	-0.08
$\mathbf{E}_{tot}$ **[kWh]**	**0.99**	**1.03**	-0.02

Table 5.12: Case 4 quantitative analysis

Sailing Full: Case 5 (d = -20 m to -24 m, s > 5.2 nm & v = 11.8 kn to 13.5 kn)

For the sailing full cases, the Case 5 results are shown in Figure 5.30 and Table 5.13. From the quantitative analysis it can be seen that despite the improvement of estimation accuracy for acceleration and deceleration, the free sailing estimation is leading. The small inaccuracy in free sailing causes the overall energy estimation to be less accurate. The main cause of the error is, from the figure, in the considered length of acceleration, where free sailing has already started. However, the estimation tool does show a representative fit of the total trip whereas the power usage is estimated more accurately according to Table 5.14.

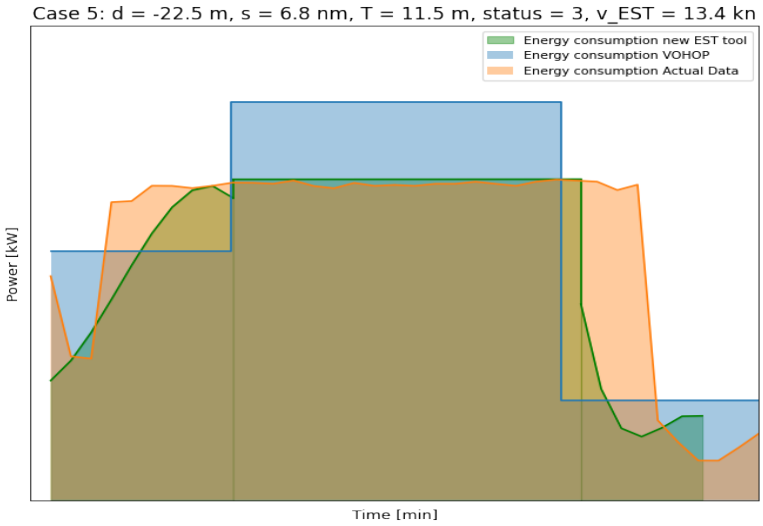

Figure 5.30: Case 5: Comparison improved estimation tool

Case 5	VOHOP/ACT	EST/ACT	Improvement
E_{acc} [kWh]	1.25	1.20	+0.05
E_{free} [kWh]	0.91	0.77	-0.14
E_{dec} [kWh]	3.89	2.06	+1.83
E_{tot} [kWh]	1.06	0.89	-0.05

Table 5.13: Case 5 quantitative analysis

Free Sailing	VOHOP/ACT	EST/ACT	Improvement
Power [kW]	1.27	1.02	+0.25

Table 5.14: Case 5: estimation of power

Sailing Full: Case 6 (d = -24 m to -28 m, s > 5.2 nm & v = 11.8 kn to 13.5 kn)

The results of Case 6 are shown in Figure 5.31 and Table 5.15. The results show an improvement for the acceleration phase and deceleration phase. The free sailing phase has a small deterioration, however Table 5.16 shows that the power usage during this phase is estimated more accurate. However, the overall energy consumption estimation does have an improvement. For this example the acceleration phase was taken account for a to long duration, which caused a too low free sailing estimation.

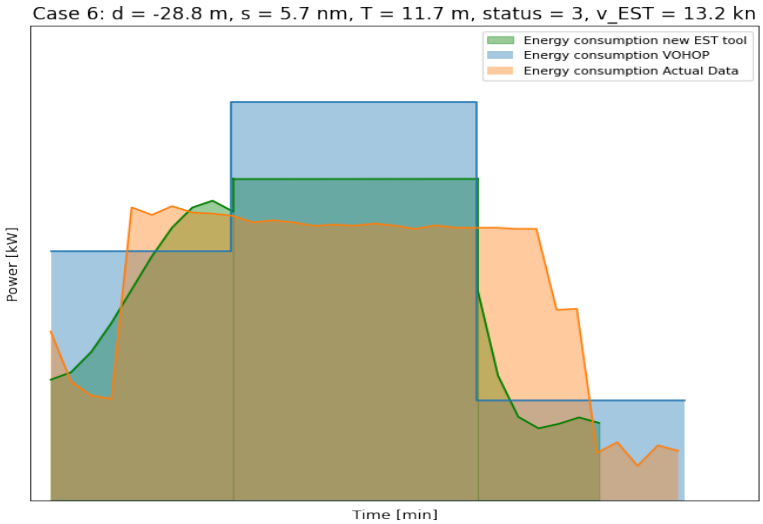

Figure 5.31: Case 6: Comparison improved estimation tool

Case 6	VOHOP/ACT	EST/ACT	Improvement
E_{acc} [kWh]	1.30	1.16	+0.14
E_{free} [kWh]	0.99	0.81	-0.18
E_{dec} [kWh]	3.25	1.84	+1.41
E_{tot} [kWh]	1.18	0.94	+0.12

Table 5.15: Case 6 quantitative analysis

Free Sailing	VOHOP/ACT	EST/ACT	Improvement
Power [kW]	1.38	1.12	+0.26

Table 5.16: Case 6: estimation of power

Sailing Full: Case 7 (d = -28 m to -35 m, s = 3.2 nm to 5.2 nm & v = 10.5 kn to 12.5 kn)

The results for Case 7 are shown in Figure 5.32 and Table 5.17. Despite large inaccuracies for acceleration and deceleration, the estimation tool shows a total improvement for the energy consumption. This is due to the relative small energy consumption for deceleration and the accurate estimation for free sailing. Besides, the power usage shows improvement of estimation by the new estimation method compared to VOHOP shown in Table 5.18.

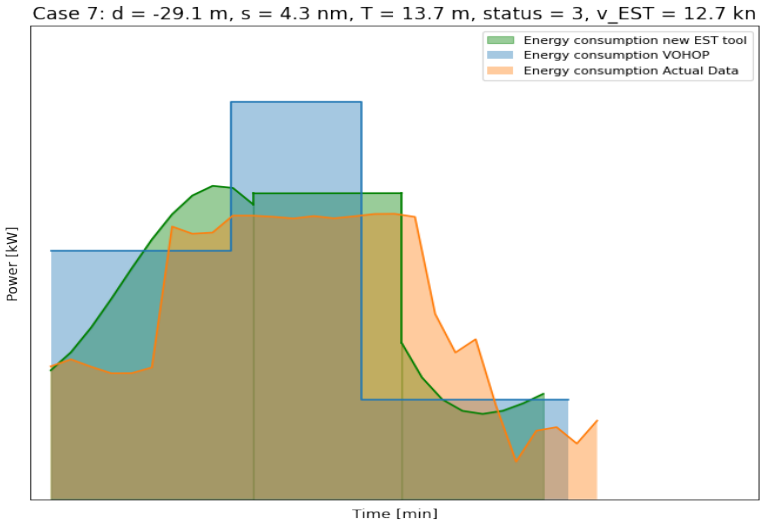

Figure 5.32: Case 7: Comparison improved estimation tool

Case 7	VOHOP/ACT	EST/ACT	Improvement
E_{acc} [kWh]	1.14	1.25	-0.11
E_{free} [kWh]	1.12	0.97	+0.09
E_{dec} [kWh]	1.02	0.71	-0.27
E_{tot} [kWh]	1.11	1.02	+0.09

Table 5.17: Case 7 quantitative analysis

Free Sailing	VOHOP/ACT	EST/ACT	Improvement
Power [kW]	1.41	1.08	+0.33

Table 5.18: Case 7: estimation of power

Sailing Full: Case 8 (d = -35 m to -59 m, s < 3.2 nm & v = 8.0 kn to 12.0 kn)

The last treated case, Case 8, shows a significant improvement. This can be seen in Figure 5.33 and Table 5.19. It shows an improvement of accuracy in every phase of the trip. The VOHOP estimation considered the sailing distance too short to reach free sailing. The figure shows that this interpretation can be of discussion as there is no clear distinction between accelerating and decelerating. However, the estimation tool, also takes into account a very small duration of free sailing. Despite the fact that there is no free sailing calculated by VOHOP, the power usage is still shown for the estimation and for the actual data to show the accuracy, see Table 5.20. The resulting comparison leads to an overall improvement of energy consumption estimation. However, for this short sailing distances it is observed that the power fit has large deviations. This makes estimating the energy consumption more difficult as the next trip could deviate again and could show different results.

Case 8	VOHOP/ACT	EST/ACT	Improvement
E_{acc} [kWh]	1.60	1.15	+0.45
E_{free} [kWh]	0.00	1.35	+0.65
E_{dec} [kWh]	2.04	1.13	+0.91
E_{tot} [kWh]	1.33	1.19	+0.14

Table 5.19: Case 8 quantitative analysis

Free Sailing	VOHOP/ACT	EST/ACT	Improvement
Power [kW]	-	1.15	-

Table 5.20: Case 8: estimation of power

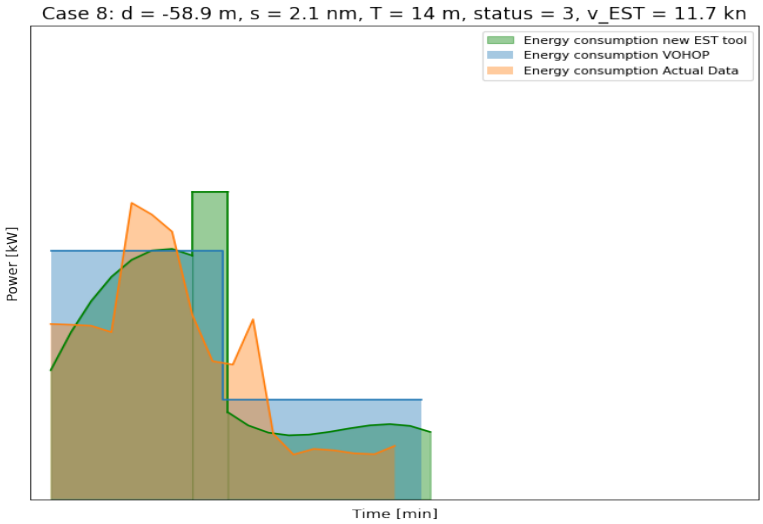

Figure 5.33: Case 8: Comparison improved estimation tool

5.2.2 Case Study Evaluation

The case studies show the comparison between the VOHOP estimation method and the newly created estimation method. Some key findings from the case study are pointed out. The acceleration estimation shows an improvement in 7 out of 8 cases, only case study 7 does not show improvement in estimating acceleration comapred to VOHOP, which might be due to the generalised definition of acceleration used in the new estimation tool. This causes the new estimation tool to take certain time of free sailing into account as acceleration, leading to a too high energy consumption for acceleration. Remarkable is the consistent overestimation conducted by VOHOP for acceleration, free sailing and deceleration. For free sailing, the results are fluctuating (either lower compared to actual data or higher compared to actual data), where an improvement is only shown in half of the case studies. From the figures, it is observed that the reason for possible miss-estimations is not due to a wrong power estimation, but due to a wrong duration estimation. From the tables, the maximum fluctuation in estimated power usage by the new estimation method is a factor 1.15 of the actual used power. The fluctuation estimated by VOHOP shows a fluctuation that increases up to 1.65 times the actual power usage. For deceleration, the results are fluctuation even more significantly than for the free sailing phase. The reason for this might be due to external factors, that play a more significant role in decelerating, however play a less important role in the total energy consumption. The main takeaway from the case study is that the results indicate that the new estimation tool does actually show improvement compared to the VOHOP estimation. However some improvements are usefull in defining the duration of acceleration and free sailing in order to improve accuracy of the new estimation tool even more. To summarize on the improvements of energy estimation for the case studies, Table 5.21 shows an overview of all cases and the resulting improvement for total energy and power consumption.

	Improvement Etot	**Improvement Ptot**
Case 1: d = -8m to -14m, s > 5 nm & v = 13.8 kn to 14.6 kn	+0.27	+0.57
Case 2: d = -14m to -19m, s > 5 nm & v = 13.8 kn to 14.6 kn	+0.33	+0.36
Case 3: d = -19m to -29m, s < 5 nm & v = 11.7 kn to 13.3 kn	+0.12	+0.19
Case 4: d = -29 m to -59m, s < 5 nm & v = 11.7 kn to 13.3 kn	-0.02	None
Case 5: d = -20m to -24m, s > 5.2 nm & v = 11.8 kn to 13.5 kn	-0.05	+0.25
Case 6: d = -24m to -28m, s > 5.2 nm & v = 11.8 kn to 13.5 kn	+0.12	+0.26
Case 7: d = -28m to -35m, s = 3.2 nm to 5.2 nm & v = 10.5 kn to 12.5 kn	+0.09	+0.33
Case 8: d = -35m to -59m, s < 3.2 nm & v = 8.0 kn to 12.0 kn	+0.14	None

Table 5.21: Overview of case results

The research concerns multiple variations in depth, distance and draught. Figure 5.34 and Figure 5.35 show the range of which depth, distance or draught is observed for the sailing empty and the sailing full stage respectively. It therefore also shows which situations have not been examined and are useful to do research on in a further study. To elaborate on the figures, Figure 5.34 shows that in this research, for sailing empty a maximum draught of T $\approx$ 9 m is observed. If the estimation tool is used for empty dredging vessels with a larger draught than this value, deviations might occur as no research is done towards this situation. For the

observed depth range the same limitations hold as this research only observed up to a depth of d ≈ 60 m. A situation of larger depth is therefore not taken into account in this research and might lead to deviating results. At last for the distance there are different ranges that are treated in this research. For the relatively smaller depths (d ≈ 8 to 14 m) this research created an estimation based on a relatively large sailing distance (s ≈ 7.5 nm). From the figure it can be observed that for a relatively large depth, this range of distance is not treated. The same holds for a relatively smaller distance paired with a smaller depth as this is also not observed in this research.
To add on the limitations, the green area in Figure 5.34 and Figure 5.35 corresponds to data observed by means of observing a relatively smaller amount of data (the Project B project). For this reason, the output of an estimation in this area will be less reliable than for the other areas.

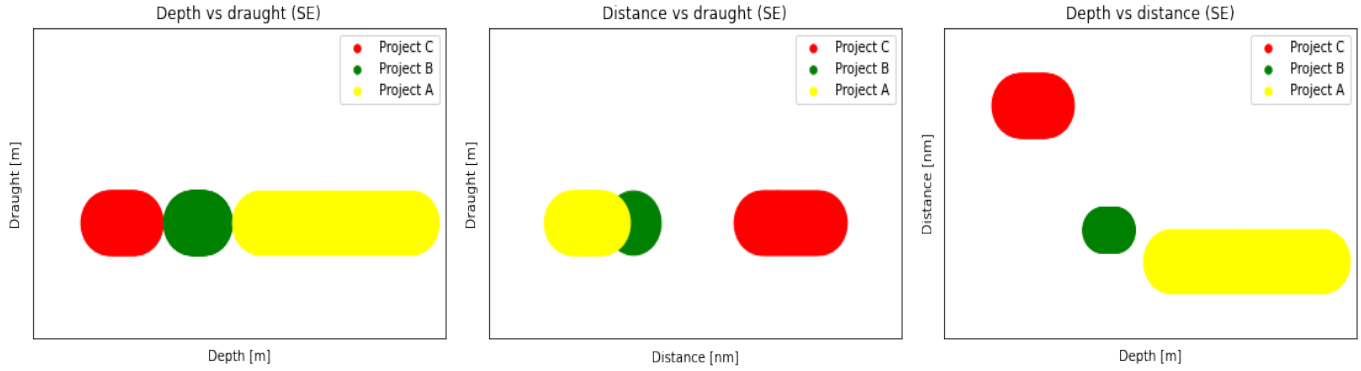

(a) Relation of depth and draught (SE) (b) Relation of distance and draught (SE) (c) Relation of depth and distance (SE)

Figure 5.34: Relation between depth, distance and draught (SE)

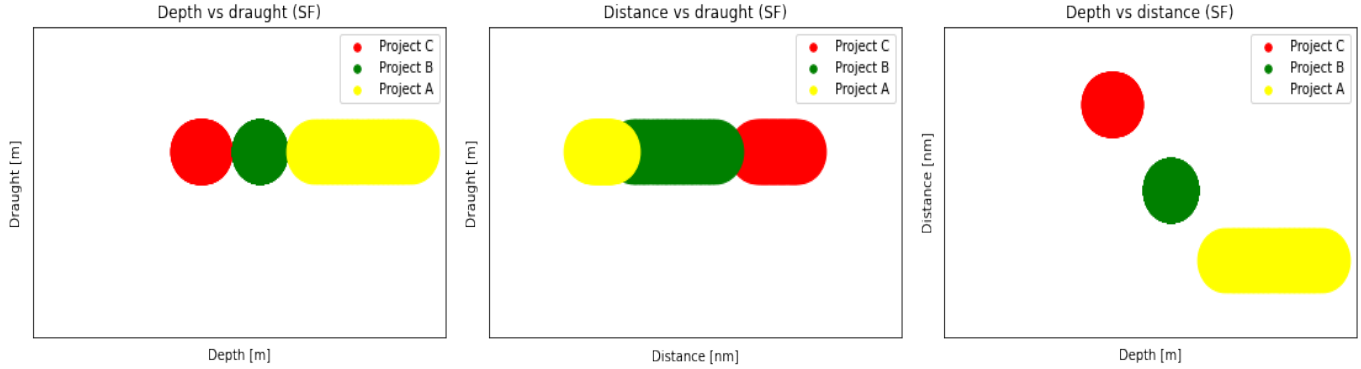

(a) Relation of depth and draught (SF) (b) Relation of distance and draught (SF) (c) Relation of depth and distance (SF)

Figure 5.35: Relation between depth, distance and draught (SF)

5.3 Conclusion

In this chapter, the estimation analysis and the actual data are compared to each other to evaluate the difference and subsequently to create an improved method for estimation. After this, the improved method is tested to verify whether the results of the estimation are more accurate. This is done by observing estimation results of eight different cases, considering different depth and distance. The depths and distances that are selected for the case studies are based on the created power fits mentioned in the previous paragraphs in order to make the comparison representative.

First the free sailing phase is evaluated. The comparison showed that the modified HM approach (HM including Karpov correction), which is the base of the new estimation tool, has a too low estimation for deep situations. The estimation is considered to be accurate for limited depth situations, however, small deviations cause significant miss-estimations. After analysing the contribution of each resistance term per different depth, the conclusion is drawn that the inaccurate estimation of the modified HM approach is caused by the inaccurate estimation of wave resistance. The reason for this is either the discrete distribution of this variable, combined with the significant increase of this variable for decreasing depth. This causes both the too low estimation for deeper depths and the high sensitivity for inaccurate estimations for more limited depths. Therefore the wave

resistance is re-calculated. This is done by analyzing multiple trips of actual data (30+ trips) and analyzing the correction that is needed for an accurate estimation of free sailing only. The pattern that is found, is a relation in increase of wave resistance paired with an increase in draught. A new formula is created for estimating the wave resistance based on draught, which shows accurate estimations for the actual data (based on 50+ trips). However, this estimation is only tested on little amount of data and further research is needed to verify whether this estimation is correct for every situation.

For the acceleration phase, the evaluation of the actual results showed that there are two types of situations that might occur. This considers the pitched situation and the non-pitched situation. The non-pitched situation described an instant increase of power, where the maximum power is reached earlier than the maximum velocity. The pitched situation describes an incremental increase of power. It is observed that the energy consumption can be decreased by using the pitched situation, however this might lead to extra duration of the trip. As the extra duration of a trip causes a too high cost pattern due to the costs of the vessel, this pitched situation is only rarely used. Therefore, the non-pitched situation is used in the estimation improvement. This improvement is done by evaluating a power fit that shows a consequent fit the acceleration follows over time. After analyzing the fit for different depth regions, where reached velocity is linked to sailed distance, different power fits were created based on distance and depth. A formula is created for which the power fit can be estimated for each situation. This lead to the resulting new estimation method for accelerating. For this phase it is important to notice that the amount of data used to create the power fit is significantly different for different depth and distances. This might lead to inconsistent results or less accurate results that need to be validated by using more data.

The deceleration phase is evaluated in a similar way as the acceleration phase. Certain depth regions are defined and reached velocity is linked to the sailed distance. The power fits are created for sailing empty and sailing full based on the common form of the deceleration pattern. The created formulas are then used to function as estimation method for decelerating. However, for the deceleration phase it is observed that large deviations take place and creating a common pattern is more difficult than for the other phases. This might have to do with possible influence of external activities. In this research a common fit is chosen, however more research and the use of more data could lead to a more accurate result.

Now that all the improvements are created for each phase of the sailing trip, the results have to be validated to state whether there is an actual improvement or not. This is done by comparing the estimation of VOHOP with the new estimation tool that is based on power fits and a proposed version of the modified HM approach. By comparing these methods with actual data, the improvement is validated by means of eight case studies for different depths and distances. Concluding from the case studies:

- E_{acc}
  Zooming into the phases of the sailing trip, the new created estimation method shows improvement on estimating the energy consumption for acceleration. In 100% of the cases, the VOHOP estimation shows an overestimation for acceleration. The new estimation method shows an improvement in 87.5% of the cases, where also for the new estimation method, the estimation is an overestimation in all cases.

- E_{free}
  The free sailing phase shows deviating results. Only in 4 out of 8 cases there is an improvement of estimation. The main pattern that is seen is an underestimation of the new estimation method. This might occur due to the definition of acceleration whereas the energy consumption that is not accounted for in the sailing free phase, is accounted for in the acceleration phase.

- E_{dec}
  For the deceleration phase, the estimation tool shows fluctuating results. As already mentioned the reason for fluctuations might be caused by external factors that play a role in the deceleration process, such as traffic. The average improvement is 35%, however this results seems unreliable as the fluctuations range from reduction in accuracy of 50% to improvement of 183%.

- E_{tot}
  For the improvement of the total estimated energy consumption, the newly created estimation method shows in 75% of the cases an improvement (based on eight cases). The estimation has an average improvement of total energy consumption of 12.75% over the eight cases compared to VOHOP. In 100% of the cases the improvement is caused, due to an overestimation of energy consumption by VOHOP, where the new estimation tool reduces this overestimation. After analysing, the main improvement in accuracy is found to be in estimating the power usage. increasing the estimation of free sailing duration might lead to even more improvement.

Overall, the new estimation tool for energy consumption shows an improvement compared to the estimation done by VOHOP. This improvement is based on implementing the parameters depth and distance and thereby creating a more accurate estimation. The resulting cases indicate that the estimated power level only shows small deviations from the actual data, with a maximum fluctuation of a factor 1.15 and minimum fluctuating factor of 0.77 compared to the actual data and shows an average inaccuracy of power estimation of 12% of the actual data. The VOHOP estimation shows a maximum fluctuation of 1.65 times the actual data and has an average miss-estimation of 1.44 times the actual power use. However, the duration of the phases shows more fluctuations, which causes miss-estimations. Overall the result is an improvement compared to the current estimation method. Therefore, this chapter contributes to answering the fourth sub-question (iv.): How to **develop** and **validate** a model to evaluate and improve the estimation of energy consumption. Nonetheless, the research shows some deviating results that make room for discussion. Therefore in the next chapter, the Discussion and Conclusion is treated.

6 Discussion and Conclusion

This chapter explains and analyzes the results of this study. Section 6.1 consists of the discussion that summarizes the main findings of this study and identifies certain interpretations of the results. The discussion section is designed to address the significance, importance and relevance of the results after which the some limitations of the research are mentioned followed by the recommendations for practical actions or scientific studies that should follow this research. Section 6.2 contains the conclusion of this study. This section provides the answer to the main objective of the research. A reflection is made by summarizing the research. The main insights are stated and certain arguments that emerged are mentioned.

6.1 Discussion

This chapter describes the discussion of this study. The interpretation of the results is explained, along with the implication of why the results are important. Any limitations are acknowledged and explained, followed by certain recommendations.

6.1.1 Summary of Results

The main research problem, as mentioned in Section 1.2, consisted of the inaccuracy of the current estimation method used by Van Oord, called VOHOP, for the arising complex situations consisting of shallow water dredging or short distance sailing. This research was done to develop an improved method for estimating energy consumption. After identifying that improvement in the sailing phases of a dredging cycle is most valuable, the research focused on these phases only. Alternative estimation methods are analyzed and selected to be used as a new estimation method, allowing the use of both empirical and physical estimates. The results indicate that by taking into account the effect of varying depths and varying sailing distances, an improvement in the method for estimating energy consumption is achieved using the estimation method proposed by Holtrop & Mennen (HM) inlcuding modifications for shallower depths as a basis. The analysis of the modified Holtrop & Mennen estimation method shows that the actual energy consumption observed in historical data is significantly higher than the modified HM method suggests. Further analysis shows the relationship between wave resistance and vessel draught with respect to depth and identifies the steps needed to improve the estimate of energy consumption, with all findings based on actual data. The overall result is a new estimation tool that is based on both the estimation method proposed by modified Holtrop & Mennen and real data and is able to more accurately estimate energy consumption for different depths and distances. This improvement is based on either a created data based correction for the free sailing part of the sailing stage and the use of a generalized power fit for acceleration and deceleration depending on the observed parameters based on the historical data. In addition, the results indicate a significant improvement in accuracy for the estimation of power consumption during free sailing, suggesting that there are other parameters, such as trip duration, that play a role in the remaining inaccuracy of the estimation method.

6.1.2 Interpretations and Implications

Before indicating the interpretation of the study, it is important to state the implications in relation to the existing literature reviewed. The purpose of this section is to ascertain whether the results of this study are in line with previous studies. In addition, this section indicates whether the results are in line with the expectations of the study and to explain certain unexpected results. The modified HM estimation method is found to be suitable for estimating energy consumption and is tested using actual data. The results indicate that, consistent with other studies on the Holtrop & Mennen (1982) approach, the energy consumption estimation results are considered to be too low. Other studies performed by Rotteveel (2013) and Zeng (2018) have pointed out that for limited water depths, the HM approach is considered inaccurate and therefore created modifications based on limited water depths. The results verify this claim by comparing the estimation method with actual results and providing a new understanding of the relationship between water depths and wave

resistance estimations. Whereas other studies have focused on the required correction for limited water depths, these results demonstrate that despite the proposed modifications for limited water depths, the modified HM estimation shows an asymptotic behaviour for decreasing depths which causes the estimation to become sensitive. In addition, the method also shows deviations in estimation accuracy for increasing depth. Therefore the importance of a correction factor for both limited water depths and deeper water depths is stated. The expected outcome of the study is to demonstrate the correlation of shallow depths with higher power consumption, as more resistance is expected at the same speed for limited depths. However, contrary to the hypothesis, the relationship between depth and power consumption appears to be fluctuating. analyzing acceleration, free sailing and deceleration separately indicates that the free sailing phase shows a significant correlation between the draught of the vessel with respect to the depth and the power used by the vessel. For the acceleration and deceleration part, the results are fluctuating, since limited depths do not necessarily lead to the highest power consumption. Another hypothesis of this research is to demonstrate the correlation between a lower achieved speed and a short sailing distance and, in addition, the influence of the acceleration and deceleration phase that becomes more significant at smaller sailing distances. The results of this study are consistent with this hypothesis since this expectation is met for both sailing empty and sailing full. In addition, the values of the achieved speed were linked to the sailing distance in order to produce an improved estimation tool. The resulting estimation tool shows improvement in estimating the total energy during a sailing trip. The results suggest that the fluctuations are mainly caused by incorrect estimations of duration rather than power consumption, since the estimation of power consumption has a significantly higher accuracy.

6.1.3 Limitations

During the study, some limitations came to light that may affect the results. Therefore, these limitations are listed and discussed. The nature of the limitations may vary from the general design of the study to specific methodological choices. After mentioning the limitations, their effect is evaluated.

The first limitation of this study concerns the scope of the study. The current results are based on a certain type of TSHD solely. This limitation means that the results are only valid for this type of vessel and other types of vessels, carrying different equipment, may produce different results. However, the method for evaluating and improving the estimation method is useful for other vessel types. In addition to the limitation of scope, this study focuses only on the sailing phases, while the overall dredging cycle consists of other phases as well. Whereas the current estimation method for sailing was based only on a small number of parameters, and was therefore chosen to evaluate, an improvement for the other phases could also be valuable.

Another limitation concerns the amount of data, where a smaller sample size increases the uncertainty of the results. After analyzing several projects, the three selected projects were found to have the most data, and the most workable data. However, the results show that, despite the selection process, the sample size of one of the projects is considered small (less than 120 trips) and therefore the results of the analysis of this project are less certain. Nevertheless, the exclusion of this project limits the possibility of providing some insight into the depths, as the other selected projects had more limited depths. In addition, when validating the results, the created estimation method was compared to VOHOP in eight different cases. These cases covered different types of situations to show what the results are. However, by expanding the number of experiments, the reliability of the results also increases.

The number of filters applied to the data is limited, increasing the likelihood of using unreliable data in the study. The reason for using a limited number of filters is the small amount of data, where applying more filters would result in even less data to use. This lack of data also decreases reliability. In addition, some of the filters are based on visual interpretation, which is less reliable than statistically determined filters. This limitation makes it difficult to determine the uncertainty of the data and thus the uncertainty of the results.

In this study, averaging and fitting of data is used. When performing this process, the reliability of the outcome decreases. To determine the reliability of the data used, or in other words, to test how uncertain the data is, a goodness of fit test is needed. This test is performed to analyze how reliable the speed and propulsion values used are, but this procedure must be performed for each time the data set is generalized. In particular, when the power fit is established for acceleration and deceleration, assumptions are made that give more uncertainty to the result.

To simplify the understanding and workability of the system, several assumptions are made. First, certain parameters are assumed to remain constant during the trip, such as depth and draught. This allows the user to proceed, where without assumptions the study would face uncertainties. Second, the results do not take into account external influences such as weather conditions, currents or traffic conditions. The estimation and

analysis of energy consumption assumes that the vessel has no limitations with respect to these external activities. Especially at limited depths, the influence of currents can become more significant and disregarding these effects gives more uncertainty to the results. It could also give a clear picture of why certain fluctuations occur. Another assumption includes the definition of acceleration, free sailing and deceleration. The assumptions are tested using a visual perspective, which also emerges in the study. However, these definitions are not yet firm and other perspectives could give rise to changes in the definition. Using a different definition for the phases could lead to anomalous results. In addition, the chosen definition of shallow depth and deep depth is only divided into four different regions of depth, where between these regions there could be a large variability in energy consumption.

6.1.4 Recommendations

The results of this study indicated that although the estimation model created shows an increase in accuracy for the total energy consumption of a sailing phase, there are still deviations in the estimation model from the actual data. However, the results showed that the estimation of the power use was not the main cause of the anomalous results of the estimation, as the resulting power use was similar to the actual energy consumption. Therefore, it is suggested that the difference in energy consumption is caused by the estimated duration of the phases of a trip. A follow-up study on improving the estimation of the duration of a sailing trip will provide more insight into the duration per phase, increasing the probability of an accurate estimate when the accurately estimated duration is combined with the, already, accurately estimated power consumption.

The estimation tool created in this study can be used to estimate energy consumption for future projects with multiple input variables. However, more research on the influence of other external factors could increase the number of input variables, thus increasing the accuracy of the estimation tool. Whereas only depth and distance were considered in this study, other influences, such as current, could provide more accurate results. By calculating the effect of external factors and including them in the calculation proposed in the new estimation tool, a more certain estimate can be made.

A follow-up study is recommended using the same methodology as this study, but with a larger amount of data. The quality and lack of data decreased the reliability of this study. By using more data and selecting the right data, the research becomes less uncertain. In addition, the data results are more accurate which will improve the quality of the estimate. An increase in sample size also allows more variations of situations to be observed. This study distinguished only a few levels of depth and distance, whereas more data could provide sufficient material to draw conclusions from more specific types of situations.

This study focuses only on the sailing phases of a dredging cycle, as it has been determined that this is the least accurate phase in which estimates are made. However, an evaluation and, if necessary, improvement of the estimation accuracy for the other phases (loading and discharging) could be of value. Further study of all four phases of the dredging cycle is needed to arrive at an estimation tool for the entire dredging cycle, where the estimate is based on real data. By using the estimation tool in combination with the simulation software OpenCLSim, the energy consumption of dredging projects can be simulated in the future, before they are implemented. In addition to this recommendation, a further study is needed to provide the possibility of implementing different dredging strategies in the estimation tool. In this way, different dredging strategies can be compared, resulting in an overview where the user can choose the optimal outcome. The methodology for implementing this recommendation is by reusing the same methodology as in this study and providing an estimate based on actual data.

A further study that validates the correctness of certain assumptions is required. In general, of the assumptions implemented in this study, it is first necessary to clarify their consequence by providing a coefficient of determination that indicates the level at which the reliability of the results is affected by the assumptions. Then, after quantifying this goodness of fit, it is important to take into account this measure of reliability when observing the results. Finally, measures can be taken to increase this goodness of fit, and thus the reliability of the study. In this study, depth was assumed to remain constant throughout the trip, while in reality fluctuations occur. A follow-up study on the influence of increasing or decreasing depth will provide more information on the estimation accuracy for this type of situation. By choosing the specified situation (e.g., increasing depth during deceleration) as the type of situation, the study is conducted using a similar methodology as this study. The starting point of deceleration (or the ending point of acceleration) could depend on the increase or decrease in depth for a specified situation. Implementing this feature in the estimation tool would allow the user to take these specific situations into account. In addition to this recommendation, further research on the assumption of the definition of acceleration, free speed, and deceleration provides more certainty in the estimation tool. Currently, the definition of the three phases is based only on three projects and on visual observation. A clear

and justified definition increases the reliability of the results.

This research mainly focuses on the non-pitched situation, where the power is instantly increased to the maximum value, while the velocity cannot handle this instant increase and thus energy is lost. Using the pitched situation, where the power is incrementally increased, saves energy but leads to a longer time duration. A cost-benefit analysis is important. In the current situation, Van Oord's vessels mainly use the non-pitched situation because the extra time it takes to use the pitched situation does not outweigh the extra costs it entails. However, with the upcoming charges for non-pitched procedures and the rising cost of fuels, this could become leading in the near future. A closer study of the trade-off between time and energy will give insight into what this situation is like now, and may give an idea of what impact certain sanctions and taxes have. In addition, with the earlier recommendation to allow the user to adopt different strategies, including different types of fuels, the user could be given the opportunity to switch between sustainable and non-renewable options before the project is implemented, and gain insight into the energy pattern.

The results of this study show fluctuating results in the power fit during the acceleration, but especially, during the deceleration phase. Possible reasons for this have already been mentioned: traffic, increased maneuverability and other external influences such as currents or increasing depths when reaching the coastal zone. However, these influences are still assumed. Further investigation into the actual reason for the fluctuation for both the acceleration and deceleration phases will provide more clarity in the results. It also provides an opportunity to conduct research on predicting certain external influences prior to project implementation so that these predictions can be implemented in the estimation tool, increasing its certainty and therefore accuracy.

6.2 Conclusion

This section describes the conclusion of this research. In this section, the answer to the research objective is clearly stated. A summary is given showing the research and the relevance of this study.

This study was conducted to evaluate and improve the current estimation method used by Van Oord, called VOHOP. VOHOP does not meet the situations that arise today, such as sailing over short distances and limited depths. The need to improve the energy consumption estimation is the increased environmental awareness. More consequences for performing over- or underestimates of fuel consumption are emerging as certain penalties begin to play a role. This required improvement in accuracy for estimating energy consumption for these emerging complex situations lead to the following research objective:

"To improve estimation of energy consumption for dredging activities based on actual data."

This research goal is achieved by first conducting a literature review stating the basic principles of a dredging cycle and the relevance of improving the estimation. After identifying that improvement of the estimation of the sailing phases of the dredging cycle is considered valuable, this research only focused on the sailing phases. Several existing estimation methods for estimating energy consumption during sailing activities are discussed, of which the method proposed by Holtrop & Mennen (HM) is selected as the most suitable for comparison with the VOHOP. The literature review revealed some existing corrections that have already been applied to the Holtrop & Mennen approach, mainly aimed at estimating the energy consumption for limited depths. One of the proposed corrections was introduced by Karpov (Rotteveel, 2013), a correction based on the ratio of depth to draught, which discreetly increased the wave resistance for shallower depths. After analyzing the difference between the original method proposed by Holtrop & Mennen and the modified form including Karpov's correction, it was considered to use the modified method in this study, since the application of the correction is useful for the situations to be observed (limited depths).

To indicate the difference between VOHOP and the chosen modified Holtrop & Mennen approach, both estimation methods are compared and the differences are analyzed. Where the difference is compared for a given base-case situation, resulting in a higher energy use for VOHOP. The calculations were performed in a Python environment, using the software application OpenClSim, which simulates the dredging cycle. The reason for using the OpenCLSim environment is that this package has already been tested by previous studies and has proven to be useful for simulating recurrence concepts. In addition, it allows the user to easily vary input variables to create a new estimation method, and reduces time by sequentially estimating energy consumption for the dredging cycles. Now that the difference in estimation methods has been validated, it is important to find out which estimation method is more accurate, and how modified HM can be improved to produce a better estimate of energy consumption.

Historical data provided by Van Oord has been analyzed to serve as comparison material. The actual data used is based on a TSHD. Before the data can be used for comparison, filters are applied so that only representative data is used such as removing zero-valued sensor data or cutting out outliers in data. After applying the different filters, the data is compared using the modified Holtrop & Mennen approach, where each part of the sailing phase, consisting of acceleration, free sailing and deceleration, is treated separately. The new estimation method was developed to provide an accurate estimate of energy consumption in complex situations encountered today, such as reduced depths and short sailing distances. Accordingly, the type of situations observed consist of varying depths and distances, where limited distances lead to a limited speed achieved, since the vessel is not able to reach the maximum speed in the short distance. Within the sample size of the data, three projects were selected to be representative because of the difference in depth and distance and because of the volume of data available for these projects.

With the estimation model chosen (modified HM) and the actual data selected and filtered, the two are compared. Two conclusions are drawn from the comparison of the free sailing part: The modified Holtrop & Mennen approach is considered to have too low estimate for deep depth situations, and is too sensitive for both deep depth and limited depth. The reason for the low estimate is the insignificant contribution of wave resistance for deeper depths, and furthermore, after analyzing the relationship between the actual power used and various parameters, larger draughts with respect to water depth are related to larger wave resistance. A correction factor is created that corrects the value of wave resistance based on varying draughts so that the total resistance is accurately calculated according to actual data. The corrected estimate for free sailing is tested for different cases of actual data.

Second, the acceleration phase and the deceleration phase are observed. For these phases, a comparison of the modified Holtrop & Mennen approach with the actual data is unusual, since the actual data indicates the power used including certain phenomenon such as propeller slip, while the estimation method calculates the power required. Because of the large differences, and the untenable method of acceleration, the comparison is not made on behalf of modified HM. The improved estimation is made by looking for a fit to be found between power consumption during acceleration/deceleration and making the corresponding fit for different areas of depth and distance. This has led to the creation of estimation fits for both limited depths and short sailing distances, which is applied in the new estimation tool.

The newly created estimation tool consists of three phases: acceleration, free sailing and deceleration. Each estimation tool has as input variables the different depth/draught and distance considered, where the distance sailed is related to the velocity achieved. The new estimation tool is compared with VOHOP to validate whether there is an actual improvement. Eight cases of actual trips consisting of different depths and different sailing distances are used to validate the results. The comparison indicates the following:

- An improve in estimation is found for estimating the acceleration phase based on depth and distance by using the new estimation method
- Estimating the free sailing phase has either improvements and reductions in accuracy. The reason for fluctuations is the definition of free sailing for the estimation method.
- Estimating the deceleration phase shows improvements in accuracy, however estimating deceleration is considered to be difficult due to large fluctuations.
- In total, the estimation of energy consumption has improved in accuracy for the new estimation method compared to the method used by Van Oord based on the eight cases.

The result of this research is a new estimation tool based on real data that shows an improvement in the accuracy of energy consumption estimation, which meets the main objective of this research. However, the study also suggests a significant improvement in the accuracy of the power consumption estimates during the free sailing phase. Where the energy estimate shows some deviations from the actual data, the power consumption shows similar results. With the known anomalous results for estimating energy consumption and the accurate estimation of power consumption, it is suggested that the estimation of the duration of a sailing trip is the most important factor in causing erroneous estimates. Despite the validated results within this study, a follow-up study is recommended to improve the reliability of the results and to increase the accuracy of the estimate. As mentioned, a follow-up study to increase the accuracy of the estimation of the duration of each stage will provide more insight into the energy consumption during a trip, which will increase the possibility of further improving the new estimation tool as power consumption is indicated to show an accurate result.

Bibliography

1. Althens. (2022). Rekstrookjes | Althen Sensors. Retrieved June 19, 2022, from https://www.althensensors.com/nl/sensoren/rekstrookjes/:%7E:text=De%20werking%20van%20een%20rekstrookje,hoogte%2Dbreedteverhouding%20van%20deze%20rechthoek.

2. Anzanello, D. (2014, October 22). How To Determine Propeller Slip. Teague Custom Marine. Retrieved June 19, 2022, from https://teaguecustommarine.com/teagueblog/how-to-correctly-determine-propeller-slip/

3. Bertram, V., Schneekluth, H. (1998). Ship Design for Efficiency and Economy (2nd edition). Elsevier. https://doi.org/10.1016/B978-0-7506-4133-3.X5000-2

4. Bianconi, G. (2002). Shallow Seas Ecosystems. eLS. https://doi.org/10.1038/npg.els.0003193

5. Bolt, E. (2003, October 22). Schatting energiegebruik. DOCplayer. Retrieved June 15, 2022, from http://docplayer.nl/8600238-Schatting-energiegebruik-binnenvaartschepen.html

6. Chakraborty, S. (2021, December 6). What's The Importance Of Bulbous Bow Of Ships? Marine Insight. Retrieved February 7, 2022, from https://www.marineinsight.com/naval-architecture/why-do-ships-have-bulbous-bow/

7. Corporate Finance Institute. (2022, May 7). R-Squared. Retrieved June 19, 2022, from https://corporatefinanceinstitute.com/resources/knowledge/other/r-squared/

8. Data Science Team. (2020, May 8). R-Squared Definition. DATA SCIENCE. Retrieved June 19, 2022, from https://datascience.eu/mathematics-statistics/r-squared-definition/

9. Dutch Water Sector. (2016). Van Oord completes ground improvement on reclaimed land for Al-Zour refinery, Kuwait | Dutch Water Sector. Retrieved June 19, 2022, from https://www.dutchwatersector.com/news/van-oord-completes-ground-improvement-on-reclaimed-land-for-al-zour-refinery-kuwait

10. ECN Planbureau voor de Leefomgeving. (2014, September). EU-doelen klimaat en energie 2030: Impact op Nederland (No. 1394). https://www.pbl.nl/sites/default/files/downloads/pbl-2014-eu-doelen-klimaat-en-energie-2030-impact-op-nederland_01394.pdf

11. European Commission. (2022). EU Emissions Trading System (EU ETS). Retrieved November 14, 2021, from https://ec.europa.eu/clima/eu-action/eu-emissions-trading-system-eu-ets_en

12. EUC. (2020). Langetermijnstrategie voor 2050. European Commission. Retrieved December 18, 2021, from https://ec.europa.eu/clima/eu-action/climate-strategies-targets/2050-long-term-strategy_nl

13. European Dredging Association. (2022). EuDA - About dredging - Dredging - Reasons for Dredging. EuDA. Retrieved November 8, 2022, from https://european-dredging.eu/Reasons_for_Dredging

14. Goldsworthy, L., Goldsworthy, B. (2013). Modelling of ship engine exhaust emissions in ports and extensive coastal waters based on terrestrial AIS data - An Australian Case Study. Elsevier, 45–60. https://www.sciencedirect.com/science/article/pii/S136481521400262X

15. Grosse, C. (2010). Acoustic emission (AE) evaluation of reinforced concrete structures. Non-Destructive Evaluation of Reinforced Concrete Structures, 185–214. https://doi.org/10.1533/9781845699604.2.185

16. Haldar, S. K. (2013, January 1). Elements of Mining. ScienceDirect. Retrieved November 7, 2022, from https://www.sciencedirect.com/science/article/pii/B9780124160057000118

17. Holtrop, J., Mennen, G. (1982). An Approximate Power Prediction Method. Repository TU Delft. Retrieved February 7, 2022, from https://Repository.tudelft.nl

18. IHC. (2001). HAM318 23,000m3 Trailing Suction Hopper Dredger. dredgepoint.org. Retrieved February 14, 2022, from https://www.dredgepoint.org/dredging-database/sites/default/files/attachment-equipment/ham_318.pdf

19. International Towing Tank Conference. (2002, February 2). ITTC- Recommended Procedures. ITTC. Retrieved February 4, 2022, from https://ittc.info/media/2021/75-02-02-02.pdf

20. Jackson, R. (2017). The Effects of Climate Change. Climate Change: Vital Signs of the Planet. Retrieved October 5, 2021, from https://climate.nasa.gov/effects/

21. Jajodia, P. (2017). Removing Outliers Using Standard Deviation in Python. KDnuggets. Retrieved June 3, 2022, from https://www.kdnuggets.com/2017/02/removing-outliers-standard-deviation-python.html

22. Janssen, D. G. J. (2022). Production for varying velocities [Graph].

23. Jassal, R. (2022). What is block coefficient of a ship ? - MySeaTime. MySeaTime. Retrieved February 7, 2022, from https://www.myseatime.com/discussion/what-is-block-coefficient-of-a-ship

24. Jiang, M., Segers, L. J. M., van der Werff, S. E., Hekkenberg, R. G., van Koningsveld, M., Delft University of Technology, Van Oord Marine Contractor. (2022). Enabling corridor scale estimation of inland shipping related energy consumption, fuel use and emission patterns. ., 2022, 1–20.

25. Kort, G., Hollmann, L. (2021, August 2). Onderweg naar 55% minder uitstoot in 2030: Europese Commissie presenteert 'Fit for 55' – pakket - Europa. Europa decentraal. Retrieved November 12, 2021, from https://europadecentraal.nl/europese-commissie-presenteert-fit-for-55-pakket/

26. Laboyrie, P., van Koningsveld, M., Aarninkhof, S., van Parys, M., Lee, M., Jensen, A., Csiti, A., Kolman, R., Central Dredging Association, International Association of Dredging Companies. (2018). Dredging for sustainable infrastructure. CEDA.

27. Mermaid Consultants. (2021). WAVE MAKING RESISTANCE IN SHIPS. SHIP DESIGN | NAVAL ARCHITECTS | MARINE CONSULTANTS | OFFSHORE ENGINEERING | INDIA. Retrieved March 18, 2022, from https://www.mermaid-consultants.com/ship-wave-making-resistance.html

28. Miedema, S. A. (2015). The Delft Sand, Clay Rock Cutting Model (2nd ed.). Delft University Press. https://dredging.org/media/ceda/org/documents/resources/othersonline/miedema_s.a._the_delft_sand_clay__rock_cutting_model_3rd_edition.pdf

29. Miedema, S. A., Vlasblom, W. J. (1996). Theory for Hopper Sedimentation. Researchgate, 1–23. https://www.researchgate.net/publication/271443631_THEORY_FOR_HOPPER_SEDIMENTATION

30. Miola, A., Ciuffo, B. (2011, April 1). Estimating air emissions from ships: Meta-analysis of modelling approaches and available data sources. ScienceDirect. Retrieved December 2, 2022, from https://www.sciencedirect.com/science/article/pii/S1352231011000872

31. Moreno-Gutierrez, J., Calderay, F., Saborido, N., Boile, M., Valero, R. R., Duran-Grados, V. (2015, June 15). Methodologies for estimating shipping emissions and energy consumption: A comparative analysis of current methods. ScienceDirect. Retrieved December 15, 2021, from https://www.sciencedirect.com/science/article/pii/S0360544215005502fd2

32. Murphy, J. T. (2012, June). Fuel Provisions For Dredging Projects. Fuel Provisisons for Dredging Projects. Retrieved October 21, 2021, from https://westerndredging.org/phocadownload/ConferencePresentations/2012_SanAntonioTX/2B-4%20Murphy.pdf

33. Navalapp. (2022). What is the Froude number? Navalapp - Sailing Yacht Design Performance. Retrieved February 7, 2022, from https://navalapp.com/articles/what-is-the-froude-number/

34. NovAtel. (2022). Real-Time Kinematic (RTK). Retrieved June 19, 2022, from https://novatel.com/an-introduction-to-gnss/chapter-5-resolving-errors/real-time-kinematic-rtk

35. Panagiotopoulos, T. (2022). Propeller slip and its role to the boat's performance. E-Ribbing.Com. Retrieved June 19, 2022, from https://e-ribbing.com/en/propellers/296-propeller-slip-and-its-role-to-the-boat-performance.html

36. Raunek, R. (2022, April 21). The Importance of Vessel Tracking System. Marine Insight. Retrieved June 19, 2022, from https://www.marineinsight.com/marine-safety/the-importance-of-vessel-tracking-system/

37. Rawson, K. J. (2001, January 1). Basic Ship Theory. ScienceDirect. Retrieved February 7, 2022, from https://www.sciencedirect.com/science/article/pii/B9780750653985500054

38. Rijkswaterstaat. (2021, September 21). CO2-prestatieladder. Retrieved November 14, 2021, from https://www.rijkswaterstaat.nl/zakelijk/zakendoen-met-rijkswaterstaat/inkoopbeleid/duurzaam-inkopen/co2-prestatieladder

39. Rijkswaterstaat. (2021, December 1). Energie en klimaat. Retrieved November 2, 2022, from https://www.rijkswaterstaat.nl/zakelijk/duurzame-leefomgeving/energie-en-klimaat

40. Roh, M. I., Lee, K. Y. (2017). Computational Ship Design. Springer Publishing. https://doi.org/10.1007/978-981-10-4885-2_5

41. Rotteveel, E. Delft University of Technology. (2013, September). Investigation of inland ship resistance, propulsion and manoeuvring using literature study and potential flow calculations.

42. Russel, D. A. (2015). Longitudinal and Transverse Wave Motion. ACS. Retrieved March 12, 2022, from https://www.acs.psu.edu/drussell/demos/waves/wavemotion.html

43. Segers, L. J. M. (2020, April). Mapping Inland Shipping Emissions in Time and Space for the Benefit of Emission Policy Development: A Case Study on the Rotterdam-Antwerp Corridor (Thesis). TU Delft.

44. Statista. (2021, November 22). Annual global emissions of carbon dioxide 1940–2020. Retrieved June 18, 2022, from https://www.statista.com/statistics/276629/global-co2-emissions/

45. The Express Tribune. (2017). Pakistan's first deep-water terminal to be ready in April. Retrieved June 19, 2022, from https://tribune.com.pk/story/1294318/karachi-port-pakistans-first-deep-water-terminal-ready-april

46. United Nations Climate Change. (2021). The Paris Agreement. UNCC. Retrieved November 13, 2021, from https://unfccc.int/process-and-meetings/the-paris-agreement/the-paris-agreement

47. Van de Ketterij, R., Stapersma, D., Kramers, C., Verheijen, L. (2009, April 2). CO2 INDEX: MATCHING THE DREDGING INDUSTRIES NEEDS WITH IMO LEGISLATION ER -. Researchgate. Retrieved November 12, 2021, from https://www.researchgate.net/publication/340387122_CO_2_INDEX_MATCHING_THE_DREDGING_INDUSTRIES_NEEDS_WITH_IMO_LEGISLATION

48. van der Bilt, V. (2019, July). Assessing Emission Performance of Dredging Projects (Thesis). TU Delft.

49. van der Schrieck, V. G. L. M. (2015). Dredging Technology CIE5300: Lecture Notes. TU Delft.

50. van Koningsveld, M., Verheij, H., Taneja, P., Vriend, H. J. (2021). Ports and Waterways. TU Delft. https://doi.org/10.5074/T.2021.004

51. Van Oord. (2016). Indrukwekkend grondverbeteringsproject in Koeweit opgeleverd | Van Oord/. Retrieved June 19, 2022, from https://www.vanoord.com/nl/updates/indrukwekkend-grondverbeteringsproject-koeweit-opgeleverd/

52. Van Oord. (2017). DPC Innovation award voor Van Oord project in de Malediven | Van Oord/. Retrieved June 19, 2022, from https://www.vanoord.com/nl/updates/dpc-innovation-award-voor-van-oord-project-de-malediven/

53. van Rhee, C. (2020, October).TU Delft Dredging Technology. Brightspace. Retrieved November 10, 2021, from https://brightspace.tudelft.nl/d2l/le/content/289203/viewContent/1961844/View

54. Ventura, M. (2022). Bulbous Bow Design. Instituto Superior Tecnico. Retrieved February 7, 2022, from http://www.mar.ist.utl.pt/mventura/Projecto-Navios-I/EN/SD-1.5.4-Bulbous%20Bow%20Design.pdf

55. Vivian, C. M. G., Murray, L. A. (2009). Dredging - an overview | ScienceDirect Topics. ScienceDirect. Retrieved November 10, 2022, from https://www.sciencedirect.com/topics/earth-and-planetary-sciences/dredging

56. Vlasblom, W. J. (2007, May). Trailing Suction Hopper Dredger. CEDA. Retrieved February 7, 2022, from https://dredging.org/documents/ceda/downloads/vlasblom2-trailing_suction_hopper_dredger.pdf

57. Vosta LMG. (2019). Jet Pumps - Components | VOSTA LMG - Dredging Technology. Retrieved October 12, 2021, from https://vostalmg.com/components/pumping-systems/jet-pumps

58. Wartsilia. (2022). Coefficients of form. Wartsila.Com. Retrieved February 7, 2022, from https://www.wartsila.com/encyclopedia/term/coefficients-of-form

59. Weng, J., Shi, K., Gan, X., Li, G., Huang, Z. (2020, March 1). Ship emission estimation with high spatial-temporal resolution in the Yangtze River estuary using AIS data. ScienceDirect. Retrieved December 2, 2021, from https://www.sciencedirect.com/science/article/pii/S0959652619341678bib17

60. Zeng, Q., Thill, C., Hekkenberg, R., Rotteveel, E. (2018). A modification of the ITTC57 correlation line for shallow water. Journal of Marine Science and Technology, 24(2), 642–657. https://doi.org/10.1007/s00773-018-0578-7

A | Appendix

A.1 Calculations

The formula for calculating 1+k2 is:

$$1 + k2 = \sum \frac{S_{APP} * 1 + k2}{\sum S_{APP}} \tag{A.1}$$

With the approximate values for 1+k2 shown in Figure A.1.

Approximate $1 + k_2$ values	
rudder behind skeg	1.5 – 2.0
rudder behind stern	1.3 – 1.5
twin-screw balance rudders	2.8
shaft brackets	3.0
skeg	1.5 – 2.0
strut bossings	3.0
hull bossings	2.0
shafts	2.0 – 4.0
stabilizer fins	2.8
dome	2.7
bilge keels	1.4

Figure A.1: Approximate Values 1+k2

A.1.1 Karpov

The calculation for enhancing wave resistance factor α_{xx} is calculated by the following discrete equation:

$$F_{nh} = V_0/np.sqrt(g * h) \tag{A.2}$$

if F_{nh} <= 0.4:
if 0 <= h / T < 1.75:

$$\alpha_{xx} = (-4 * 10^{(-12)}) * F_{nh}^3 - 0.2143 * F_{nh}^2 - 0.0643 * F_{nh} + 0.9997 \tag{A.3}$$

if 1.75 <= h / T < 2.25:

$$\alpha_{xx} = -0.8333 * F_{nh}^3 + 0.25 * F_{nh}^2 - 0.0167 * F_{nh} + 1 \tag{A.4}$$

if 2.25 <= h / T < 2.75:

$$\alpha_{xx} = -1.25 * F_{nh}^4 + 0.5833 * F_{nh}^3 - 0.0375 * F_{nh}^2 - 0.0108 * F_{nh} + 1 \tag{A.5}$$

if h / T >= 2.75:

$$\alpha_{xx} = 1 \tag{A.6}$$

if F_{nh} > 0.4: if 0 <= h / T < 1.75:

$$\alpha_{xx} = -0.9274 * F_{nh}^6 + 9.5953 * F_{nh}^5 - 37.197 * F_{nh}^4 + 69.666 * F_{nh}^3 - 65.391 * F_{nh}^2 + 28.025 * F_{nh} - 3.4143 \tag{A.7}$$

if 1.75 <= h / T < 2.25:

$$\alpha_{xx} = 2.2152 * F_{nh}^6 - 11.852 * F_{nh}^5 + 21.499 * F_{nh}^4 - 12.174 * F_{nh}^3 - 4.7873 * F_{nh}^2 + 5.8662 * F_{nh} - 0.2652 \quad \text{(A.8)}$$

if 2.25 <= h / T < 2.75:

$$\alpha_{xx} = 1.2205 * F_{nh}^6 - 5.4999 * F_{nh}^5 + 5.7966 * F_{nh}^4 + 6.6491 * F_{nh}^3 - 16.123 * F_{nh}^2 + 9.2016 * F_{nh} - 0.6342 \quad \text{(A.9)}$$

if 2.75 <= h / T < 3.25:

$$\alpha_{xx} = -0.4085 * F_{nh}^6 + 4.534 * F_{nh}^5 - 18.443 * F_{nh}^4 + 35.744 * F_{nh}^3 - 34.381 * F_{nh}^2 + 15.042 * F_{nh} - 1.3807 \quad \text{(A.10)}$$

if 3.25 <= h / T < 3.75:

$$\alpha_{xx} = 0.4078 * F_{nh}^6 - 0.919 * F_{nh}^5 - 3.8292 * F_{nh}^4 + 15.738 * F_{nh}^3 - 19.766 * F_{nh}^2 + 9.7466 * F_{nh} - 0.6409 \quad \text{(A.11)}$$

if 3.75 <= h / T < 4.5:

$$\alpha_{xx} = 0.3067 * F_{nh}^6 - 0.3404 * F_{nh}^5 - 5.0511 * F_{nh}^4 + 16.892 * F_{nh}^3 - 20.265 * F_{nh}^2 + 9.9002 * F_{nh} - 0.6712 \quad \text{(A.12)}$$

if 4.5 <= h / T < 5.5:

$$\alpha_{xx} = 0.3212 * F_{nh}^6 - 0.3559 * F_{nh}^5 - 5.1056 * F_{nh}^4 + 16.926 * F_{nh}^3 - 20.253 * F_{nh}^2 + 10.013 * F_{nh} - 0.7196 \quad \text{(A.13)}$$

if 5.5 <= h / T < 6.5:

$$\alpha_{xx} = 0.9252 * F_{nh}^6 - 4.2574 * F_{nh}^5 + 5.0363 * F_{nh}^4 + 3.3282 * F_{nh}^3 - 10.367 * F_{nh}^2 + 6.3993 * F_{nh} - 0.2074 \quad \text{(A.14)}$$

if 6.5 <= h / T < 7.5:

$$\alpha_{xx} = 0.8442 * F_{nh}^6 - 4.0261 * F_{nh}^5 + 5.313 * F_{nh}^4 + 1.6442 * F_{nh}^3 - 8.1848 * F_{nh}^2 + 5.3209 * F_{nh} - 0.0267 \quad \text{(A.15)}$$

if 7.5 <= h / T < 8.5:

$$\alpha_{xx} = 0.1211 * F_{nh}^6 + 0.628 * F_{nh}^5 - 6.5106 * F_{nh}^4 + 16.7 * F_{nh}^3 - 18.267 * F_{nh}^2 + 8.7077 * F_{nh} - 0.4745 \quad \text{(A.16)}$$

if 8.5 <= h / T < 9.5: if $F_{nh} < 0.6$:

$$\alpha_{xx} = 1 \quad \text{(A.17)}$$

if $F_{nh} >= 0.6$:

$$\alpha_{xx} = -6.4069 * F_{nh}^6 + 47.308 * F_{nh}^5 - 141.93 * F_{nh}^4 + 220.23 * F_{nh}^3 - 185.05 * F_{nh}^2 + 79.25 * F_{nh} - 12.484 \quad \text{(A.18)}$$

if h / T >= 9.5: if $F_{nh} < 0.6$:

$$\alpha_{xx} = 1 \quad \text{(A.19)}$$

if $F_{nh} >= 0.6$:

$$\alpha_{xx} = -6.0727 * F_{nh}^6 + 44.97 * F_{nh}^5 - 135.21 * F_{nh}^4 + 210.13 * F_{nh}^3 - 176.72 * F_{nh}^2 + 75.728 * F_{nh} - 11.893 \quad \text{(A.20)}$$

$V_2 = V_0 \ / \ \alpha_{xx}$

A.2 Formula fits

This section remains confidential.

List of Figures

List of Tables